NOTE TO USERS

DISRUPTION OF THE *ard* EXPRESSION, ENCODING A SUBUNIT OF *DROSOPHILA* NEURONAL NICOTINIC ACETYLCHOLINE RECEPTOR BY MITOMYCIN C-OLIGONUCLEOTIDE CONSTRUCT AND RIBOZYME

by

MAREK PIERZCHALA

A dissertation submitted to the Graduate Faculty in Biochemistry in partial fulfillment of the requirements for the degree of Doctor of Philosophy. The City University of New York

2005

INFORMATION TO USERS

The quality of this reproduction is dependent upon the quality of the copy submitted. Broken or indistinct print, colored or poor quality illustrations and photographs, print bleed-through, substandard margins, and improper alignment can adversely affect reproduction.

In the unlikely event that the author did not send a complete manuscript and there are missing pages, these will be noted. Also, if unauthorized copyright material had to be removed, a note will indicate the deletion.

ProQuest Information and Learning Company
300 North Zeeb Road
P.O. Box 1346
Ann Arbor, MI 48106-1346

This manuscript has been read and accepted for the Graduate Faculty in Biochemistry in satisfaction of the dissertation requirement for the degree of Doctor of Philosophy.

4/11/05
Date

Chair of Examining Committee

April 19th, 2005
Date

L. Davenport
Executive Officer

Supervisory Committee

The City University of New York

ABSTRACT

Disruption of the *ard* expression, encoding a subunit of *Drosophila* neuronal nicotinic acetylcholine receptor by mitomycin C-oligonucleotide construct and ribozyme

by

Marek Pierzchala

Advisor: Professor Thomas Schmidt -Glenewinkel

The goal of this studies it to disrupt the expression of the *ard* gene encoding one of the subunits of the nAChR in *Drosophila*. The results may lead to better understanding of the role the ARD subunit plays and the function and structure of the nicotinic receptor. Out of many approaches to influence the expression of the *ard* gene we had chosen two direct methods; first – using MC-oligonucleotide conjugate – we attempted to induce small mutation in crucial stretch of *ard* DNA sequence, and second-using ribozyme- we tried to reduce or abolish *ard* mRNA , thus preventing or reducing efficient translation. Mitomycin C is able to alkylate and cross-link DNA strands; it is also a potent mutagen. MC-oligonucleotide constructs were designed and synthesized. The cross-linking was done *in vitro* on M13mp18 vector. M13mp18 vector from the cross- linking reaction was transformed into *E. coli* to investigate the nature of the potential mutations. Also, cross-linking that could lead to a mutation was attempted *in vivo* in *E. coli*. In addition, similar

attempt was tried in *Drosophila* by injecting MC-oligonucleotide constructs into thousands of *Drosophila* embryos. In spite of laborious screenings potential mutations were not identified.

Another method to disrupt efficient gene expression is through destruction of mRNA by employing targeted ribozymes. We used several ribozymes against *ard* mRNA. DNA coding for the ribozymes was subcloned into pP{CaSpeR-hs} vector. Using P-element mediated transformation several transgenic *Drosophila* lines were established. *Drosophila* embryos from each line were heat-shocked to allow the subcloned ribozyme DNA, that was under the control of heat-shock promoter, to be transcribed into the specific ribozyme and cleave the *ard* mRNA. Immunoblotting experiments indicate that the ARD protein level, in the larvae hatched form the heat-shocked embryos, was substantially decreased, presumably by the action of the hairpin ribozyme.

ACKNOWLEDGMENTS

I wish to express my highest regards to my mentor Dr. Thomas Schmidt-Glenewinkel who spent so much time trying to help me in any possible way to finish successfully my Ph. D. research. He guided me through the project with a patience worth of a saint. He advised me on many aspects of Ph. D. work. Whenever I encountered an impediment his profound knowledge of sciences helped me to overcome many problems. He was very generous in his support. Also, on personal level I owe my mentor a lot.

I am very thankful to Dr. Maria Tomasz for supplying me with all necessary protocols, scientific instruments, and materials, including mitomycin. Her technical advice was of great help to me.

I am really grateful to my colleagues, Vita Vernace (for helping me in diverse ways in my project), Dong Dong Ma, Jinguo Ma, Zhiyou Wang, Sneha Mathew. I have to also express gratitude to Julie Russak and Judy Zhu who contributed to my project considerably.

Thank you to all my friends.

TABLE OF CONTENTS

TITLE.....i

COPYRIGHT.....ii

APPROVAL PAGE.....iii

ABSTRACT.....iv

ACKNOWLEDGEMENTS.....vi

TABLE OF CONTENTS.....vii

LIST OF TABLES.....xi

LIST OF FIGURES.....xii

LIST OF ABBREVIATIONS.....xv

I. INTRODUCTION.....1

A. Background.....3

1. Structure and function of nAChRs.....2

a. nAChRs in vertebrates.....2

Neuromuscular junction – muscle nAChRs.....2

Neuronal AChRs.....9

b. nAChRs in *Drosophila melanogaster* 11

2. The advantages of using *Drosophila* as a model system for studying neuronal nAChR..... 15

3. Mitomycin C-oligonucleotide adduct as a tool to mutagenize the *ard* gene. 17

4. Ribozyme as a tool to inactivate *ard* mRNA..... 21

B. Specific Aims.....29

a. design and generate mitomycin C - oligonucleotide conjugates.....32

b. produce cross-linking *in vitro* and optimize its conditions using M13mp18 DNA.....32

c. introduce mutations into M13mp18 DNA and screen for it.....33

d. introduce mutations in the *Drosophila white* gene.....33

e. introduce mutation in the *Drosophila ard* gene.....34

f. predict secondary structure of the *ard* mRNA and find target sequences in it.....34
g. design and prepare ribozyme constructs.....35

h. generate transgenic flies.....35
i. heat-shock activate the ribozyme and disrupt the *ard* mRNA.....36

II. MATERIALS AND METHODS.....37

A. Materials.....37

1. Sources of materials.....37

2. Bacterial strains and plasmids.....38

3. *Drosophila* strains 38

B. Generation of mitomycin C-oligonucleotide conjugates.....39

1. Synthesis of oligonucleotides with aminolinker for the conjugates.....39

2. Attachment of mitomycin A to oligonucleotide with aminolinker.....40

C. Formation and optimization of cross-linking *in vitro*..... 41

1. Large-scale preparation of single-stranded M13mp18 DNA..... ...41

2. 3'-end labeling of MC-oligonucleotide conjugate with cordycepin 42

3. Purification of cordycepin-labeled conjugate 42

4. Preparation of microsomal NADPH-cytochrome c (P-450) reductase from rat liver 43

5. NADPH-cytochrome P-450 reductase quantitation 44

6. Determination of NADPH-cytochrome P-450 reductase activity.....45

7. Cross-linking of MC-oligonucleotide conjugate to ss(c) M13mp18 DNA 46

D. *In vivo* experiments in *E. coli* 47

1. Preparation of Frozen Storage Competent Cells 47

2. Preparation of single-stranded DNA template for sequencing.....47

3. Screening for a mutation (plaque lifts).....47

E. *In vivo* experiments with *Drosophila* 49

Microinjections of MC-oligonucleotide constructs.....49

F. Prediction of the *ard* secondary structures.....50

G. Preparation of the ribozyme delivery construct.....50

H. Generation of transgenic flies.....51

I. Heat-shock activation of ribozyme 54

J. Drosophila head / larva membrane protein preparation and solubilization.....55

K. Western blotting 57

III. RESULTS.....59

Design and generation of mitomycin C-oligonucleotide conjugates. 59

Introduction of cross-linking *in vitro* between MC-oligonucleotide construct and ssDNA.....68

In vivo experiments in *E. coli* 76

A. Identification and analysis of potential mutation in M13mp18 DNA 76

B. Cross-linking *in vivo* catalyzed by the intracellular reductases of *E. coli* 78

Introduction of mutations into *Drosophila white* and *ard* genes.....78

Prediction of the *ard* mRNA secondary structures 82

Ribozyme design and the preparation of the ribozyme delivery construct..... 83

Generation of transgenic flies. 88

Lowering of ARD protein level by degradation of the *ard* mRNA..... 88

IV. DISCUSSION 93

V. BIBLIOGRAPHY 100

LIST OF TABLES

Table 1. List of identified nicotinic AChR subunit genes in *Drosophila melanogaster*...13

Table 2. cDNAs of four subcloned ribozyme constructs.....84

LIST OF FIGURES

Figure 1. Schematic drawing of the events taking place during arrival of an action potential and synaptic transmission at the synaptic cleft with a participation of acetylcholine and acetylcholine receptors.....3

Figure 2. Schematic drawing of the nACh receptor 5

Figure 3. Schematic drawings of the nACh receptor and one of its subunits.....7

Figure 4. Schematic drawings of the nAChR subunits undergoing a rotation between closed - and open-channel forms.....10

Figure 5. Semi-schematic representation of the neuronal nicotinic Ach receptor.....9

Figure 6a. Chemical diagram of mitomycin C (MC). 19

Figure 6b. MC cross-links with DNA.....21

Figure 7. Predicted secondary structure of a hammerhead ribozyme and the substrate RNA.....25

Figure 8. Predicted secondary structure of the hairpin ribozyme-substrate RNA complex 26

Figure 9. Schematic diagram of the hammerhead ribozyme based on the X-ray crystal structure.....27

Figure 10. Drawings of four mitomycin C conjugated oligonucleotides.....60

Figure 11. M13mp18 DNA target sequence, including EcoRI recognition site, with four different length oligonucleotides complementary to this sequence.....61

Figure 12A-D. The course of the coupling reaction 62-65

Figure 13A. The diagram of the HPLC chromatogram 66

Figure 13B. UV-visible spectrum of MC-oligonucleotide conjugate (21-mer) 67

Figure 14. Phosphoimage of the purification products of cordycepin 5'-triphosphate labeled conjugates.....71

Figure 15. The comparison of the two reductase samples used for the cross-linking reaction.....72

Figure 16. Phosphoimage of the cross-linking reaction product and control for the 21-mer conjugate.....74

Figure 17. Phosphoimage of the cross-linking reaction products and control for 21-mer conjugate run in glyoxal loading buffer.....75

Figure 18. M13mp18 DNA sequence with EcoRI recognition site and complementary 18-mer oligonucleotide probe.....77

Figure 19. *Drosophila white* gene target sequence with conserved motif and complementary 18-mer oligonucleotide.....79

Figure 20. *ard* mRNA optimal secondary structures.....83

Figure 21. Enlarged region of the *ard* mRNA optimal secondary structures 83

Figure 22. Schematic diagram of the hammerhead ribozyme delivery construct (top) and the target *ard* mRNA together with ribozyme 85

Figure 23. Schematic diagram of the hairpin ribozyme delivery construct and the *ard* mRNA with the ribozyme.....86

Figure 24. pP{CaSpeR-hs} vector.....87

Figure 25. Picture of the SDS-polyacrylamide gel with solubilized membrane protein preparation from *Drosophila* head.....89

Figure 26. Protease digestion of the solubilized larval membrane preparation

and the results of the increased amount of protease inhibitors.....90

Figure 27. Western blotting results of heat-shock experiments.....92

LIST OF ABBREVIATIONS

aa	amino acids
Ach	acetylcholine
AChR	acetylcholine receptor
AEL	after egg laying
BSA	bovine serum albumin
HPLC	high performance liquid chromatography
MA	mitomycin A
MC	mitomycin C
mRNA	messenger RNA
ms	millisecond
nAChR	nicotinic acetylcholine receptor
nt	nucleotides
O.D	optical density
PE	phosphodiester
PS	phosphorothioate

I. INTRODUCTION

A. Background

Efficient communication between neurons is crucial to the normal functioning of the nervous systems which are the most complex, least understood, but recently widely investigated organ systems in animals. Nerve cells communicate, that is propagate nerve impulses, or action potentials, via specialized cellular structure known as the synapse – a junction at which the axon of the presynaptic neuron terminates at some location on the postsynaptic neuron. At electric synapses action potential simply travels from one cell to the next through specialized channels, called gap junctions, which connect the two cells. But most cells communicate via chemical synapses. These cells are separated by a synaptic cleft, a space, which prevents direct passage of action potentials. Instead, chemicals called neurotransmitters are employed to communicate the signal from one cell to the next. Some neurotransmitters are excitatory and depolarize the next cell, thus increasing the probability that an action potential will be fired. The process by which this information is communicated is called synaptic transmission – a signaling process that neuroscience has intensely been trying to unravel for the last several decades. One of the excitatory neurotransmitters is acetylcholine (Ach), a simple molecule synthesized from choline and acetyl-CoA, which activates ACh receptors, some of which belong to a class of neurotransmitter receptors known as ligand-gated ion channels. AChR is a transmembrane protein found mostly in the postsynaptic membrane. It mediates fast transmission of nerve signal from one neuron to another or to a muscle or gland cell. Two main classes of AChRs have been identified on the basis of their responsiveness to

either the toadstool alkaloid, muscarine, or to nicotine: the muscarinic receptors and the nicotinic receptors, respectively. Both receptor classes are abundant in human brain. Nicotinic AChR has the distinction of being the first ligand-gated ion channel sequenced. It has been most thoroughly investigated and best characterized by biochemical, alignmimmunological, electrophysiological and molecular biology methods. Postsynaptic membranes are densely populated with this receptor; 20,000 per square micrometer (Mathews, 2000) When action potential reaches the end of an axon, calcium channels are opened which leads to the release of Ach into the presynaptic cleft. Binding of Ach to the nACh receptor in the post-synaptic cell activates this receptor, its cation channel opens transiently, an influx of Na^+ into the cell takes place, resulting in a depolarization of the postsynaptic membrane (Fig.1, next page).

As more and more studies become available, more subtypes of nicotinic ACh receptor are being discovered. The broadest division puts nAChRs into two classes, based on function and position in organism: muscle nAChR (present at neuromuscular junction) and neuronal nAChR (present in the nervous system).

1. Structure and function of nAChRs

a. nAChRs in vertebrates

Neuromuscular junction – muscle nAChRs

The molecular biology of nACh receptors is much better understood in vertebrates than in insects.

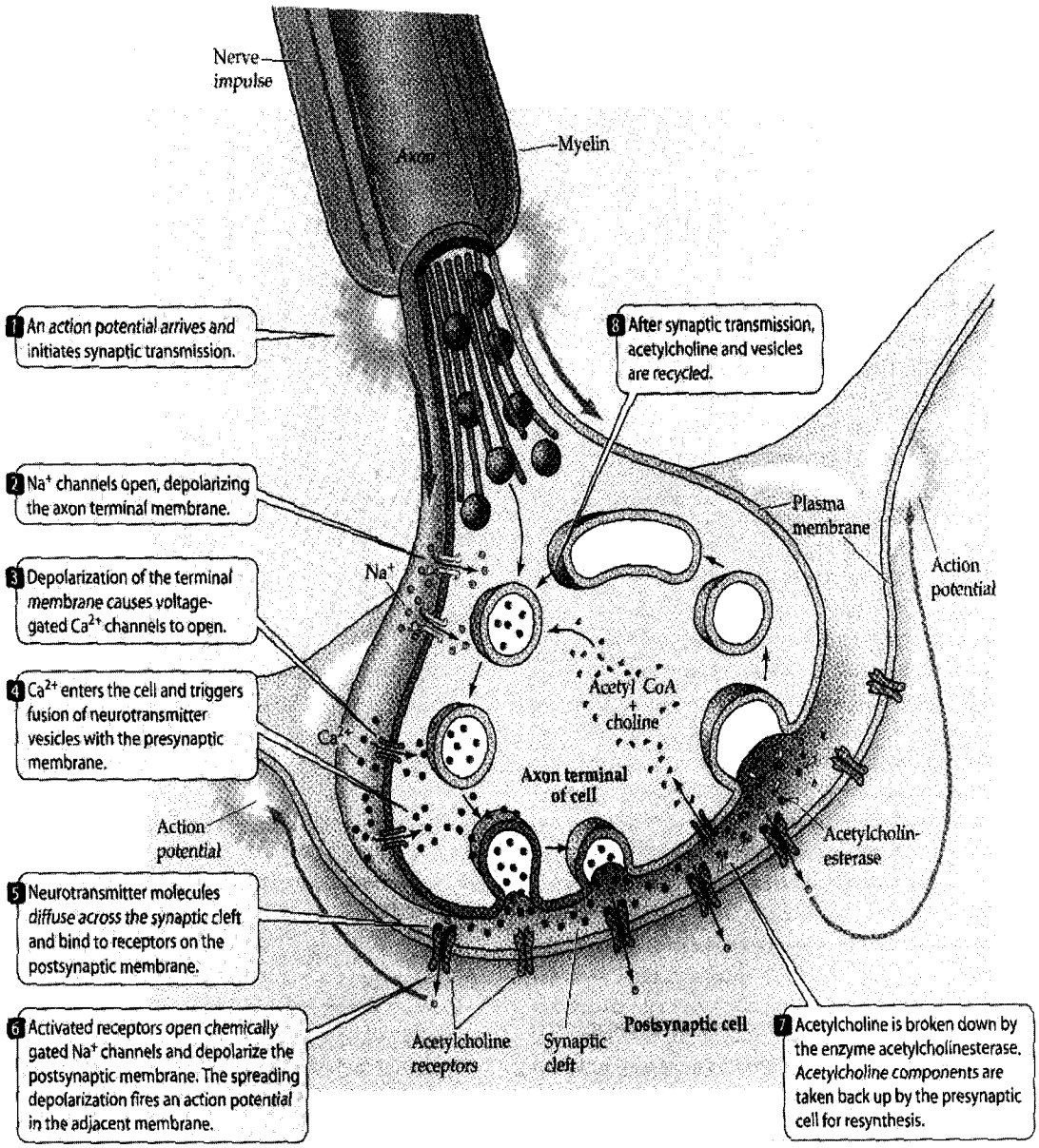

Figure 1 Schematic drawing of the events taking place during arrival of an action potential and synaptic transmission at the synaptic cleft with a participation of acetylcholine and acetylcholine receptors.
From "Life: the science of biology" (Purves et al., 2001), p.787.

The prototype of nAChRs are those of the neuromuscular junction of vertebrates and the electric organ of *Torpedo californica* (Grutter and Changeux, 2001; Millar, 2003; Ortiz-Acevedo et al., 2004) .It was found that during development, nAChR not only changes in amount and distribution, but also in several of its properties. Only the molecular basis of a postnatal change in its channel properties is now relatively well understood. The embryonic muscle receptor is a pentameric protein consisting of four different but homologous subunits assembled with a stoichiometry of $\alpha_2\beta\gamma\delta$. The change in postnatal properties results from the change in subunit composition: postsynaptic nAChRs containing a γ subunit ($\alpha_2\beta\gamma\delta$) are replaced by nAChRs containing a homologous ε subunit ($\alpha_2\beta\varepsilon\delta$). The switch is transcriptional: the abundance of γ subunit mRNA declines and that of ε subunit mRNA increases. This substitution affects the channel properties of the nAChR, as the γ nAChR has a smaller single-channel conductance and opens for a longer time than the ε nAChR. The physiological significance of this change may be that γ nAChRs are more effective in depolarizing the smaller muscle fibers of embryonic muscles than the ε nAChRs ((Hall and Sanes, 1993).

The shape and dimensions of the nAChR at the muscular junction were deduced from electron microscopy study (approaximately 12.5nm x 8nm) (Fig.2, next page) (Hucho et al., 1996) Binding of acetylcholine to the two α-subunits is thought to be the essential signal to transiently open the integral cation channel. All subunits are membrane-spanning glycoproteins with sugar residues on the extracellular side and peripheral membrane protein anchoring the subunits to the cell's cytoskeleton. The subunits display significant similarity with each other and across species, and have a similar structural organization.

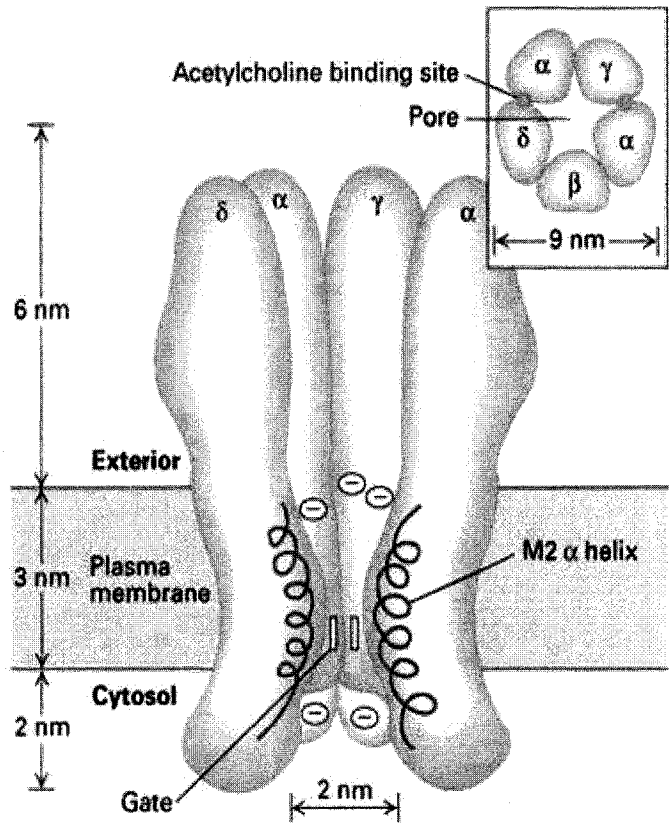

Figure 2 Schematic drawing of the nACh receptor.
The receptor is imbedded into the plasma membrane at the neuromuscular junction. The approximate dimensions of the receptor, both for the pore size and for the subunits are shown. This drawing was taken from the website: www.zoology.ubc.ca

A model (Fig.3, page 7) predicts each subunit to be a long string of amino acids that goes in and out of the muscle cell membrane 4 times, forming 4transmembrane regions (M1-

M4) that correspond to the parts of the receptor within the membrane, but not to the tails and loops outside the membrane. The amino acid composition of this string varies in each subunit. The M2 helices of the five subunits are presumed to line the pore of the ion channel. An essential element of the ligand-binding site of the α subunit is located just upstream of the M1 in the extracellular N-terminal domain and is characterized by two adjacent cysteine residues, in the so called loop C of the nAChR-binding site. Other specific residues in smaller loops of α subunits contribute to the ACh binding. The cytoplasmic loop between M3 and M4, and short extracellular C-terminal tail are highly variable both in sequence and length (Ortiz-Acevedo et al., 2004).

The structure of the open-channel form of nAChR has been determined from electron images of *Torpedo* ray postsynaptic membranes activated by brief (<ms) mixing with droplets containing ACh and freezing rapidly. Comparison with the closed-channel form shows that ACh initiates small rotations of the subunits in the extracellular domain, which trigger a change in configuration of α-helices lining the membrane-spanning pore. The open pore tapers towards the intracellular membrane face, where it is shaped by a 'barrel' of α-helices having a pronounced right-handed twist as suggested by Unwin, based on 9Å studies (Unwin, 1995); Fig.4, page 8).

In another model, based on substituted cysteine accessibility mutagenesis (SCAM), Karlin and colleagues suggested that α M2 domains undergo significant changes in secondary structure, from non-helical to α-helical, during gating (Karlin and Akabas, 1995; Wilson and Karlin, 1998). No matter which model is right, those conformational changes provide a structural basis for explaining the remarkably rapid and efficient response of this synaptic protein to the neurotransmitter, its precise permeation and its

almost total impermeability to ions when the neurotransmitter has dissociated (Hille, 2001). It seems likely that other types of nAChRs and other ligand-gated channels would use similar principles to open their pores and allow passage of ions.

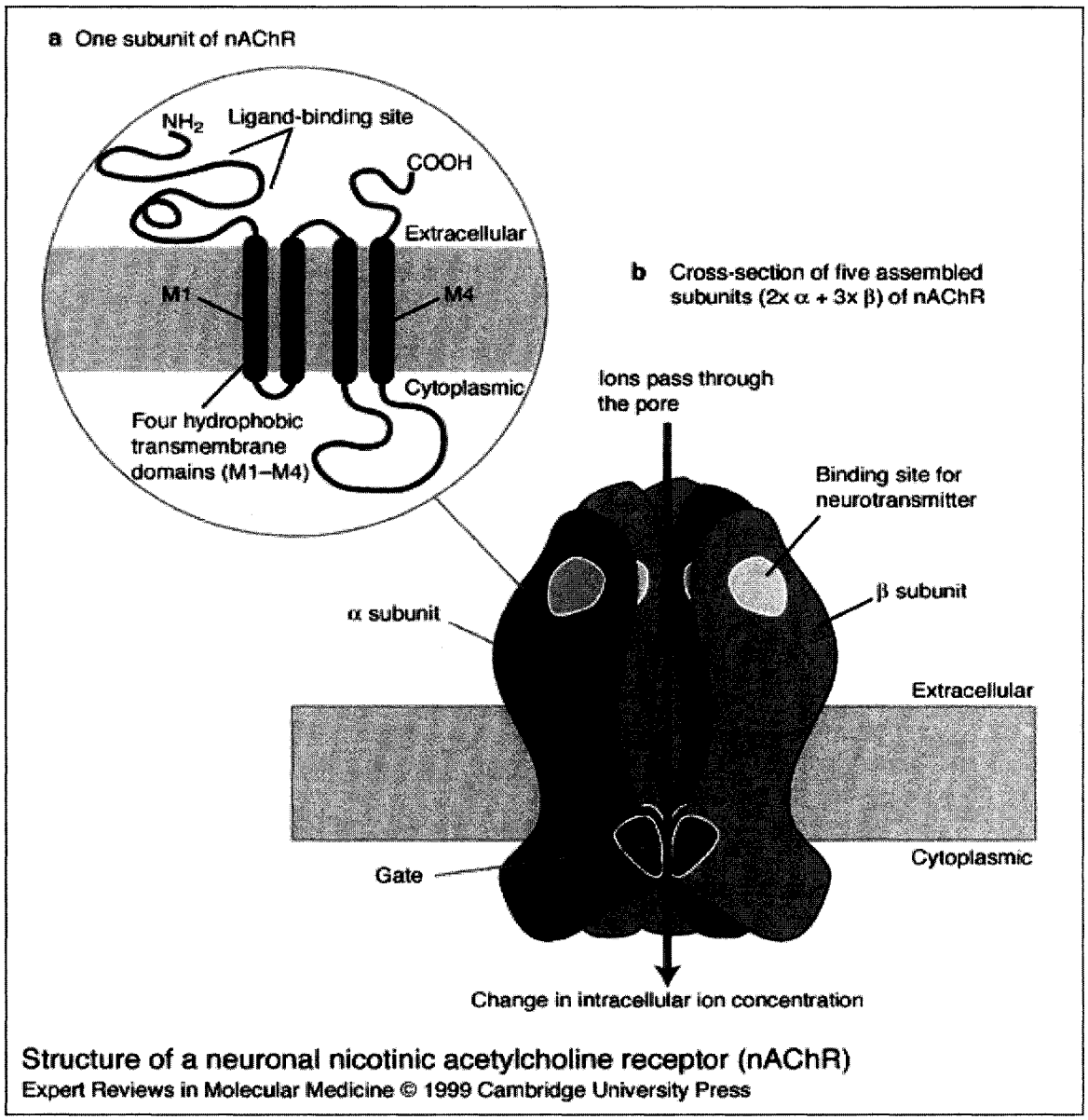

Figure 3 Schematic drawings of the nACh receptor.
Part **a** shows just one subunit with 4 transmembrane regions (domains of long chains of amino acids) M1-M4. Part **b** shows the cross-section of the receptor. This drawing was taken from the website: www.ermm.cbcu.cam.ac.uk.

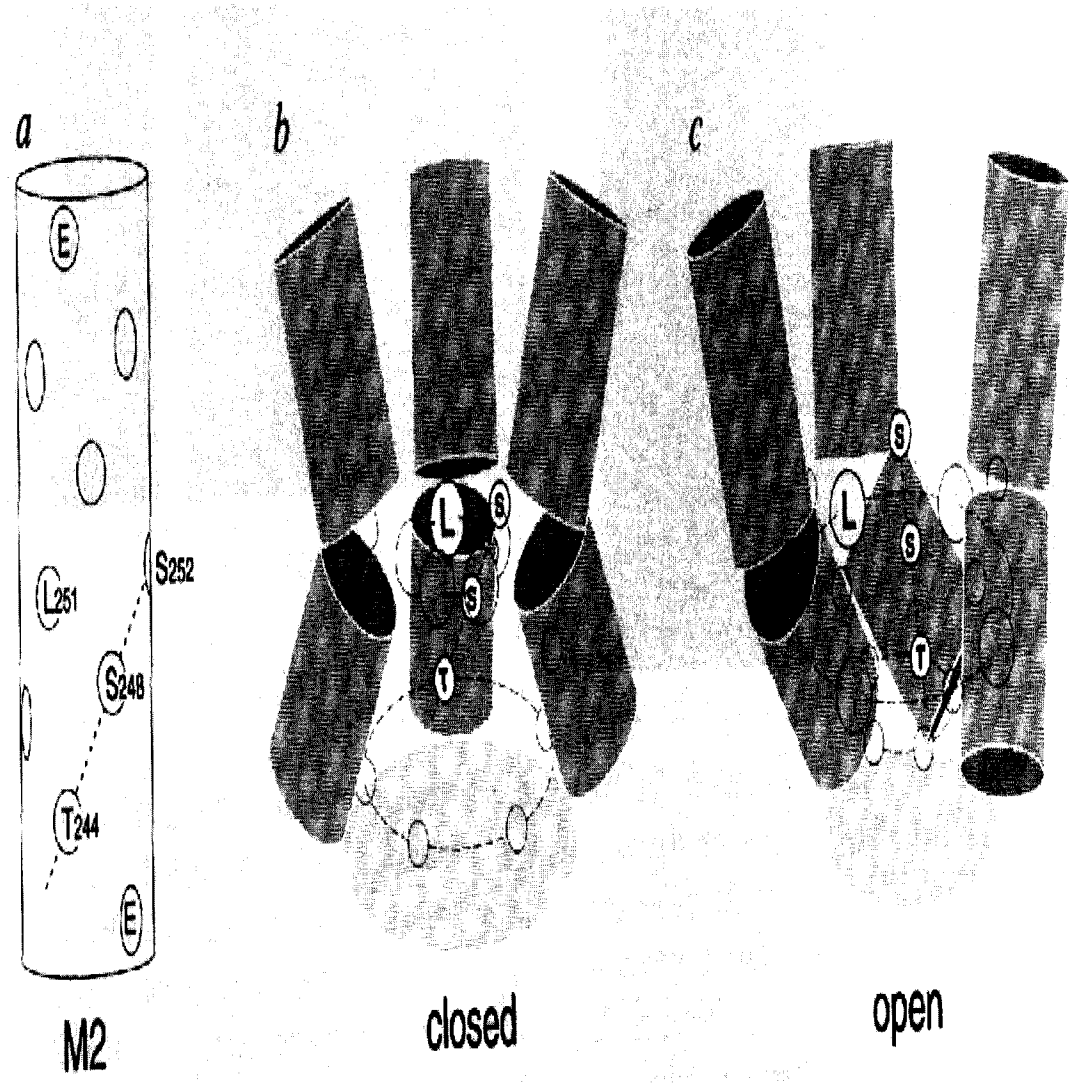

Figure 4 Schematic drawings of the nAChR subunits undergoing a rotation between closed- and open-channel forms.
The figure appears in (Unwin, 1995)

Neuronal nAChRs

In addition to nACh receptors expressed at the neuromuscular junction, a distinct group of receptors called neuronal nAChRs is found in the vertebrate peripheral and central nervous systems (Fig.5).

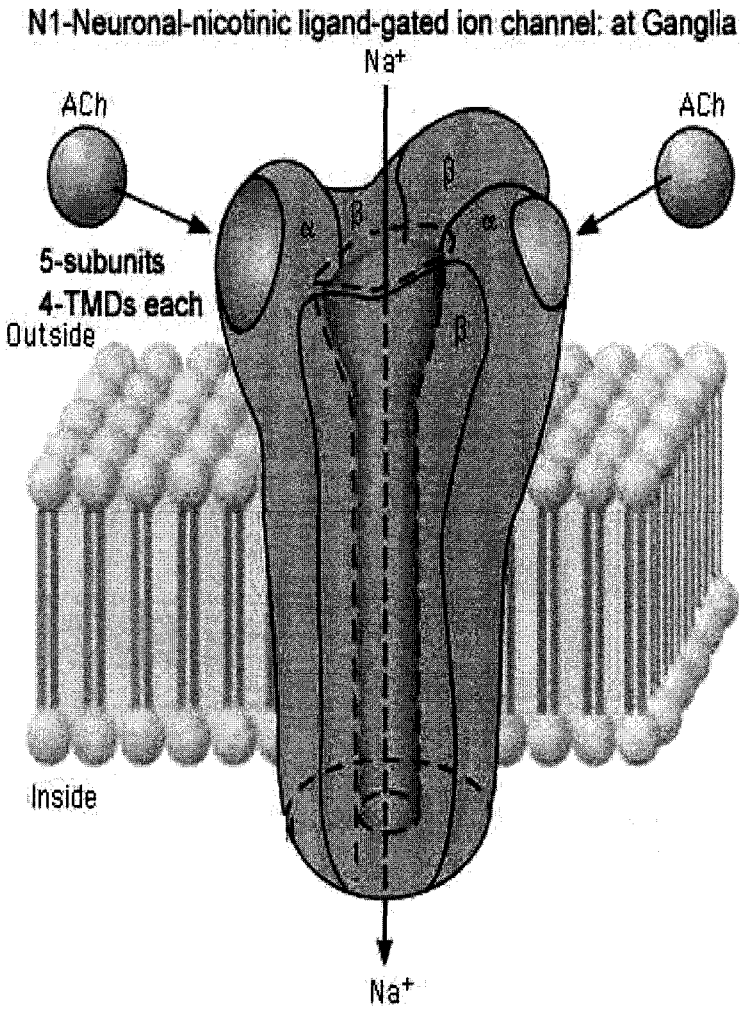

Figure 5 Semi-schematic representation of the neuronal nicotinic Ach receptor. The figure is on the website: www.usc.edu.

Unlike muscle nAChR, neuronal nAChRs comprise two classes. One class is heteropentameric receptor consisting of two types of subunits: ligand-binding α-subunits characterized by two adjacent cysteines and structural β-subunits that carry complementary ligand-binding domains (Grauso et al., 2002; Millar, 2003). The other class is homopentameric receptor consisting of only α-subunits, e.g. α7 nAChR (Millar, 2003; Nai et al., 2003). The neuronal nAChRs are more complex than neuromuscular nAChRs with twelve genes encoding twelve subunits identified so far (rat), which are divided into nine ligand-binding α-subunits (α2-α10) and three structural β-subunits (β2-β4 in rat; non-α-1 to 3 in the avian system (Boorman et al., 2000; Gotti and Clementi, 2004; Millar, 2003; Sargent, 1993).

The α-subtypes are similar to the muscle α-subunit (α1), and the β-subunits fulfill a structural role and are analogous to β1, γ/ε, and δ subunits in the muscle receptor of *Torpedo californica*. Each of these subunit genes exhibits distinct temporally and spatially restricted patterns of expression in the nervous system (McGehee and Role, 1995). Combinations of neuronal α- and β-subunits form ACh-gated channels on expression in *Xenopus* oocytes, a finding confirming that functional nAChRs can in fact assemble from two types of subunits (Boulter et al., 1987). These include homopentameric receptor (α7, α8, and α9) channels with different pharmacological and physiological profiles (Arias, 2000; McGehee and Role, 1995; Millar, 2003) It is possible that the functional diversity exhibited by the neuronal nAChR family results from the differential expression of these subunits leading to incorporation of different subunits into mature receptors (Millar, 2003; Sargent, 1993).

All neuronal nAChRs found so far are presumed to regulate cation fluxes as do muscle nAChRs. This presumption is based primarily on the homology of sequencies from central and peripheral nervous tissues, with nAChRs genes expressed in vertebrate skeletal muscles. Since the functional nature of the channel in vertebrate muscle is well established, it follows that the channel of the homologous neuronal receptors would have a similar function. Regulation of cation fluxes by the neuronal nAChR allows it to receive and process natural chemical signals carried by the neurotransmitter, acetylcholine. Receipt and processing of these signals are critical to modulation of fast synaptic transmission, regulation of autonomic nervous system, participation in pharmacological action of drugs, such as the effects of nicotine in brain (including addiction as well as analgesia, enhanced cognition, memory and attention) (Grutter and Changeux, 2001). Mood, thinking, and many forms of sensory perception, like auditory function, is also controlled in part by neuronal nAChRs.

In contrast to muscle nAChRs, where Na^+ is main permeating ion, some neuronal nAChRs have a significant permeability to Ca^{2+}, although they can still conduct Na^+ (Sargent, 1993)

b. nAChRs in *Drosophila melanogaster*

In insects, cholinergic synaptic transmission is restricted to the nervous system. Homology screening with cDNA probes from vertebrate nAChR subunits and subsequently with *Drosophila* receptor-derived probes, and sequence similarity searches based on BLAST method using previously cloned *Drosophila* nAChR genes, have led to

the isolation of a family of cDNAs and genes encoding ten different putative subunits of the *Drosophila* nAChRs (Grauso et al., 2002; Gundelfinger, 1992; Gundelfinger and Hess, 1992; Lansdell and Millar, 2002; Lansdell et al., 1997; Millar, 2003), see Table1, next page. Four of these subunits, known as ALS/ Dα1, SAD/Dα2, Dα3, and Dα4, contain two adjacent cysteines characteristic of ligand-binding α-subunits (Baumann et al., 1990; Bossy et al., 1988; Gundelfinger, 1992; Lansdell and Millar, 2002; Millar, 2003). In Dα5, Dα6, and Dα7 these two cysteines are separated by thirteen amino acids (Grauso et al., 2002). Three subunits: ARD, SBD, and Dβ3, are lacking above cysteine residues and thus most likely represent structural non α-subunits (also called β-subunits) (Lansdell et al., 1997; Sawruk et al., 1990).

The recently sequenced genome of *Drosophila melanogaster* has renewed interest in molecular and functional diversity in the *Drosophila* nAChR gene family. This contributed to the cloning of Dα5, Dα6, Dα7, and Dβ3 putative nAChR subunit genes and has provided evidence of genetic variation, alternative splicing and site-specific mRNA editing events (Grauso et al., 2002; Lansdell and Millar, 2002) Until now, despite intensive efforts, it has not been possible to generate functional neuronal nAChRs from *Drosophila* by heterologous expression of any combination of known subunits. It has, however, been possible to express functional hybrid receptors when Drosophila α–subunits are co-expressed with vertebrate β-subunits in *Xenopus* oocytes (Lansdell and Millar, 2002).

The putative nAChR subunits in *Drosophila* display a higher sequence homology to vertebrate neuronal nAChRs than to vertebrate muscle receptors.

GENES	Synonyms	Chromosomal location	Protein length (aa)	Reference
als	*nAcRa-96Aa,* CG5610	96A1-A2	567	Bossy B, Ballivet M, Spierer P. (1988)
Da2	*nAcRa-96Ab,* CG6844	96A3	576	Jonas *et al.* (1990)
Da3	*nAcRa-7E* CG2302	7E1-E2	783, 795	Schulz *et al.* (1998)
Da4	*nAcRa-80E*	80F1-F3	568 384	Lansdell and Millar (2000)
Da5	*nAcRa-34E,* CG4498, BG:DS05899.4	34F3-F4	807, 482 570	Grauso *et al.* (2002)
Da6	*nAcRa-30D* CG4128	30D1-D3	523,544 509, 494	Grauso *et al.* (2002)
Da7	*nAcRa-18C* CG8109, CG8082	18C2-C3	219, 545	Grauso *et al.* (2002)
ard	*nAcRb-64B,* CG12606	64B6	521	Hermans-Borgmeyer et al. (1986)
sbd	*nAcRb-96A,* CG6798, *Db2*	96A5	519	Sawruk *et al.*, (1990)
Db3	*nAcRb-21C,* CG11822	21D1	541	Lansdell and Millar, (2002)

Table 1 List of identified nicotinic AChR subunit genes in *Drosophila melanogaster.*

They share a similar predicted structural organization and up to 50% sequence similarity with nAChR subunits of vertebrates. They have cleavable signal peptides at the N-termini and the putative mature proteins consist of 493 (SBD), 497 (ARD), 546 (ALS), 535 (Dα2), 807 (Dα5), and 563 (Dα6) amino acids (Grauso et al., 2002; Gundelfinger and Hess, 1992).

In order to establish the identity of the deduced proteins as functional nAChR subunits and to study their assembly, two ligand-binding subunits, ALS and Dα2, as well as structural subunit ARD proteins are studied widely and intensively at physiological and pharmacological level in *Drosophila* (Bertrand et al., 1994; Schulz et al., 2000).

The snake venom, α-bungarotoxin (α-Btx), a nicotinic receptor blocker, has been shown to antagonize nAChRs in insects (Lees et al., 1983). At least two different classes of binding complexes by α-Btx have been reported in *Drosophila* (Schloss et al., 1988). By immunoprecipitation experiments, the precipitation of binding complex of protein and ^{125}I-α-Btx can be detected (Schloss et al., 1991). With the aid of antibodies against bacterially expressed fusion proteins of cloned receptor subunits ALS and ARD have been proved to be components of the class I high-affinity α-Btx binding sites (Schloss et al., 1991). These results are consistent with the assumption that both proteins could be subunits of the same hetero-oligomeric receptor complex with ALS as ligand-binding subunit and ARD as structural subunit.

Similar assumption - that both proteins might be subunits of the same hetero-oligomeric receptor complex - could be extended to another pair of nAChR subunits, Dα3 and ARD, since Dα3 antibodies co-immunoprecipitated Dα3 and ARD proteins and, vice versa,

anti-ARD antibodies co-precipitated ARD and Dα3 in another set of like experiments (Chamaon et al., 2000).

2. The advantages of using *Drosophila* as a model system for studying neuronal nAChR

Drosophila melanogaster is well suited to genetic, molecular, and physiological approaches to investigate nAChR function in nervous system. The fly's intermediate level of complexity, as compared to unicellular organisms vs. vertebrates, and its highly advanced genetics, makes it great model organism to the researchers. *Drosophila* has many advantages for genetic analysis studies: a small size and a short generation time make feasible raising of large number of individuals for the many generations required for genetic analysis. It also has a small genome, 1/20 the size of a typical mammalian genome, which facilitates molecular genetic analysis (Rubin, 1988). There is a wide range of tools available for use with this organism, like germline transformation that provides diverse easy ways to generate mutations in the nervous system.

Drosophila nervous system is an unusually rich source of nicotinic receptors and there is substantial evidence that acetylcholine is a widely used excitatory neurotransmitter in the insects central nervous system. The concentration of nAChR in the CNS of *Drosophila* is very high (20,000 per square micrometer) comparing with that in the electric organ of the electric eel, and nAChRs occur only in the nervous system, since the neuromuscular junction in insects uses glutamate as neurotransmitter (Gundelfinger and Hess, 1992; Schafer, 2002).

Nicotinic AChRs are highly conserved from *Drosophila* to mammals in nervous system. Insect nAChR α subunits more closely resemble in sequence vertebrate neuronal α subunits, than vertebrate muscle α subunits (Grauso et al., 2002).

Recently, more knock-out mice have been generated to study the effect of deletions on the structure and functions of the nervous system. They all display behavioral phenotypes. The lack of the α7 (Orr-Urtreger et al., 1997) and β2 (Picciotto et al., 1995) subunits in the neuronal nAChR in mice led to a very subtle phenotype with no obvious macroanatomical changes. Changeux and his associates are studying the roles of some subunits of neuronal nAChRs in vertebrates by generating knock-out mice. They found nicotine self-administration was reduced or suppressed in β2 and α4 mutant mice. These data support the view that the β2-containing and α4-containing receptors are involved in mediating the reinforcing properties and nicotine-elicited antinociception of nicotine (Lena and Changeux, 1999; Marubio et al., 1999). They also found α2 (Marks et al., 1999) and α7 (Corringer et al., 1999) subunits are involved in nicotine sensitivity. However, such type of mutations in mammalian systems is more subtle and is usually compensated, while mutations in *Drosophila* have frequently a more dramatic effect and may cause lethality.

What makes studies with this fruit fly easier is the fact that in the year 2000 the genome of *Drosophila melanogaster* was completely sequenced. This contributed to the identification of four new putative subunits of nAChR in *Drosophila*. In spite of these new findings the complexity of nAChRs appears to be lower in fruit fly than in vertebrates, what stresses the attractiveness of *Drosophila* as a model system to study the nAChR.

3. Mitomycin C-oligonucleotide adduct as a tool to mutagenize the *ard* gene.

Effective long-term or permanent, heritable inhibition of gene expression might be achieved by targeting a selected gene directly in the chromosomal or viral DNA. Although cellular DNA occurs in a duplex form, it can be expected that under certain conditions the DNA will be accessible for binding by an oligonucleotide:

1. temporary, local unwinding of DNA during replication and transcription.
2. triple helix (strand) formation.

Experimental evidence supports these two possibilities. It has been shown *in vitro* that transcription of the β- lactamase gene by *E. coli* RNA polymerase was specifically inhibited by a oligonucleotide-acridine conjugate complementary to the β-lactamase promoter site (Helene et al., 1985). It is well known that triple helix formation can occur between homopyrimidine oligonucleotides recognizing complementary homopurine / homopyrimidine sequences in the major groove of duplex DNA (Moser and Dervan, 1987). Homopyrimidine oligonucleotides bind in parallel orientation (pyrimidine motif) while homopurine oligonucleotides bind in antiparallel orientation (purine motif) compared to the homopurine strand of the double helix (Sandor and Bredberg, 1994). Subsequent studies demonstrated that the oligonucleotide and DNA strand homogeneity does not have to be strict: purine rich oligonucleotide can have several pyrimidines; corresponding anti-parallel DNA strand has thus to be purine rich (Maher et al., 1991). Rigas (Rigas et al., 1986) demonstrated formation of a stable DNA triple helix *in vitro* between duplex DNA and a complementary 43-mer oligonucleotide catalyzed by Rec A protein.

The binding of the oligonucleotide to its complementary target segment in the duplex DNA is necessary but obviously not sufficient for introduction of site-specific mutation and subsequent inactivation of a particular gene. A functional group has to be attached to the oligonucleotide in order to cross-link the oligonucleotide to the DNA fragment or to introduce other modifications. Several functional groups have been used to cause site-specific cleavage of the target DNA *in vitro* when covalently attached to a sequence specific oligonucleotide. A few of the most elegant examples of the so called "chemical nucleases" are: EDTA-Fe^{3+} (Moser and Dervan, 1987), phenanthroline-Cu^{2+} (Chen and Sigman, 1986; Francois et al., 1988), or porphyrin-Fe^{3+} (Ward et al., 1986). These redox-active metal complexes affect the cleavage by metal-bound or free hydroxyl radicals. It is also important that triple-helix stability can be enhanced since some metal compounds are intercalating agents, f.e. phenanthroline-Cu^{2+} (Helene, 1991). Unfortunately, difficulties arise in trying to use such conjugates *in vivo* because of the high cation concentration required. More promising approach relies on conjugates which reactive groups can be activated by light to create cross-links within a target DNA sequence. Two of these groups are azidoproflavine (Le Doan et al., 1987) and azidophenacyl (Praseuth et al., 1988). These alkylating reagents can cross-link the oligonucleotide to only one DNA strand. However, another alkylating group - psoralen derivatives - can form interstrand cross-links after UV irradiation (Takasugi et al., 1991). Aminotriethyl psoralen conjugated to oligonucleotides targeted against vesicular stomatitis virus mRNA sequences showed virus protein synthesis inhibition in virus infected cells when irradiated (Miller and Ts'o, 1987). In another set of experiments, a psoralen derivative conjugated to the oligonucleotide directed against the promoter region of the NF-KB

transcription factor - chloramphenicol acetyltransferase (CAT) construct - strongly reduced expression of the transferase after the cells were irradiated. Isolation of the plasmid from the irradiated cells clearly showed the two plasmid DNA strands were cross-linked (Helene et al., 1992).

In our experiments we are using a different reactive group: the antitumor drug mitomycin C (Fig.6a).

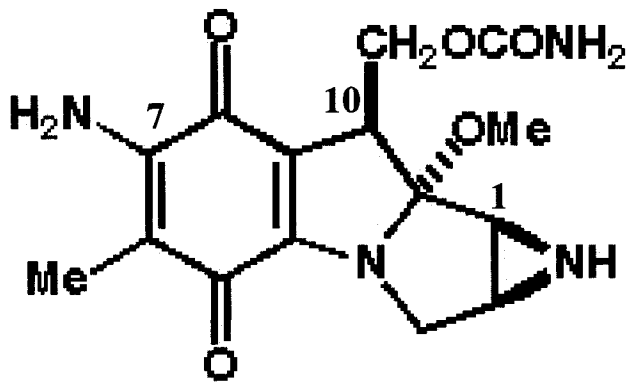

Figure 6a Chemical diagram of mitomycin C (MC).
Carbon atoms are numbered in order to see which of them participate in the cross-linking with DNA. These carbons are #1, if there is only one cross-link and #10, if MC acts in bifunctional activation pathway and forms two cross-links with DNA (see page 21, Fig.6b). An oligonucleotide will be attached to carbon #7 through an aminolink.

Mitomycin C (MC), which is used clinically against cancer cells is able to alkylates DNA preferentially at 5'-d(CG) sequences (Paz et al., 1999). It can be conjugated via $(-CH_2-)_n$ aminolinker to 5'-end of oligonucleotide (Maruenda and Tomasz, 1996). This construct can form cross-linked products with single-stranded DNA under bioreductive conditions

if the oligonucleotide has a sequence complementary to DNA fragments. The hybridization is thus sequence-specific and directs the mitomycin C moiety of the conjugate to chosen CG, which becomes alkylated at the 2-amino group of a guanine base (Fig. 6b, next page). The introduced cross-link is expected to be repaired by the repair system of the organism into which the construct was injected or into which the cross-linked product was transformed (Srikanth et al., 1994). This may lead to a mutation of the DNA target sequence if the error-prone repair system does not repair the cross-linking correctly, for example by substituting a wrong base (nucleotide). It has been shown that mitomycin C is an effective mutagen *in vivo* in *E. coli, Drosophila*, and eukaryotic cells (Fram et al., 1986; Georgiev et al., 1990; Nishiyama et al., 1997). When linked to an oligonucleotide, the non-covalent affinity of this oligonucleotide to its complementary sequence is greatly increased (Chawla and Tomasz, 1988). Also, *in vitro* studies had shown that even without cross-linking the conjugate effectively blocked movement of the replication fork (Basu et al., 1993). MC - oligonucleotide conjugates are shown to be sensitive *in vivo* to both endo- and exonucleases. From studies in tissue culture, it appears that oligonucleotides are degraded mostly by exonucleases (Helene et al., 1985; Zamecnik et al., 1986). To overcome this difficulty chemical modifications of the oligo(dN) could be necessary as in phosphothioates and methylphosphonates. The replacement of the natural β-anomers of nucleoside units by their synthetic α-anomers also confers a high resistance to nucleases (Helene, 1991). Therefore, different types of chemically modified oligonucleotides should be used.

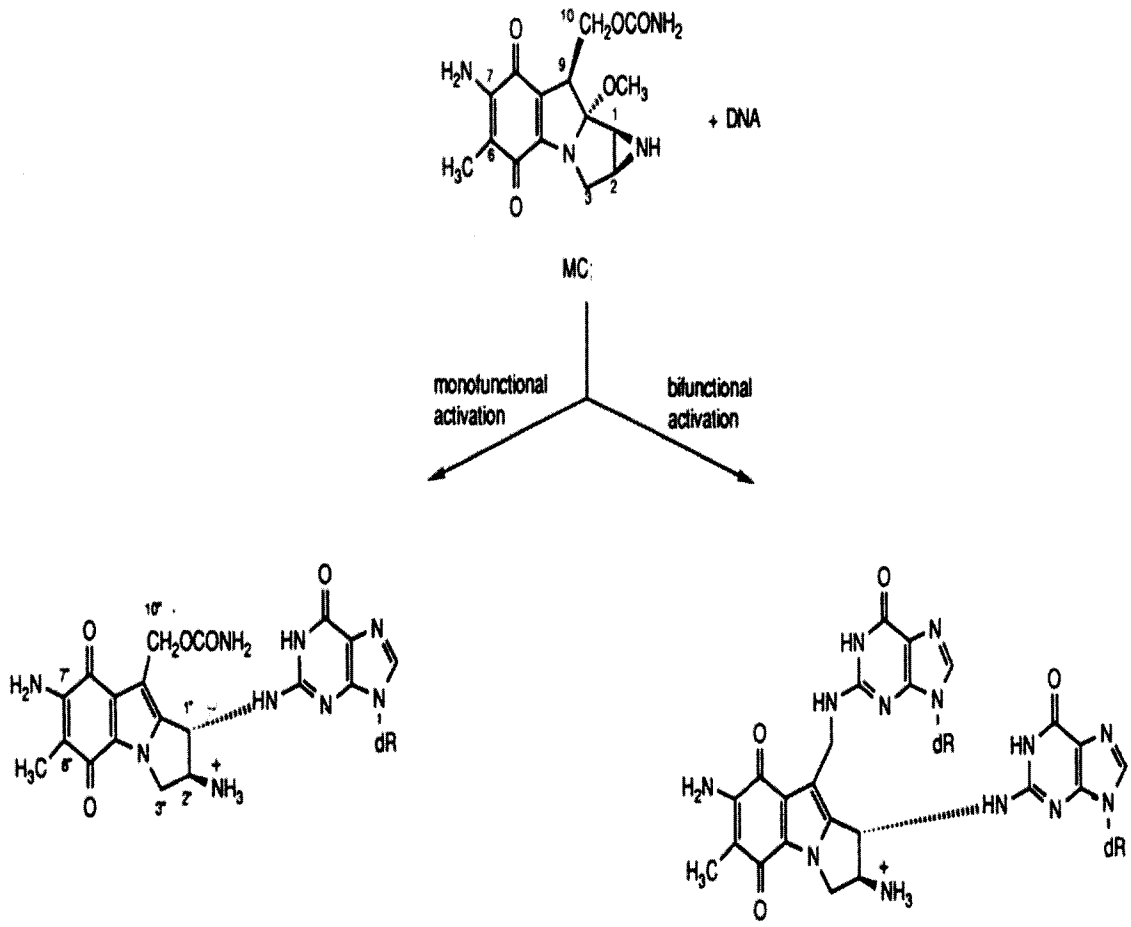

Figure 6b Schematic diagram of MC activation leading to cross-links.
MC forms one cross-link (monofunctional activation) or two cross-links (bifunctional activation) with DNA by alkylating 2-amino group of a guanine base. Modified from (Basu et al., 1993).

4. Ribozyme as a tool to inactivate *ard* mRNA.

RNA catalysis was first described in 1990 with the discovery of the RNA component of RNase P and the group-I intron. This was the first time that biochemical

catalysis had been observed without the presence of protein-based enzymes, and such ribonucleotides were named ribozymes (Birikh et al., 1997). Since then three more classes of ribozymes were described based on their unique characteristics, shape and sequence:

1. the hepatitis delta virus ribozyme
2. hairpin ribozyme
3. hammerhead ribozyme

They are antisense RNA molecules able to cleave RNA at a specific site after binding to it by the binding domains (arms) through Watson-Crick base pairing. *Cis* –acting ribozymes catalyze intramolecularly (self-cleavage) and *trans* – acting ribozymes catalyze intermolecularly.

Their potential for the sequence-specific inhibition of gene expression and their anticipated use as therapeutics has drawn a lot of interest. They have been successfully tested against target sequence *in vitro* mutagenesis (Haseloff and Gerlach, 1992). In recent years, ribozyme-mediated gene inactivation has been explored as a method to effect gene expression in AIDS research (Jackson et al., 1998); a number of investigators has demonstrated the ability of ribozymes to suppress HIV replication (Sun et al., 1997) and to reduce susceptibility to HIV infection in ribozyme-expressing transgenic cells (Andang et al., 1999). Other numerous potential applications for ribozymes are being actively explored, including immunology, neurobiology, analyses of gene function, the development of therapeutics for genetic and other viral diseases.

First successful experiments using ribozyme in *Drosophila* were done by generating transgenic flies carrying a ribozyme targeted against the *fushi tarazu (ftz)* gene (Zhao and

Pick, 1993). These researchers created conditional knock-out mutations by introducing a targeted heat-inducible hammerhead ribozyme. They were able to distinguish two developmental phases of *ftz* function after they had induced timely the ribozyme. This experimental approach is very useful particularly in cases where the functions of genes that are express several times during development are often obscured in the later stages because of disruptions caused by the absence of early gene function (Zhao and Pick, 1993) . Being under the control of time-dependent inducible promoter the ribozyme can be delivered to a specific region and heat-shock activated at a specific time corresponding to a certain developmental stage of an organism. In this way, potential problems with the low expression, time- and cell type (region)-dependent expression of the genes under investigation can be circumvented. These aspects of working with ribozymes are very useful in nAChR research, because the *ard* gene, like other genes encoding the subunits of *Drosophila* nAChR, is characterized not only by time-dependent expression but also is expressed throughout the CNS, and not in other regions. Northern blot analysis done by many *Drosophila* researchers have demonstrated that the transcripts from the genes that encode nAChRs can be detected at all developmental stages starting from mid-aged embryos (10 hrs old, stage13) through adult fly (Jonas et al., 1990; Sawruk et al., 1990; Wadsworth et al., 1988). But these studies have also shown the developmental regulation of the level of nAChR subunit transcripts; they are high during late embryogenesis, in late pupae and in young adults, and decrease during larval life and in aging fly. The periods of high expression of them correlate well with periods of terminal neuronal differentiation and synapse formation in *Drosophila* CNS. Because of the time-dependent expression of the genes and their expression levels, it is important to specify our studies

on the critical regulatory gene function at deferent developmental phases. Ribozyme, with its site- and time-specific action, will fit very well in these studies.

The best understood classes of ribozymes are hammerhead and hairpin ribozymes-named after the approximate shape of their secondary structures (Fig.7 and 8, next pages).

Hammerhead ribozyme is a type of natural catalytic RNA structure that was originally discovered within the satellite RNA of a plant pathogenic virus. Since then, its distribution has been seen to extend to other satellite RNAs, viroids and virusoids, where it participates in the processing of multimers produced during rolling circle replication. The hammerhead catalytic motif consists of three base-paired helices (I-III), connected by two single-stranded regions (loops) and a bulged nucleotide (Fig.9, page 27). The single-stranded regions were found to be invariant, except at position 7, and were presumed to form a conserved catalytic core. In contrast, the base-paired helices (I-III) showed little sequence similarity. In nature, two of the hammerhead's helical arms are terminated by nucleotide loops and thus the ribozyme catalyzes the intramolecular (*in-cis)* cleavage of a phosphodiester bond (Birikh et al., 1997). By separating the catalytic domain from the ribozyme and attaching antisense arms (that can recognize a specific sequence) to the catalytic core, a particular mRNA stretch can be targeted and cleaved in the intermolecular (*in- trans)* fashion. Therefore, almost any RNA may be targeted if it displays favorable secondary structures and proper target sequence.

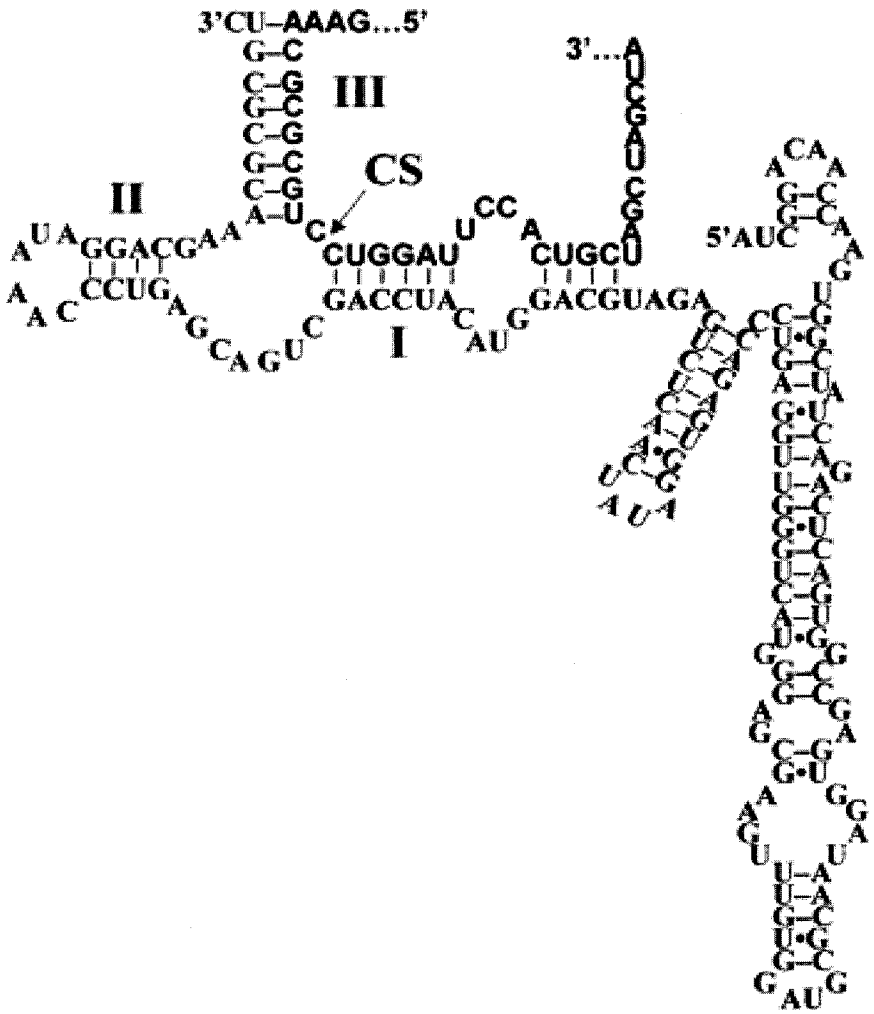

Figure 7 Predicted secondary structure of a hammerhead ribozyme (associated with the SMα DNA family from the human parasite *Schistosoma mansoni*) and the substrate RNA. The ribozyme with its elongated part towards the bottom of the page is shown in lighter fonts. The substrate RNA is on top, in darker fonts. The hammerhead is in the I / III format (I, II, and III are ribozyme helices) and cleaves at SC site indicated by arrow (Vazquez-Tello et al., 2002).

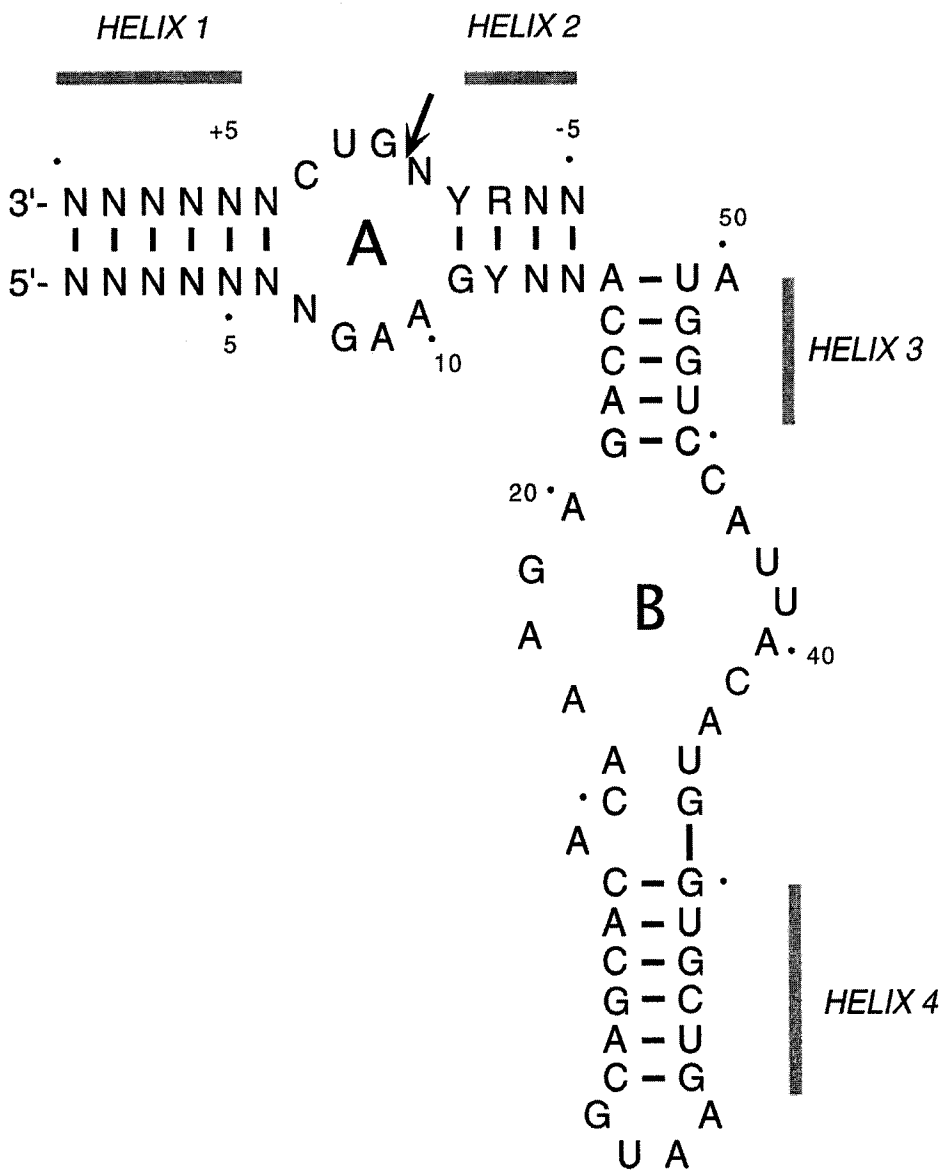

Figure 8 Predicted secondary structure of the hairpin ribozyme-substrate RNA complex. The arrow marks the cleavage site, and dashes indicate Watson-Crick base pairs. Ribozyme nucleotides are numbered 1-50. Substrate nucleotides are numbered consecutively from the cleavage site. *A* and *B* indicate the two internal loops within domains A and B of the ribozyme - substrate complex. Helices are numbered 1-4. The figure is from (Yu et al., 1998).

For hammerhead ribozyme this sequence is 5'-↓GUH-3' (where H represents C or A or U), with GUC triplet being optimal (Haseloff and Gerlach, 1992), and for hairpin ribozyme the optimal sequence is defined as 5'-RYN↓GUC-3' (where R could be A or G; Y represents C or U; N is any nucleotide).

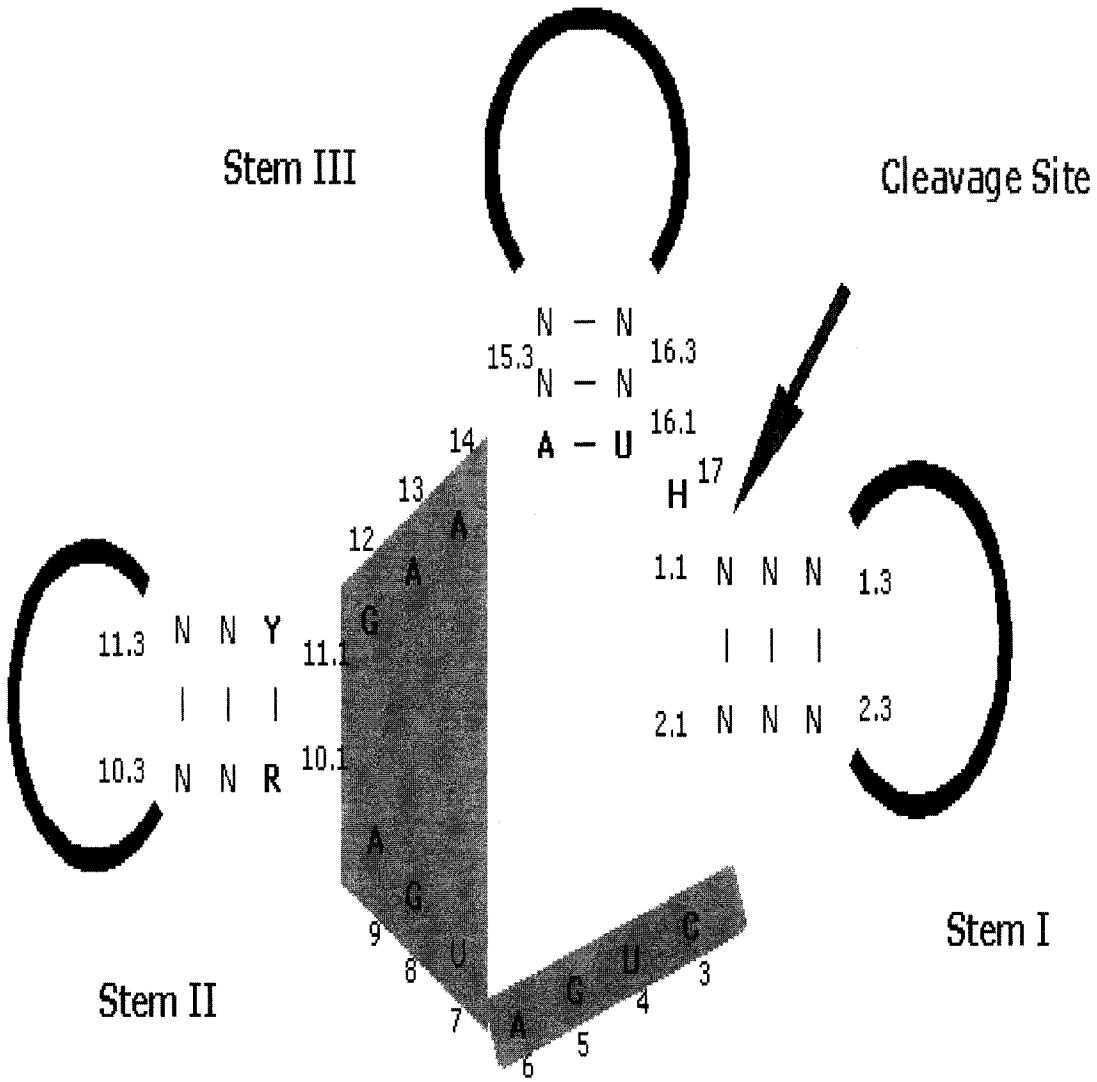

Figure 9 Schematic diagram of the hammerhead ribozyme based on the X-ray crystal structure.
Conserved nucleotides are shown in bold. N represents any nucleotide; H stands for C, U or A nucleotide. Cleavage triplet (optimal is GUC), here $NU_{16.1}H_{17}$, is at the end of Stem III (Birikh et al., 1997).

Other RNA substrates may be cleaved but with lower activity (Yu et al., 1998). Some researchers indicated that BN↓GUC (B is C or G or U) sequence gives efficient cleavage by hairpin ribozyme.

Ribozymes share certain characteristics with antisense oligodeoxynucleotides, which are used for the same purpose. However, because of their catalytic power, ribozymes are expected to be more efficient than antisense oligonucleotides (Birikh et al., 1997) since a single ribozyme molecule can inactivate many molecules of the target RNAs. This is dependent on the secondary structure of the mRNA around the target site and also on the ribozyme structure. There is a set of rules, dealing with this and other problems facing researches in designing proper ribozyme against specific target RNA, proposed by Zhao and Lemke (Zhao and Lemke, 1998):

1. *Target sequences predicted to be embedded within a long base-paired stem (double-stranded region) are to be avoided.* For reliable design, these unfavorable regions must be predicted to appear in both minimum and near minimum free energy structures calculated by a conformation energy analysis computer program, such as MFOLD, RNAdraw or other RNA folding program based on free energy minimization.
2. *For hammerhead ribozymes, the selected cleavage site should fall within a loop that is not smaller than four nucleotides.* A loop in the target is essential for the formation of the hybridization complex. However, a large loop (>25nt) should be avoided, since it may be involved in the formation of a tertiary RNA structure.
3. *Short antisense segments (7-12 nucleotides for each arm of a hammerhead ribozyme) are better than longer ones.* Long antisense segments have a

significant propensity to form stable secondary structures on their own, so they should be avoided. Also, too long arms may bind too strong to the target RNA and the ribozyme will cleave both correct and incorrect targets indiscriminately; turnover number may decrease too. On the other hand, if the length of the binding arms is very short, the rate of dissociation of the ribozyme from the target RNA may exceed the rate of cleavage, resulting in poor efficiency (Rossi, 1997). For hairpin ribozyme, the optimal length of arm (helix) I is 4nt and of helix II is 5-9 nt (Hampel et al., 1997).

Target sequences within the first several hundred nucleotides of a large RNA molecule are favored. The predicted secondary structures in this region are more likely to form in a nascent mRNA molecule and are less likely to be affected by the structure of the 3' region of the mRNA.

B. Specific Aims

Nicotinic acetylcholine receptors are ligand-gated ion channels important in transmission of signals between neuronal cells in central and peripheral nervous systems. They influence synapse development and modulation of neurotransmitter system. nAChRs are pentamers variously composed of alpha and beta subunits. Different subunits vary in their distribution and properties; α subunits have ligand-binding properties and β subunits are thought to be structural parts of nAChR.

One of the major research in our laboratory concentrates on the investigation how mutations and changes in the expression of the *ard* gene, encoding one of the subunits of

neuronal nicotinic acetylcholine receptors in *Drosophila melanogaster*, can influence the structure, development, regulation and functioning of this receptor, and its effect on the functioning of *Drosophila* nervous system.

There is more and more evidence that links malfunction and alterations in nAChR number to such diseases and disorders like Parkinson's and Alzheimer's, schizophrenia, attention deficit-hyperactivity disorder (ADHD), mood disorders, and others affective disorders. Since nAChRs are conserved from *Drosophila* to humans, studying them in the fruit fly could lead to better understanding of the molecular mechanisms involving nAChR in humans and contribute to battling these various disorders of mammalian nervous system caused by nAChR abnormalities.

The main goal of this study is to disrupt the expression of the *ard* gene that encodes ARD subunit of the nAChR in *Drosophila melanogaster*. This is a structural subunit important in proper assemble of the nicotinic receptor. Our laboratory want to investigate how nAChR will function, how it will be distributed throughout the central nervous system and how it influence the neurotransmitter signal pathways in *Drosophila* when ARD protein becomes synthesized in insufficient amounts, if at all. Disruption of the expression of the *ard* gene may also cause some morphological changes in the nervous system, such as gain or loss of neurons, abnormal positioning of neurons, defects in axon pathways, abnormal neuron morphology and abnormal distribution of ARD subunits. By knocking down the *ard* gene or destroying its mRNA these phenomena could be studied and elucidated.

In particular, we want to introduce a site-specific mutation into the *ard* gene via organism's repair system that would cause a mutation by imperfect repair of cross-linking

made between mitomycin C-oligonucleotide conjugate and organism's DNA. The strategy for using the conjugate is that the oligonucleotide part of it will be complementary in sequence to the DNA stretch of the *ard* gene, so that after hybridization mitomycin C, known DNA cross-linking agent and mutagen, will be poised to form cross-link with the selected nucleotide.

In general, site-specific mutations are very difficult to achieve. Most form of mutagenesis do not permit targeting the event to a predetermined gene, as in knock-out technique with mice (Greenspan, 2004). Using free chemical mutagens not linked to any oligonucleotide sequence leads to random mutations, scattered around the genome. This makes it practically impossible to find out how many and where all mutations were made, and which mutation is responsible for which phenotypic change. Site-specific mutation eliminates these uncertainties. It can help to unravel the function of a gene under investigation and its relationship to a certain phenotype. In spite of finishing sequencing of whole *Drosophila* genome the functions of large number of its genes are still unknown. Employing targeted mutations (with, for example, MC-oligonucleotide construct as a tool) would greatly speed up deciphering the functions of scores of genes or groups of genes in *Drosophila.* In other organisms, particularly in those on higher evolutionary level than fruit fly, site-specific mutations can bring similar, and many more, benefits. Being able to cause targeted mutation in practically any part of a gene would allow "probing" the gene for important regulatory sequences involved, for example, in gene replication or transcription, like promoter region, enhancer sequences, etc. This could lead to the opportunity of the modulation of gene expression; upregulation or downregulation of a gene. It would wide open new horizons in medicine for gene

therapy: deleterious gene products could be eliminated, or significantly reduced, and beneficent products could be increased by the over-expression of a certain gene. Aberrant genes could be silenced. Many conditions, disorders, and diseases related not only to the nicotinic receptor but to the broad range of improper gene expressions, could be alleviated or cured. Therefore, a simple way of making site-specific mutations could bring unlimited benefits.

Specific aims that will lead to the fulfillment of the objective of the introduction of the targeted mutation into the *ard* gene , using MC-oligonucleotide conjugate, can be formulated as follows:

a. design and prepare MC-oligonucleotide conjugates

The design has to take into account unknown positioning of the aminolinker part of the conjugate carrying mitomycin C moiety for "attack" against target G residue. Therefore, different length conjugates have to be designed; this can be made by varying the length of the oligonucleotide part of the construct.The adducts will be generated according to the information supplied by Prof. Maria Tomasz from Chemistry Department, Hunter College.

b. produce cross-linking *in vitro* and optimize its conditions using M13mp18 DNA

The cross-linking reaction is rather difficult one. The conjugates used in this reaction disintegrate during storage after several months even if kept at -70^0C. Also, acidic conditions favor disintegration. This puts certain restraints on the reaction conditions. The mitomycin C moiety of the adduct has to be first reductively activated to

form a cross-link. This requires a reductant, reducing enzyme, and constant steady flow of argon gas through the reaction tube to give needed anaerobic environment.

Optimization experiments will be done on single-stranded M13mp18 vector. Different length conjugates will be used in the cross-linking reactions in order to find the adduct which will give the highest yield of cross-linked product. The reaction conditions, volume, argon flow, ratio of the reactants, and amount of the reductase will be varied to achieve a high yield. Phosphoimaging techniques will be employed to visualize the cross-linked products, compare their relative amounts, and estimate the yields.

c. introduce mutation into M13mp18 DNA and screen for it

The repair of the cross-link between the MC-oligonucleotide conjugate and the 5'-d(CG) in the target fragment of M13mp18 DNA can lead to a mutation in this fragment. *E. coli* repair system is capable of repairing cross-linking in DNA (Min et al., 1996). Therefore, after the cross-linking reaction, its product will be transformed into *E. coli* strain JM101 which repair system is intact. Transformed cells will be plated with X-gal and IPTG to identify mutated DNA. Screening bacteriophage plaques with radiolabeled oligonucleotide probes complementary to the DNA target sequence containing possible mutations will be performed. Further, direct transformation with the conjugate and M13mp18 DNA will take place without cross-linking step *in vitro*; the cross-linking will depend on the intracellular activation of the MC-oligonucleotide conjugate.

d. introduce mutations in *Drosophila white* gene

Before we employ MC-oligonucleotide construct against *Drosophila ard* gene, we propose to use it initially targeted against *Drosophila white* (w) gene. A good target for the MC-oligonucleotide conjugate is a conserved Gly-Lys sequence. Mutation of this motif is known to create a white eye color phenotype that can be easily identified. Preceding the glycine is an alanine - the nucleotide sequence is GCC GGA AAG for the three amino acids, generating the required 5'-d(CG) fragment. The conjugates will be injected into *Drosophila* eggs circumventing a potential problem of construct delivery. Also, during the first 1 hour after egg laying the nucleus of the *Drosophila* egg undergoes fast eight syncytial cleavages before cell formation begins. During this period the replicating DNA is fully accessible for interactions with the injected conjugates. I will look for white eyed flies in G_1 generation.

e. introduce mutation in *Drosophila ard* gene

If the mutagenesis by MC-oligonucleotide construct is feasible in *Drosophila* - that is, if the *white* gene becomes mutated by the construct - we will try to introduce mutation, using MC-oligo construct, in the *ard* gene.

Another major goal we want to attain is to destroy, or significantly reduce the *ard* mRNA by ribozymes. The choice of the experimental system rests on the availability of germline transformation mediated by P-elements. Transposable P-element can integrate (transpose) into a host chromosome when transposase will catalyze the reaction; DNA sequence cloned between the terminal repeat sequences of a P-element will be integrated too. This way, the ribozyme DNA can be incorporated into a host chromosome and

transcribed. Transcriptional activation depends on heat-shock, since ribozyme DNA sequence is under control of a heat-shock promoter. *Drosophila* is a perfect organism for this type of experiments with all sophisticated genetic tools available and ease of germline transformation by using microinjections to introduce P-element with subcloned ribozyme construct into fly embryo.

Specific aims that will lead to the execution of the above objective of the disruption of the *ard* mRNA can be formulated as follows:

f. predict secondary structure of the *ard* mRNA and find target sequences in it

Prediction of the *ard* mRNA secondary structures will be done using free energy minimization computer program. Then, favorable target sequences will be chosen (employing Zhao and Lemke set of rules described before) to assure efficient cleavage by the ribozymes.

g. design and prepare ribozyme constructs

Hammerhead and hairpin ribozymes will be designed to target specific favorable sites in the *ard* mRNA. Again, the design will take into account Zhao and Lemke rules. cDNA templates containing the ribozyme sequences will be constructed and subcloned into a plasmid, denoted as pP{CaSpeR-hs}, so that the ribozyme DNA transcription will be under the control of a heat-shock promoter, present in the plasmid.

h. generate transgenic flies

pP{CaSpeR-hs} plasmid with the cloned ribozyme DNA will be microinjected into *Drosophila* **yw** mutant embryos. *Drosophila* crosses will be done (as described in the Materials and Methods) to find transformants and establish the P-element insertion linkage with *Drosophila* chromosome.

i. heat-shock activate the ribozyme and disrupt the *ard* mRNA

Heat-shock will be applied to the *Drosophila* transgenic embryos. The ribozyme DNA sequence, being under the control of the heat-shock promoter, will be transcribed into the ribozyme and cleave its target *ard* mRNA. The heat shock will be applied just before the first *ard* mRNA expression peak.

Results of these experiments can contribute towards better understanding of the structure and role nAChR plays in nervous system not only in *Drosophila* but also in other organisms, including humans; the relationships between neuronal nicotinic acetylcholine receptor and neuropsychiatric disorders plaguing growing part of our population may be faster elucidated.

II. MATERIALS AND METHODS

A. Materials

1. Sources of materials

Mitomycin A was a generous gift form Prof. Maria Tomasz, Hunter College, Dept. of Chemistry. Aminolinker oligonucleotides, complementary strands of the oligonucleotides for the ribozyme constructs, primers for DNA sequencing, oligonucleotide for plaque lifts were synthesized in the Synthesis and Separation Core Facility at Hunter College. Aminolinkers [NH_2-$(CH_2)_{12}$-] were obtained as the corresponding phosphoramidates from Applied Biosystems and Glenn Research. [α^{32}P]dATP cordycepin was from Perkin-Elmer. Restriction enzymes, DNA ligase and polymerases, aprotinin, antipain, ϵ-amino cuproic acid, benzamidine HCl, bacitracin, trypsin inhibitor, IAA, Protease Inhibitor Cocktail for mammalian tissues, molecular weight protein color marker, acrylamide, bis-acrylamide, TEMED, luminal, p-Coumaric acid, β-mercaptoethanol and some oligonucleotides with aminolinker were obtained from Sigma. Terminal transferase was ordered from Boehringer Mannheim. Maxi-prep kit was obtained form Qiagen. NENSORB 20 cartridges for plasmid purification were obtained from NEN Research Products. Renex 690 was ordered from ICI. DEAE-cellulose column (Whatman DE52), Sephadex G-25 column, 2',5'-ADP Sepharose 4B column were from Pharmacia. (C_4) Dynamax-300A column was from Rainin. SuperSignal West Pico Chemiluminescent Substrate and BCA Protein Assay Kit were obtained from Pierce. Polyclonal anti-rabbit antibody was ordered from Bio-Synthesis, Inc. Nitex nylon membrane was from Sefar America. Halocarbon oil was from Halocarbon Products. PVDF membranes and transfer apparatus for immunobloting were from Immobilon.

2. Bacterial strains and plasmids

E. coli strains: (1) XL-1 Blue: *recA1 endA1 gyrA96 thi-1 hsdR17 supE44 relA1 lac* [F' *proAB lacI*^{q} *ZΔM15* Tn*10* (Tet^{r})]. (2) JM101: *supE thi-1* Δ(*lac-proAB*) [F'*traD36 proAB lacI* ^{q} *ZΔM15*]. Vectors used were pP{CaSpeR-hs} (Rubin and Spradling, 1983), pπ25.7wc (Karess and Rubin, 1984), and M13mp18. Both bacterial strains and M13mp18 vector were obtained from Stratagene. pP{CaSpeR-hs} and pπ25.7wc helper plasmid were a gift from Dr. Leslie Pick, Mount Sinai Medical School.

3. *Drosophila* strains

The *white* mutant strain used in this study was Oregon R. For P-element germline transformation **yw** mutant strain was used, in which flies had yellow body color and white eye color. w^{1118} flies (white eye color) were used for crosses with flies that eclosed from larvae when MC-oligonucleotide constructs were injected into wild-type *Drosophila* embryos.

The following balancer stocks were used to establish insertion linkages with *Drosophila* chromosomes: (1) y^{1} w^{1} sn^{3} f^{36a} ado^{4P1} / FM7a, (2) w^{1118}; EcR^{225} / CyO, (3) w^{1118}; TM3, Sb^{1} / CxD. For a description of marker genes and balancer chromosomes go to the Internet website of Bloomington Drosophila Stock Center at Indiana University: http://flystocks.bio.indiana.edu. All *Drosophila* stocks needed in this research were ordered from this center.

B. Generation of mitomycin C-oligonucleotide conjugates

1. Synthesis of oligonucleotides with aminolinker for the conjugates

Generation of mitomycin C-oligonucleotide conjugates was carried out according to Maruenda and Prof. Maria Tomasz (personal communication), with small modifications. The oligonucleotides were synthesized on a 1.0 μmol scale on an Applied Biosystems 380B automatic DNA synthesizer at Hunter's Sequencing Facilities. From the commercially available aminolinkers n=12 was chosen as close to the optimal aminolinker length (Maruenda and Tomasz, 1996). Aminolinkers [NH_2-$(CH_2)_{12}$-] were obtained as the corresponding phosphoramidates (Applied Biosystems, Glenn Research). The synthesis of the 5'-end modified aminolinker oligonucleotide was requested 'trityl on'. The synthesis cycle was modified and included extension of the last phosphoramidite coupling step to 3 min and coupling twice during the attachement of the aminolinker. This ensured 95-100% yield. The monomethoxytrityl (MMT)-protected aminolinked oligonucleotide was treated with 30% ammonium hydroxide for 16-18 hrs at 55^0C. Next, the oligonucleotide solution was rotoevaporated and the dry solid was dissolved in 100 μl of distilled water, and transferred to a microcentrifuge tube. 10 μl of 5M NaCl was added and mixed by gentle tapping. 330 μl of ice-cold 100% ethanol was added, mixed by gentle vortexing, and the tube was placed for 1 hr or longer at -70^0C. Centrifugation followed at 1500 rpm for 15-30 min at 4^0C. The supernatant was aspirated off without disturbing the pellet. 1.0 ml of 95% ethanol at RT was added, the tube was inverted several times without disturbing the pellet, and centrifuged as before. The supernatant was aspirated off, the pellet dried and 200 μl of 80% acetic acid, RT, was added to remove the trityl group. After 1 hr, the centrifugation was done as before, the solvent

removed, the pellet dried, and the ethanol precipitation was done once more. The deprotected and purified aminolinker oligonucleotide was dissolved in 100 µl of distilled water. O.D. readings at 260 and 280 nm were taken to check the purity and the amount of the oligonucleotide. Reversed-phase high performance liquid chromatography (HPLC) was employed to check the oligonucleotide for purity. 5 µg of the oligonucleotide was mixed with 10 µl of solution A (0.1M TEAA, pH 7.5) and injected into Rainin (C_4) Dynamax-300A, 10 x 250 mm size column. Solutions A and B (60%Acetonitrile in A) were used to elute the sample; 2 ml/min flow rate; gradient for B was: 0% to 60% (30min), 60% for 10min, 60% to 20% (5min).

2. Attachment of mitomycin A to oligonucleotide with aminolinker

The condensation of mitomycin A with an aminolinker oligonucleotide was performed in 0.1M TrisCl buffer, pH 9.0, at 31^{0}C, in the dark, over the period of 16-24 hrs, depending on the reaction temperature, with constant stirring. 67 µg of the oligonucleotide (21-mer) reacted with a 60-fold molar excess (210 µg) of MA dissolved in methanol. After all MA was used up in the reaction tube within several hours, about ½ of the starting amount of MA was added to drive the reaction to a completion. During monitoring the course of the reaction and separation of the final product reversed-phase HPLC was employed, and the gradient for solution B was as followed: 7.5% to 10% (10min), 10% to 20% (20min), 20% to 25% (5min), 25% to 50% (30min), 50% to 100% (5min), 100% to 7.5% (5min). The conjugates were stored in 0.01M Tris, pH 7.5, -70^{0}C.

C. Formation and optimization of cross-linking *in vitro*

1. Large-scale preparation of single-stranded M13mp18 DNA

Single-stranded M13mp18 DNA was prepared on large scale from infected *E. coli* host strain XL-1 Blue by polyethylene glycol precipitation and CsCl gradient according to the protocol in "Sequencing support service, USB, 1994, pp. 1.2-1.5 (1994), with many modifications. 5 ml of 2 x YT medium was inoculated with a single colony of *E.coli* strain XL-1 Blue to grow o/n at 37^0C, in a shaker. 100 ml of 2 x YT medium was inoculated with 200 μl of a fresh o/n culture to grow for 16 hrs at 37^0C, in a shaker. 2000 ml of the same medium was inoculated with the 25 ml culture from previous night, grown for 1-2 hrs, and M13mp18 stock was added. After 6-8 hr growth, centrifugation took place for 15 min, 12000 rpm, 4^0C. The supernatant was transferred to the centrifuge tubes and the centrifugation was repeated. The new supernatant was pour into a 2 L flask, 120 g of NaCl and 120 g of PEG 8000 were added, stirred at 4^0C until the PEG was completely dissolved. This mixture was left at 4^0C for 2 days so that the M13 vector could visibly sediment. The centrifugation was repeated, pellet was resuspended in 30-40 ml of 15 mM KPO_4, pH 7.5, 10 mM NaCl, 20 mM NH_4Cl buffer, and recentrifuged at 4000 rpm, 5 min, in a HB-4 rotor. The resuspension and recentrifugation were repeated two more times. The total volume of the M13 vector suspension was 60 ml.

CsCl step-gradients were prepared in swinging-bucket ultracentrifuge tubes as follows:

a) CsCl solutions were prepared with densities of 1.2, 1.3 and 1.4 (g/ml) in 50 mM TrisHCl, pH 7.5, 10 mM $MgCl_2$, 50 mM NaCl. For 1.2 g/ml, 13.8 g of CsCl was added to 50 ml buffer; for 1.3 g/ml, 20.2 g of CsCl was added to 50 ml buffer; for 1.4 g/ml, 26.9 gm of CsCl was added to 50 ml buffer.

b) 10 ml of 1.2 g/ml solution was placed in a centrifuge tube. Using a syringe with a long needle this solution was underlaid with 10 ml of 1.3 g/ml solution, and next with 8 ml of 1.4 g/ml solution. 6-12 gradients were required to purify all M13 vector preparation.

c) samples (10 ml of the vector preparation) were overlaid on top of the three-step gradients. The centrifugation was done for 16 hrs at 24000 rpm, 20^0C, in SW 28 rotor. The vector band was collected into a syringe. After combining all vector bands dialysis was done twice against 500 ml of TE buffer at 4^0C, 24 hrs each to remove the CsCl with gentle stirring. Phenol extraction followed and next phenol/chloroform extraction was done four times. Final extractions (three times) with one volume of chloroform each completely removed the phenol. Dialysis was performed 3 times (24 hrs each) against 1.5 L of TE buffer. The yield was 5.7 mg of pure DNA.

2. 3'-end labeling of MC-oligonucleotide conjugate with cordycepin

140 pmol (1μg) of MC-oligonucleotide conjugate (21-mer) was placed in a microcentrifuge tube containing 2.5 mM $CoCl_2$, 100μCi [α^{32}P]dATP cordycepin, 8 μl of 5 x reaction buffer [1 M potassium cacodylate, 125 mM TrisHCl, 1.25 mg/ml BSA: pH 6.6], 5 μl H_2O, and 50 units of terminal transferase; total volume was 40 μl. The reaction was incubated for 2 hrs at 37^0C and stopped by putting on ice.

3. Purification of cordycepin-labeled conjugate

The NENSORB 20 (NEN Research Products) cartridge was packed with the resin and pre-equilibrated by rinsing first with 2 ml of 100% methanol (1 drop/2 sec) and

second, with 2 ml of the Reagent A [0.1 M TrisCl, 10 mM TEA, 1 mM disodium EDTA, pH 7.7]. Labeled conjugate was diluted to 400 µl in the Reagent A, and loaded on the cartridge after which washing with 3 ml of the Reagent A took place. The washing continued with 3 ml of 10 mM TEA, pH 7.5; water wash was excluded because of its low pH (5.6-5.7) that could degenerate the conjugate. Elution was done with 5% butanol diluted with 10 mM TEA, pH 7.5. The effluent containing cordycepin-labeled conjugate was collected in 200 µl fractions in Eppendorf tubes.

4. Preparation of microsomal NADPH-cytochrome c (P-450) reductase from rat liver

The above procedure was done according to the protocol "Solubilization and Purification of Rat Liver NDPH-Cytochrome c (P-450) Reductase" (Yasukochi and Masters, 1976) with small modifications. 40 rats were sacrificed by decapitation and the livers were rapidly removed and perfused with 100 ml of ice-cold 0.9% NaCl solution. Tissue homogenates (20%, w/v) were prepared in 0.25 M sucrose containing 5 mM Tris buffer, plus 0.5 mM EDTA, pH 7.5, in a homogenizer. The homogenate was centrifuged at 1,900 x *g* for 10 min. and the supernatant was recentrifuged at 14,620 x *g* for 15 min. The resulting supernatant was centrifuged at 30,000 rpm for 60 min and the pellet was resuspended in 0.1 M sodium pyrophosphate buffer, pH 7.4, and centrifuged as last time. The microsomal pellet was resuspended to a protein concentration of 14 mg/ml in 10 mM Tris-acetate buffer, pH 7.4, containing 20% glycerol and 0.1 mM EDTA, and stored at -70^{0}C. The microsomal suspension, 50 ml, was mixed with 25.5 ml of 5% sodium cholate

and 25.5 ml of 10% Renex 690 and stirred at low speed for 1hr, 4^0C (this temperature was used for the rest of the reductase preparation). The supernatant fraction was applied to a DEAE-cellulose column (Whatman DE52, 3.0 x 16 cm) previously equilibrated with 0.025 M Tris buffer, pH7.7, containing 0.8% Renex 690, 0.05 mM EDTA, and 0.05 mM DTT, flow rate 1 ml/min. The column was washed with 400 ml of the above equilibration buffer. The reductase was eluted with 1 L of a similar solution in which KCl concentration was increasing from 0 to 0.35 M in a linear gradient. The active reductase fractions were concentrated in an Amicon concentrator and applied to a 2',5'-ADP Sepharose 4B column (1.7 X 12.4 cm) previously equilibrated with 10 mM potassium phosphate buffer, pH 7.7, containing 20% glycerol, 0.1% Renex 690, 0.02 mM EDTA, and 0.2 mM DTT. The column was washed with 150 ml of 200 mM potassium phosphate buffer, pH 7.7, containing 20% glycerol, 0.1% Renex 690, 0.4 mM EDTA, and 0.2 mM DTT. After the column was washed with 40 ml of equilibration buffer, the reductase was eluted batchwise with 150 ml of a similar solution containing 5 mM 2'-AMP. The reductase fractions were concentrated in an Amicon concentrator and passed through a Sephadex G-25 column to remove unbound 2'-AMP. The reductase was then eluted with 0.3 M potassium phosphate, pH 7.7, containing 20% glycerol, and 0.1% deoxycholate. At the end of this purification, the reductase was dialyzed against 4 liters of 50 mM potassium phosphate buffer, pH 7.7, containing 20% glycerol, 0.1 mM EDTA, and 0.1% sodium deoxycholate.

5. NADPH-cytochrome P-450 reductase quantitation

The standard procedure of modified Lowry assay (Peterson, 1977) was used.

Reaction to determine standard (BSA) curve concentration: BSA was diluted in distilled water to 50 ng/µl and for each reaction 20 µl of diluted BSA was added to water (starting from 0) so that total volume was 200 µl. These 200 µl were mixed in an Eppendorf tube with the same volume of Reagent A and vortexed, set aside for 10 min, RT, after which 100 µl of Reagent B was added, and immediately vortexed shortly to mix the content of the tube, 500 µl total volume. After 30 min standing at RT, O.D. readings at 750 nm were taken and the curve was drown. The same reaction conditions were employed for the measuring of the absorbance of the reductase sample, substituting the reductase for BSA. The reductase concentration was then read from the standard curve.

Reagents:

1. CTC (0.1% w/v $CuSO_4$ and 0.2% Potassium Sodium Tartrate, 50 ml total, mixed and stirred when 50 ml of 10% Na_2CO_3 was added slowly, to have 100 ml total)
2. Reagent A: 1 vol CTC + 2 vol of 5% w/v SDS + 1 vol of 0.8 M NaOH,
3. Reagent B: 1 vol of 2 N Folin-Ciocalteu phenol + 4 vol of H_2O

6. Determination of NADPH-cytochrome P-450 reductase activity

Eppendorf tube containing 300 µl of potassium phosphate buffer, pH 7.7, 0.1 µmol of EDTA, 40 nmol of horse heart cytochrome c, 0.4 µmol of the reductase, and H $_2$O, total volume of 1.0 ml, was incubated for 3 min at 30^0C. Next, 83 µg of NADPH was added to initiate the reaction, and O.D. readings at 550 nm were taken every 30 seconds when the diferences between the consecutive O.D. readings were approximately the same. The reductase activity was determined from the formula below:

$$\text{units/mg enzyme} = \frac{\Delta A_{550}/\text{min reaction} - \Delta A_{550}/\text{min Blank}}{(21)(\text{mg enzyme/ml Reaction volume})}$$

where ΔA is change in absorbance

(21) is millimolar extinction coefficient between oxidized and reduced cytochrome c

7. Cross-linking of MC-oligonucleotide conjugate to ss(c) M13mp18 DNA

0.62 pmol of ss(c) M13mp18 DNA in TE buffer, pH 7.5, was placed in an Eppendorf tube and dried by rotoevaporation, after which 1.86 pmol of the conjugate in 30 µl of 0.01 M Tris, pH 7.5, was added and the Tris concentration was adjusted to 0.1 M. The reaction tube was put into a 0.5 L beaker filled with water at 70-80^{0}C and set aside in dark for approximately 1 hr, until the water reached room temperature to allow hybridization of the conjugate to the complementary DNA sequence. 20 pmol of NADPH dissolved in 0.1 M Tris, pH 7.5, was added and the reaction was flushed with argon for 30 min. 0.13 units of the NADPH-cytochrome P-450 reductase were injected into the reaction tube, total reaction volume 60 µl in 0.1 M Tris, pH 7.5. The reaction was run in dark under bubbling with argon for 45 min, 37^{0}C. After this, the reaction tube was put for 10-15 min at 70-80^{0}C to inactivate nucleases present in the reductase sample.

D. *In vivo* experiments in *E. coli*

1. Preparation of Frozen Storage Competent Cells

Preparation was done as described in the published protocol #3, pp.123-125, (Glover, 1985). Several colonies of JM101 were picked off 14-16 hrs old SOB agar plate and dispersed in 100 ml SOB medium. Incubation at 37^{0}C was done in a shaker, 200 rpm,

until cell density was 4-7 x 10^7 ($O.D._{600}$=0.040-0.070). The culture was collected into 50 ml polypropylene centrifuge tubes and chilled on ice for 10-15 min. Centrifugation followed at 3000 rpm for 15 min, 4^0C. Pelleted cells were drained thoroughly and resuspended by moderate vortexing in a volume of RF1 solution, that was 1/3 of the volume collected, and incubated on ice for 15 min. Centrifugation was repeated and the cells were resuspended in RF2 solution to 1/12.5 of the original volume. Incubation on ice for 15 min was repeated, aliquots were distributed into chilled Eppendorf tubes and the competent cells were used immediately in transformation.

2. Preparation of single-stranded DNA template for sequencing

Single-stranded DNA template for sequencing was prepared from plaque on small-scale by the method described in M13 cloning / dideoxy sequencing instruction manual, pp.44-49 involving PEG / NaCl precipitation, phenol / chlorophorm extraction, and final ethanol precipitation. The presence of the template and its quality was checked by agarose gel electrophoresis and UV spectroscopy.

3. Screening for a mutation (plaque lifts)

Screening bacteriophage plaques was done by hybridization of radiolabeled oligonucleotide probe to target DNA sequence and plaque lifts as described in "Molecular cloning: a laboratory manual"(Sambrook et al., 1989), pp. 15.68-15.71, with some modifications.

JM101 cells transformed with M13mp18 extension product carrying possible mutations were plated on SOB plates with top agarose and lawn cells. Incubation was done o/n,

37^{0}C. The plates with plaques were kept at 4^{0}C. The plaques were transferred to 82 mm nitrocellulose filters which were let dry well for 30-40 min. Dry filters with the replica plaques were put for 5 min, RT, on a 3MM filter paper soaked in 0.5 M NaOH / 1.5 M NaCl solution. Next, the filters were transferred for 5 min, RT, to another 3 MM filter paper soaked in 1.0 M Tris-Cl, pH 7.5 / 3 M NaCl. The filters were then washed in 2 x SSPE solution for 30-60 seconds, let dry, RT, and baked at 80^{0}C for 1.5 hr in vacuum oven. Baked filters were washed again in 2 x SSPE solution for 2-3 min, RT, face up, and prehybridized for 2-3 hrs in a prehybridization solution, 30^{0}C. Hybridization in a hybridization solution followed with a radiolabeled probe, 10^6 cpm / ml of solution, 30^{0}C, o/n. Next day, the filters were washed twice in 6 x SSPE solution, 12 min each, RT, and checked for radioactive background. Moist, but not too wet filters were wrapped up in a plastic wrap and exposed to a Kodak X-ray film for 2.5 hrs. The film was developed. Filter wash (each time 5^{0}C higher) and autography were repeated until the wash reached melting temperature for the hybridized probe.

Solutions

1. Prehybridization solution: 6 X SSPE, 0.25% SDS, 5 x Denhard's, 100 μg/ml sonicated, boiled herring sperm DNA.
2. Hybridization solution: as above, except yeast tRNA concentration replaced sperm DNA.

E. *In vivo* experiments with *Drosophila*

Microinjections of MC-oligonucleotide constructs

Wild type *Drosophila* embryos were collected for up to 30 min on apple juice agar plates (1.5% sugar in apple juice) with a yeast paste spread on top of the plates. The embryos were brushed into a 25-ml plastic beaker containing several milliliters of water. The beaker was then filled up with the dechorionation solution (3% sodium hypochlorite), stirred and set aside for 30 sec, stirred again, and left for next 30 sec. The embryo suspension was emptied into a vial having a nylon mesh (0.25 mm opening size) instead of the plastic bottom, so that the embryos could be rinsed for 2-3 min with water, last rinsing from a wash bottle. The washed embryos were transferred to a glass microscope slide (Fisher) and positioned, using a sharp dental probe, on a strip of a double sticky Scotch tape (covering part of the slide, and touching its edge), so that posterior poles of parallel lined up embryos faced the edge. Next, the slide with the embryos was transferred for desiccation to a Petri dish containing anhydrous calcium sulphate (Drierite) for 0-5 min, depending on humidity and temperature. After this, the embryos were covered with a thin layer of Halocarbon oil that allows air to reach the embryos.

The injections were done with a glass needle pulled from a capillary (o.d. 1.0 mm, i.d. 0.5 mm; World precision Instruments) using a Vertical Pipette Puller (Model 700B; David Kopf Instruments); open sharp tip was made by touching the needle tip with a razor blade until the needle tip broke. This glass needle was attached to a needle holder mounted on an inverted microscope stage (BIO Star; Reichert Inc). The needle holder was connected to a 60-ml syringe with polyethylene tubing. For the injections, only the embryos which are not older than 1 hr were chosen; over-aged or wrinkled embryos were destroyed. The injection was done by moving the stage, so that the tip of the

needle could penetrate slightly (5-10%) embryo's posterior pole. A tiny amount of the injection buffer (5 mM KCl, 0.1 mM PO_4, pH 7.8) with dissolved conjugates was injected by pressing the syringe plunger. The needle was withdrawn quickly. Injected embryos were kept under oil on the slide in a moisture chamber (made of wet paper towel in a 150 x 15 mm Petri dish) and incubated at room temperature until larvae hatching.

F. Prediction of the *ard* mRNA secondary structures

ard mRNA secondary structure prediction was done using a computer modeling program RNA Structure,Version 3.2, created by Michael Zuker and David Steward. This is the RNA secondary structure prediction program developed to predict the minimum free energy or optimal secondary structure of the mRNA. All steps and plugging in all necessary data and parameters was done according to the detailed guidelines described in this reference (Zuker, 2003) and on the website. Free software is available on the Internet at this website: www.bioinfo.rpi.edu/applications/mfold. Two students, Julie Russak and Judy Zhu, did most of this computer work.

G. Preparation of the ribozyme delivery construct

The complementary strands of the oligonucleotides for the ribozymes were synthesized in the Synthesis and Separation Core Facility at Hunter College. The ribozyme DNA sequence was subcloned into the P-element transformation plasmid pP{CaSpeR-hs}, between EcoRI and XbaI sites, using EcoRI and XbaI restriction

enzymes. After subcloning, the delivery vector was used to transform *E. .coli* XL-1 Blue bacteria. Plasmid purification followed, using Qiagen Maxi-prep kit; the transcript consists of the *hsp70* 5' leader (~207bases) with m^7 Gppp cap and 3' trailer (~525 bases) with a polyA tail to protect the ribozyme from the degradation by intracellular ribonucleases (Zhao, JJ et al., 1993). Each construct was analyzed and the structures were confirmed by restriction enzyme analysis and DNA sequencing.

H. Generation of transgenic flies

pP{CaSpeR-hs} plasmid with a mini white gene, coding for red eye color and the subcloned ribozyme DNA was microinjected into *Drosophila* **yw** mutant embryos (not older than 1 hr) together with the helper plasmid, which is a P-element (pπ25.7 wc) containing transposase necessary for the transposition of pP{CaSpeR-hs}. By itself, the helper plasmid can not transpose, so only the vector carrying the subcloned ribozyme DNA can be incorporated into *Drosophila* chromosomes..

In order to establish the insertion linkage with *Drosophila* chromosome genetic crosses were made according to the scheme showed below:

Crosses

The vector construct pP{CaSpeR-hs}, containing the subcloned ribozyme DNA and a mini white gene (so it can be denoted in short as P[w+]), was microinjected with pπ25.7wc DNA before the formation of pole cells to the posterior end of freshly laid (not older than one hour) fly eggs.

P[w+] + pπ25.7wc
Microinject
↓
G0 ♂♂ $\frac{w}{Y}$ x $\frac{w}{w}$ ♀♀
↓
G1 $\frac{w}{Y}$; $\frac{P[w+]\ (2^{nd}\text{ or }3^{rd})}{+}$; or $\frac{w}{w}$; $\frac{P[w+]\ (2^{nd}\text{ or }3^{rd})}{+}$ or $\frac{P[w+]}{Y}$ or $\frac{P[w+]}{w}$

If mini white gene in P[w+] is expressed, the flies carrying it will have red eyes. Individual transformed G1 flies may have multiple transposon insertions, but more than 90% of them will have single insertion. As a result, rare multiple insertions can be avoided. Insertions on the 4th chromosome, which is very short, practically do not occur. Individual crosses were used as described below to establish the P-element insertion linkage with the chromosome and reserve the strains containing useful insertions with balancer for stock.

• Test for insertion on X chromosome:

G1 ♂ $\frac{P[w+]}{Y}$ x $\frac{yw\ sn^{3}f^{36a}\ ado^{4P1}}{FM7a}$ ♀ virgin
↓ Select w +, FM7a (bar red eyes)

G2 ♀ $\frac{P[w+]}{FM7a}$ x $\frac{w}{Y}$ ♂
↓

G3 $\frac{P[w+]}{w}$ or $\frac{w}{FM7a}$ or $\frac{FM7a}{Y}$ or $\frac{P[w+]}{Y}$

Balancers are artificial chromosomes containing large inversions that prevent crossing over during meiosis due to the non matching sequences. Flies with FM7a balancer will have bar shaped eyes that cause photoreceptors to develop only in specific areas. If we

get any of the four possibilities for G3 generation, it will mean that the plasmid that was injected is in the first chromosome, which is the X chromosome.

Test for insertion on 2nd chromosome:

G1 ♂♂ $\frac{w}{Y}$; $\frac{P[w+]}{+}$ x $\frac{w}{w}$; $\frac{EcR^{225}}{CyO}$ ♀♀ virgin

↓ Select w+, CyO (red eyes and curly wings)

G2 ♂ $\frac{w}{Y}$; $\frac{P[w+]}{CyO}$ x $\frac{w}{w}$; $\frac{\pm}{+}$ ♀ virgin

↓

G3 $\frac{P[w+]}{+}$ or $\frac{CyO}{+}$

If we get these two phenotypes, then we will get flies with curly wings or red eyes. There will be a separation of eye color and curly wings on the second chromosome proving that the plasmid was incorporated into this chromosome.

Test for insertion on 3rd chromosome:

G1 ♂♂ $\frac{w}{Y}$; $\frac{P[w+]}{+}$ x $\frac{w}{w}$; $\frac{TM3, Sb^1}{CxD}$ ♀♀ virgin

↓ Select w+, Sb^1 (red eyes and stubble hairs)

G2 ♂ $\frac{w}{Y}$; $\frac{P[w+]}{TM3, Sb^1}$ x $\frac{w}{w}$; $\frac{\pm}{+}$ ♀ virgin

↓

G3 $\frac{P[w+]}{+}$ or $\frac{TM3, Sb^1}{+}$

If we get these two phenotype combinations for G3, we will know that the plasmid is on the 3rd chromosome due to the separation of eye color and stubble hairs.

I. Heat-shock activation of ribozyme

For ribozyme activation by heat-shock treatment, *Drosophila* embryos homozygous for the ribozyme insert were chosen, except for one transgenic line in which the ribozyme construct was inserted on the first chromosome (the males are hemizygous for this construct). Each group of transformant flies was put into the separate large cage boxes to accommodate 10-15,000 flies. *Drosophila* eggs were laid on fly food trays with yeast paste spreaded on them, or agar/apple juice trays, in the cage boxes. The trays were switched every 12 hrs so that embryos collected for the heat-shock were 0-12 hrs old. The embryos were then allowed to age for 10 hrs at 25 °C, 50-60% humidity. Before the heat-shock the trays with the embryos were put inside the incubator to warm them up to about 34-35°C. The 45 min heat-shock was applied to 10-22 hrs old embryos in water bath, with the embryos on the trays in closed plastic containers, fully submerged, 36-37°C. In 10-22 hrs old *Drosophila* embryos transcripts of the *ard* gene are being synthesized in amounts large enough to become detectable and at this developmental time these transcripts gradually reach their first peak level. After the heat-shock, the embryos were allowed to recover when left at 25 °C until the first instar larvae hatched. When the larvae were approximately 0-24 hrs old, about 22-46 hrs after egg laying (AEL), they were harvested by rinsing them with filtered water off the trays through the first sieve nylon membrane (to separate larvae from embryos, egg membranes, food pieces, etc.) into the small beaker; the mesh opening was 0.67 mm. The larvae in the beaker filled with water were then collected on the second sieve membrane (installed in the small tube); the mesh opening was 0.25 mm) by pouring water with the larvae in it through the membrane.

Next, the larvae were rinsed well with water, 1 min, to get rid of any traces of yeast and frozen at -70°C until enough larvae were harvested to make a membrane protein preparation that was subsequently used in immunoblotting.

J. *Drosophila* head/larva membrane protein preparation and solubilization

Adult *Drosophila* flies were kept frozen at -70 °C. To disjoin *Drosophila* heads from bodies, frozen flies mixed with powdered dry ice in a container were shaken violently for several seconds and set aside for 1-2 minutes. This procedure was repeated 5-6 times until the heads separated from the bodies. To collect the heads, a stack of sieves (with sizes #40, 25, 10, from Wire Cloth Company, Newark, NJ) was used so that when the stack (with the heads, bodies and powdered dry ice mixed together) was shaken several times, the heads collected in one sieve only, and were stored at -70 °C ready for the membrane preparation.

The method employed for membrane protein preparation was the one described in the paper (Schmidt-Nielsen et al., 1977), with some modifications. This method was used previously, successfully, in our laboratory, as the initial step in the purification of the neuronal nAChR from *Drosophila* heads. Unless indicated all steps were done at 0-4°C. The heads were suspended to 100 mg/ml of the homogenization buffer (HB) (10 mM NaPi, pH 7.3, 1% (w/v) sucrose, 5 mM EDTA, 5 mM EGTA, 3 mM NaN_3, and Protease Inhibitor Mix (PIM) (1 μg/ml Aprotinin, 1 μg/ml Antipain, 1 mM EDTA, 1 mM EGTA,

5 mM Benzamidine HCl, 5mM 6-amino-n-hexanoic acid; 1mM PMSF; 5mM IAA, these last two ingredients added from stock immediately before use to the homogenized sample) and homogenized in ice-cooled homogenizer (Caframo Stirrer type RZR50 with Thomas B 246 glass container) using 20-24 pulses, each several seconds long. The homogenate was centrifuged for 10 min at 2341 rpm in SS- 34 rotor (Sorvall), filtered through a layer of cheesecloth, pellet was resuspended to a conc. 100 mg heads/ml of the homogenization buffer, and homogenized as before. Centrifugation as above followed. Two supernatants were combined, diluted by 1 volume of HB and centrifuged, 40 min, 11940 rpm in SS-34 rotor. The upper layer was collected (whitish glossy in appearance) and resuspended to yield a conc. equivalent to 160 mg/ml in HB, and homogenized as before. This fraction (named "Membrane Preparation") was used for subsequent solubilization.

The membrane preparation (0.5 ml sample) was solubilized by spinnig the sample for 25 min. in a microcentrifuge machine (Hermle, type Z 233 M2), 14000 rpm. The supernatant was discarded and pellet suspended in 200 μl of the solubilization buffer (SB) [10 mM Tris-EDTA, pH 7.5, 1%SDS, and PIM] without EGTA (interferes with the BCA protein assay). Next, the homogenization and spinning was done as before. The supernatant, which contained the solubilized membrane preparation, was collected. The amount of proteins present in the solubilized sample was determined by the Pierce BCA Protein Assay (Pierce) according to the attached instructions. After that, the sample content was adjusted to 5 mM EGTA and 5% β-Mercaptoethanol.

Larvae membrane preparation and solubilization was done following the same steps except:

1. no sieving was needed

2. no filtering of the supernatant took place

3. all pellet (not only the upper "whitish glossy" layer- since it could not be distinguished from the rest of the pellet) was collected at the last step of the membrane preparation before solubilization

4. about 5 times less SB was used, since protein concentration in larvae seems to be lower than in *Drosophila* heads

5. PIM included 20 x Protease Inhibitor Cocktail for mammalian tissues (Sigma).

Protein concentration in the solubilized larvae membrane preparation was measured using the Pierce BCA Protein Assay which is a detergent-compatible formulation based on bicinchoninic acid (BCA) for the colorimetric detection and quantitation of total protein. From 200 mg of first instant larvae about 500 μg of solubilized membrane proteins were extracted. This fraction contains nAChR, including ARD subunit.

K. Western blotting

A sample of 50 μg of larval solubilized membrane preparation was mixed with 3x SDS Gel Loading Buffer (150 mM Tris- HCl, pH 6.8, 300 mM DTT, 6 % [w/v] SDS, 0.3 % Bromophenol Blue, 30% [v/v] glycerol) in 2:1 [v/v] ratio and loaded on 12 % SDS polyacrylamide gel, 15 μl of molecular weight protein color marker was also loaded in separate lane. The gel was run for 2 hours, at 50V (stacking gel), and later at 140V (resolving gel). Next, the gel was transferred to the transferring apparatus and assembled into a "sandwich" which included 5 sponges, 2 paper filters, and PVDF membrane . The

transfer took 2 hours at 105 mA. Western Blotting was done using SuperSignal West Pico Chemiluminescent Substrate Method from Pierce. The blot was placed in Pierce Blocking Solution with 4% skim dry milk and incubated at 4 ^{0}C overnight. Next, the blot was incubated in the same solution with primary anti-rabbit antibody, directed against ARD protein, 1:200 dilution, 1 hour, RT, with gentle rocking. The blot was washed with PBS (containing 0.1 % Tween20) for three times (10min, 20min, 10min), and incubated with goat anti-rabbit secondary antibody (1: 8000 dilution), for 1 hour, RT. Washing as before followed. Incubation of the blot with Pierce Reagent took place for 5 minutes, RT, with rocking. The blot was wrapped up in Cling Wrap and put into the cassette. After the short exposure, the film was developed.

Sequence of the peptide according to which peptide-specific polyclonal anti-rabbit antibody, directed against ARD protein, was prepared (by Bio-Synthesis, Inc):

NH2-KQSKMEVMELSDLHHPNC-COOH

III. RESULTS

Design and generation of mitomycin C-oligonucleotide conjugates

For the experiments with M13mp18 and *E. coli* a set of four conjugates was designed (Fig.10, next page). They differ in length by one nucleotide each to enable testing the optimal distance of the 5'-end of an oligonucleotide to the cross-linking site. Mitomycin C is attached to the 5'-terminus of the deoxyribonucleotide via $(-CH_2-)_{12}$ tether. This gives lots of flexibility to the mitomycin C moiety in "searching" for the target. From the commercially available aminolinkers n=12 was chosen as close to the optimal aminolinker length (Maruenda and Tomasz, 1996). Four oligonucleotides (18-, 19-, 20-, 21-mer) are complementary to the (+) strand of M13mp18. They are directed against the 5'-d(CG) at the border of the EcoRI site (Fig.11, page 61).

Generation of mitomycin C-oligonucleotide conjugates was carried out according to Maruenda and Tomasz (personal communication), with small modifications.

Monitoring and completion of the reaction was established by C_4-reversed -HPLC (Fig.12, pages 62-65). Recovery of the conjugate was in the range of 10-20 %.

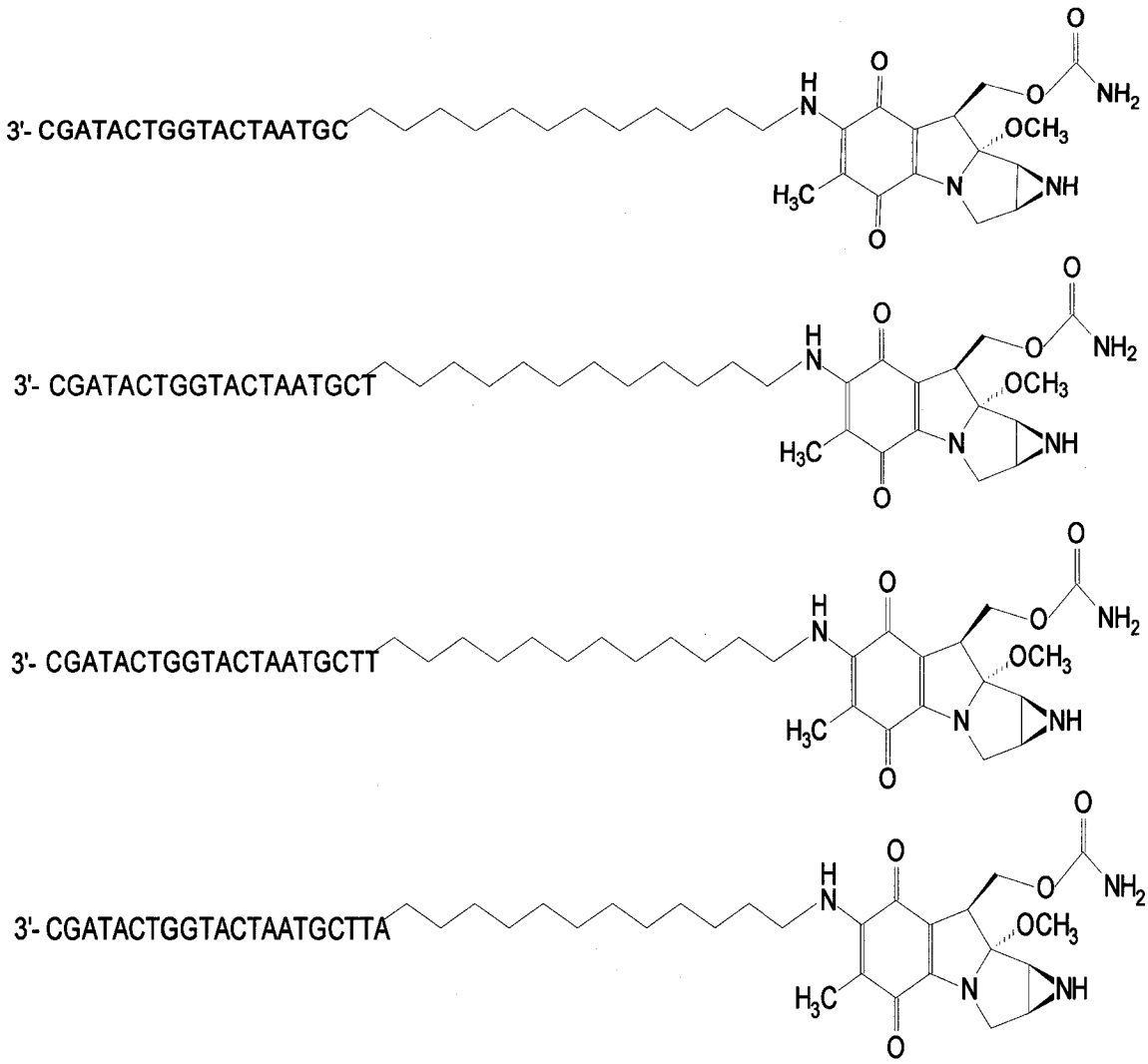

Figure 10 Drawings of four mitomycin C conjugated oligonucleotides.
Each construct consists of the mitomycin C moiety (on the right), 12 carbon-long aminolinker (in the middle), and the oligonucleotide (on the left) complementary to the EcoRI recognition site in the target sequence of the coding strand of M13mp18 DNA. Each oligonucleotide (top to bottom) is one nucleotide longer.

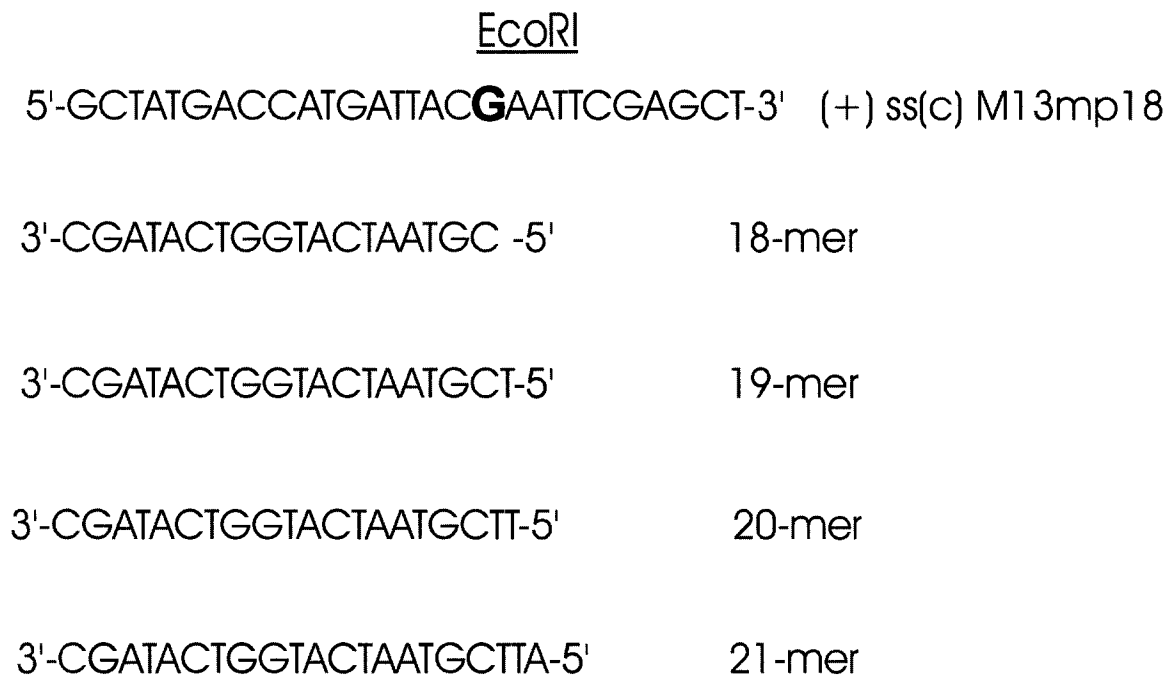

Figure 11 M13mp18 DNA target sequence, including EcoRI recognition site, with four different length oligonucleotides complementary to this sequence.
Bold G indicates guanine targeted for cross-link.

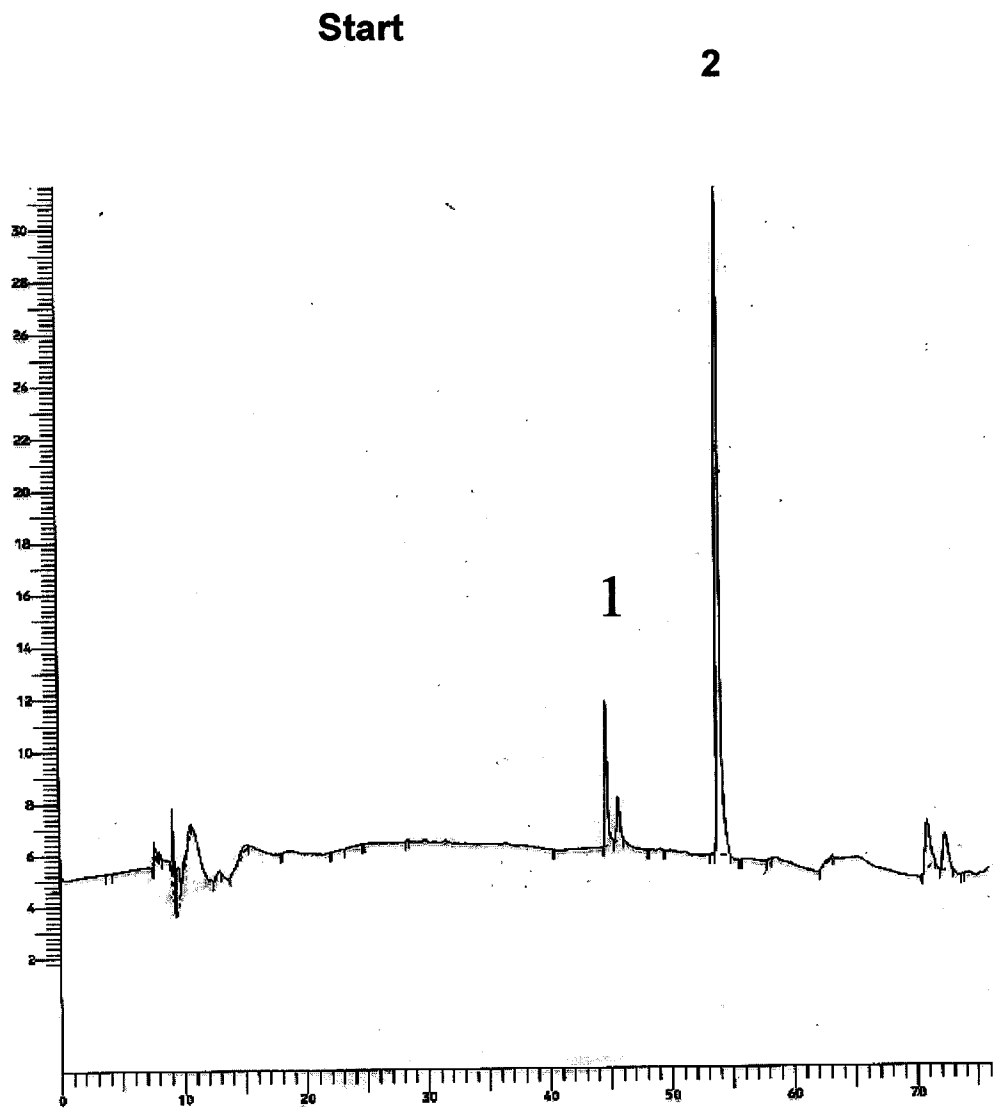

Figure 12A The course of the coupling reaction.(Start)
In the reaction MA is being attached to the aminolinker connected to the 5'-end of the 21-mer oligonucleotide.
The four diagrams were copied from the HPLC chromatograms taken at the start, after 4, 12, and 20 hrs of the coupling reaction. Numbers 1, 2, 3, indicate elution peak for the oligonucleotide, MA, and the final MC-oligo construct, respectively.
First diagram (above) represents start of the reaction

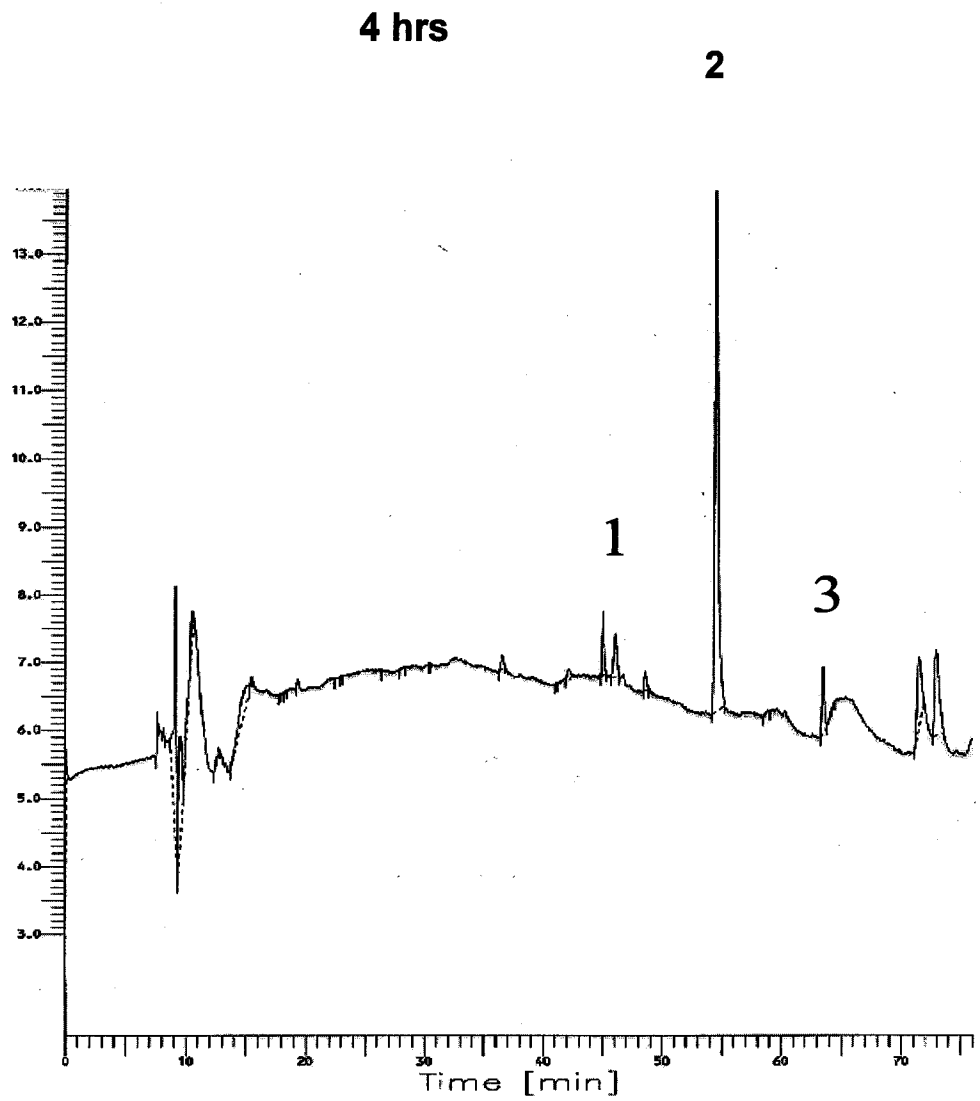

Figure 12B The course of the coupling reaction. (After 4 hours)
Elution peak for the MC-oligo construct becomes visible as the peak number 3.

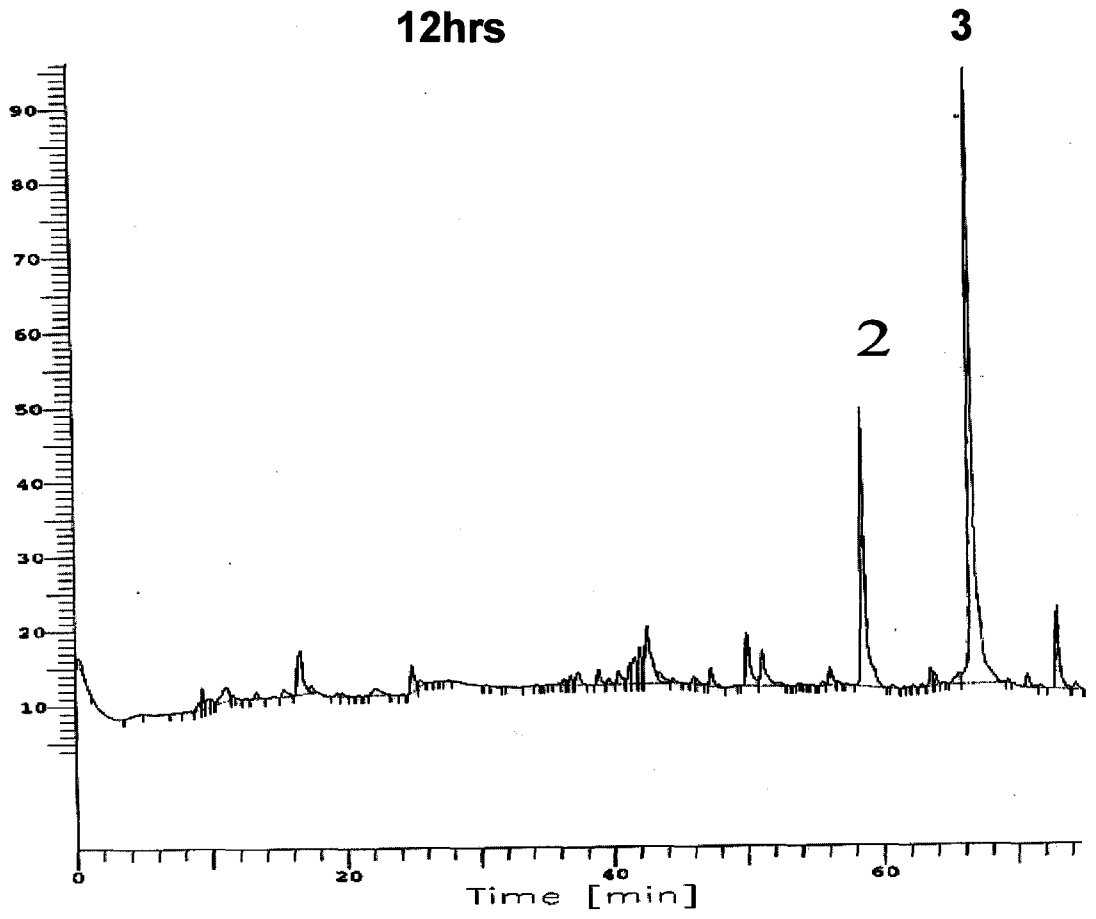

Figure 12C The course of the coupling reaction. (After 12 hours).
The elution peak for the MC-oligo construct (number 3) becomes more prominent.

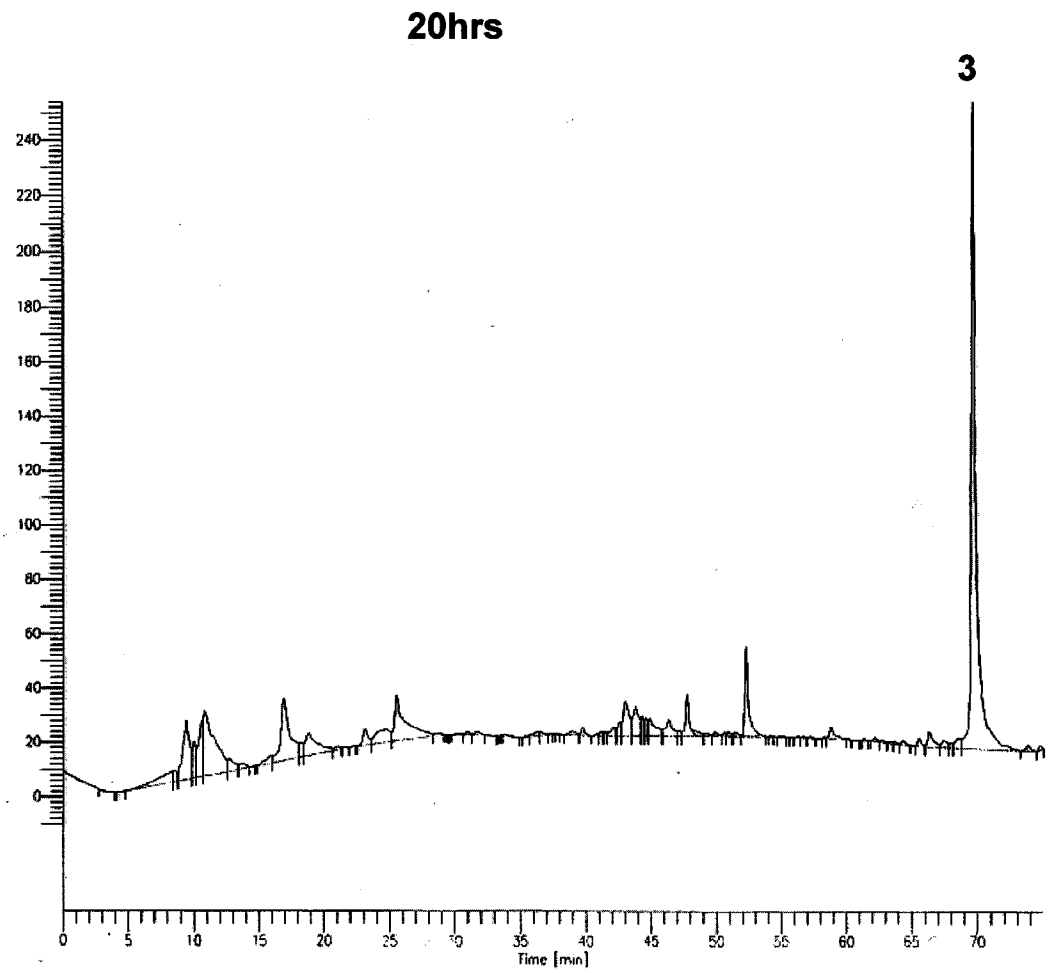

Figure 12D The course of the coupling reaction. (After 20 hours).
Only the peak for the MC-oligo construct is visible (number 3). Starting reactants, MA and the oligonucleotide with the aminolinker, were totally consumed in the reaction.

The collected peak corresponding to one of the adducts (21-mer, Fig.13A) shows high degree of purity of this adduct sample. The conjugate was characterized by UV-vis spectroscopy (Fig.13B, page 67); it had characteristic for MC-oligonucleotide adduct absorbance peaks at 260 and 374 nm (Maruenda and Tomasz, 1996).

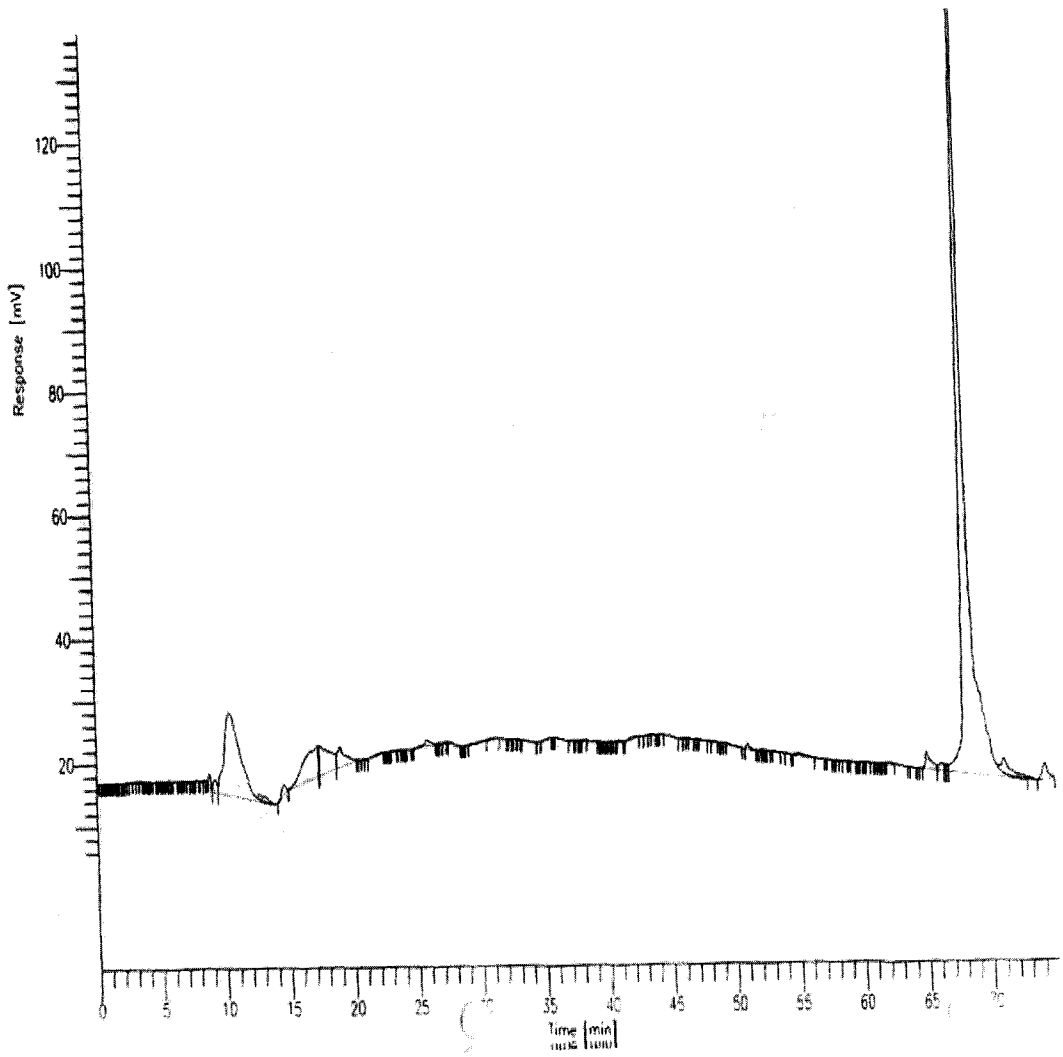

Figure 13A The diagram of the HPLC chromatogram shows the elution peak for the MC-oligonucleotide conjugate (21-mer).
The conjugate sample was separated by reversed-phase HPLC, collected, and 10μg of it was injected into Rainin (C_4) Dynamax-300A column.

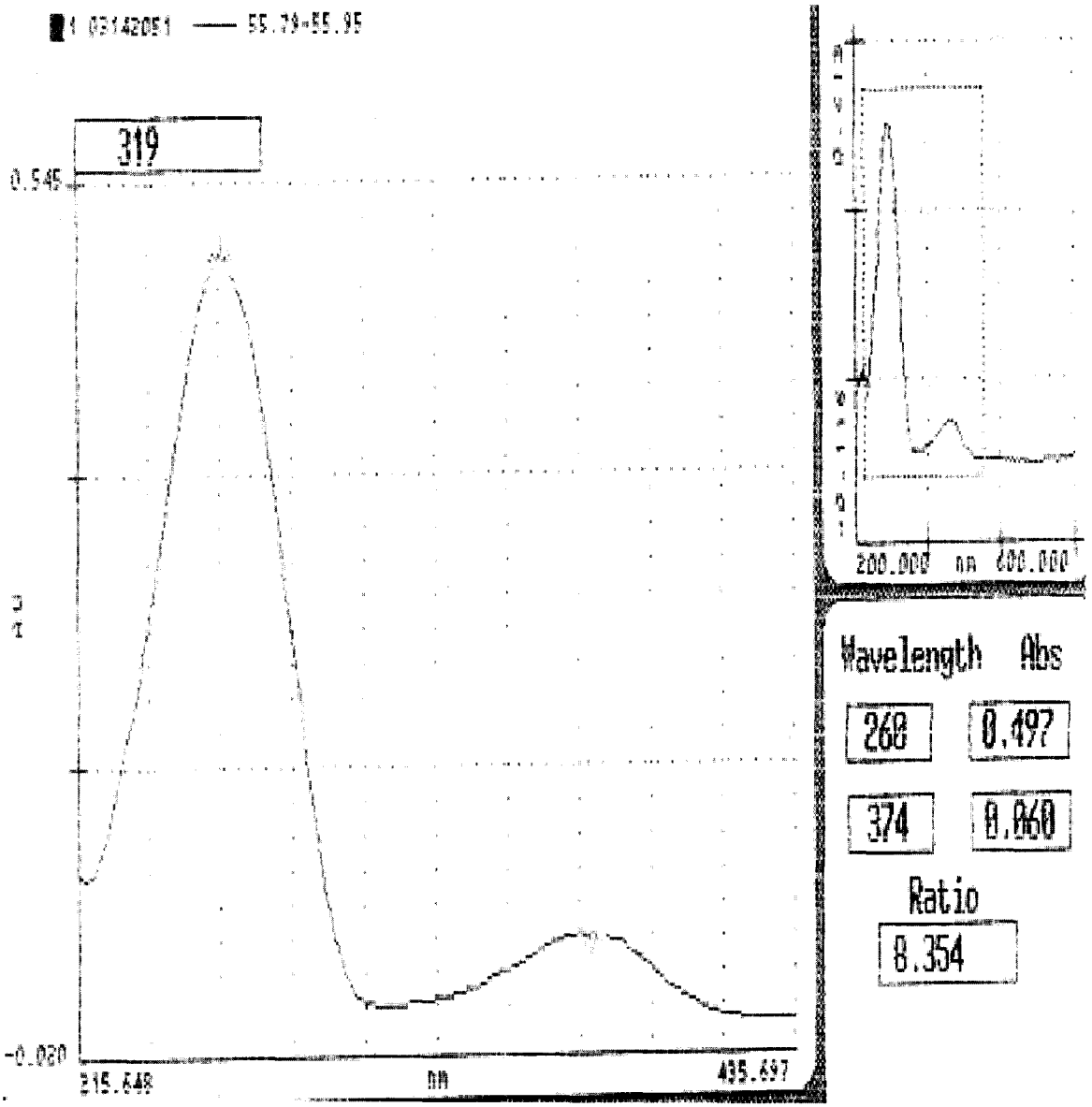

Figure 13B UV-visible spectrum of MC-oligonucleotide conjugate (21-mer).
The spectrum shows two characteristic peaks at 260 and 374 nm. The spectrum was determined by diode array scanning of eluate from (C_4) Beckman, semiprep column during HPLC.

Introduction of cross-linking in vitro between MC-oligonucleotide construct and ss DNA

Design of the cross-linking experiments aimed at establishing the optimal distance between the hybridized conjugate and the 5'-d(CG) in the target sequence, so that cross-linking of the mitomycin C moiety of the adduct to the target G residue could give high yield of the cross-linked product.

Four conjugates targeted the 5'-d(CG) at the border of the EcoRI site differred in length by one nucleotide each. This way, after annealing, each aminolinker with the attached MC could be at slightly different position during mitomycin C "attack" on G residue and form covalent bond with it during cross-linking reaction. Four cross-linking reactions had thus to be set up with radioactively (cordycepin 5'-triphosphate) labeled conjugates (plus four control reactions) to find out which of them gives the highest yield of cross-linked product. The reactions also contained M13mp18 single-stranded DNA with a target sequence, NADPH as a source of electrons for reductive activation of mitomycin C, and a reductase which would catalyze this activation. Argon gas was used to provide anaerobic environment favoring reducing conditions. Cross-linking reaction products with their radioactive label and controls were run on an agarose gel. Phosphoimage analysis had provided information if the cross-linking really took place and at what yield. Based on these experiments, the conjugate that gave the highest yield of the cross-linked product was chosen for further experiments.

The strategy for the cross-linking experiments was to use single-stranded DNA of vector M13mp18 because it has some attractive features that make DNA manipulation and search for mutations easy. M13mp18 DNA can be obtained as either single-stranded

circles or double-stranded circles at 7253 nucleotide length. Single-stranded DNA phages are male-specific; they infect male *E.coli* strains that contain an F (fertility) factor. Following infection, the M13 (+) strand DNA serves as a template for the synthesis of the complementary (-) strand DNA forming this way a double-stranded DNA, so called replicative-form (RF), which is amplified to about 200 copies per cell. After that, the (-) strand DNA is stopped being replicated; only the (+) strand DNA is being synthesized - this time the (-) strand DNA serves as a template. The (+) strand DNA circles are packaged and secreted from the *E.coli* cells through a non-lytic mechanism. Large amounts of single-stranded template DNA for dideoxy sequencing can thus be made.

Another attractive feature of M13mp18 vector is that it contains a portion of the *lacZ* gene with a polylinker containing contiguous restriction sites. If cross-linking takes place in one of these sites and its repair will lead to a mutation, after plating the plaque will be white, because it is known that most mutations in this polylinker region can be easily identified by the absence of β-galactosidase activity producing colorless or "white" plaques; without mutation the resulting plaques will be blue. Single-stranded M13mp18 DNA was prepared on large scale from infected *E. coli* host strain XL-1 Blue. The quality of the DNA was checked by UV spectroscopy and by running a 1.0% agarose gel. In order to visualize the cross-linking it was first necessary to radioactively label the conjugates with cordycepin 5'-triphosphate (3'-deoxyadenosine 5'-triphosphate); the enzyme used for labeling was terminal transferase (terminal deoxynucleotidyl transferase). It catalyzes template independent addition of deoxyribonucleoside triphosphates to the 3'-OH ends of deoxyribonucleotides, and also to double - or single stranded DNA. This 3'-end labeling reaction was done according to the

instructions attached to the enzyme sample. Labeled conjugates were separated from unincorporated radioactive nucleotides, the enzyme, and other materials by Nensorb 20 nucleic acid purification cartridge. The yield of the labeled product was 10-33%. Purity of the final product was checked by running it in a 15% polyacrylamide denaturing gel for 1.5 hour; the conjugates with the attached cordycepin 5'-triphosphate form a major product with some very faint bands indicating small amounts of side products (Fig.14, next page) that should not interfere significantly with the visualization of the cross-linking.

The enzyme employed for the cross-linking reaction was NADPH-cytochrome c (cytochrome P-450) reductase. Previously used porcine heart cytochrome c reductase (NADH dehydrogenase) obtained from Sigma was highly contaminated with nucleases (Fig.15, page 72) what made the identification of the cross-linking practically impossible. Consequently, NADPH-cytochrome c (P-450) reductase was prepared from rat liver microsomes. Purification was achieved through a DEAE (diethyl- aminoethyl)-cellulose and 2'5'-ADP agarose affinity columns according to a published procedure (Yasukochi and Masters, 1976). Quantitation of the amount of the purified enzyme was determined by using modified Lowry colorimetric method (Ashburner, 1989). Final enzyme activity was determined spectrophotometrically by measuring the increase in absorbance at 550 nm due to the appearance of reduced cytochrome c, as described in "Methods in Enzymology" (Strobel and Dignam, 1978); the activity was 1.51 units per 100 µl of concentrated reductase solution. The total recovery was 100 units which became available for my cross-linking experiments.

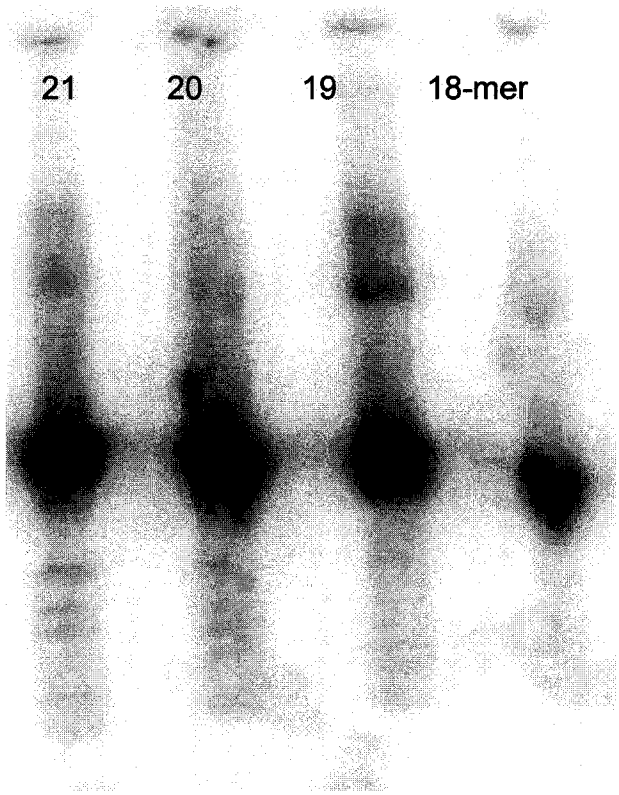

Figure 14 Phosphoimage of the purification products of cordycepin 5'-triphosphate labeled conjugates.
The conjugates were run in a 15% polyacrylamide denaturing gel for 1.5 hr. Terminal transferase catalyzed attachment of the cordycepin 5'-triphosphate to the 3'-end of the conjugates. The four labeled adducts, are (from left to right): 21-, 20-, 19-, and 18-mer, visible as big dark dots, about 2/3 -length down the gel.

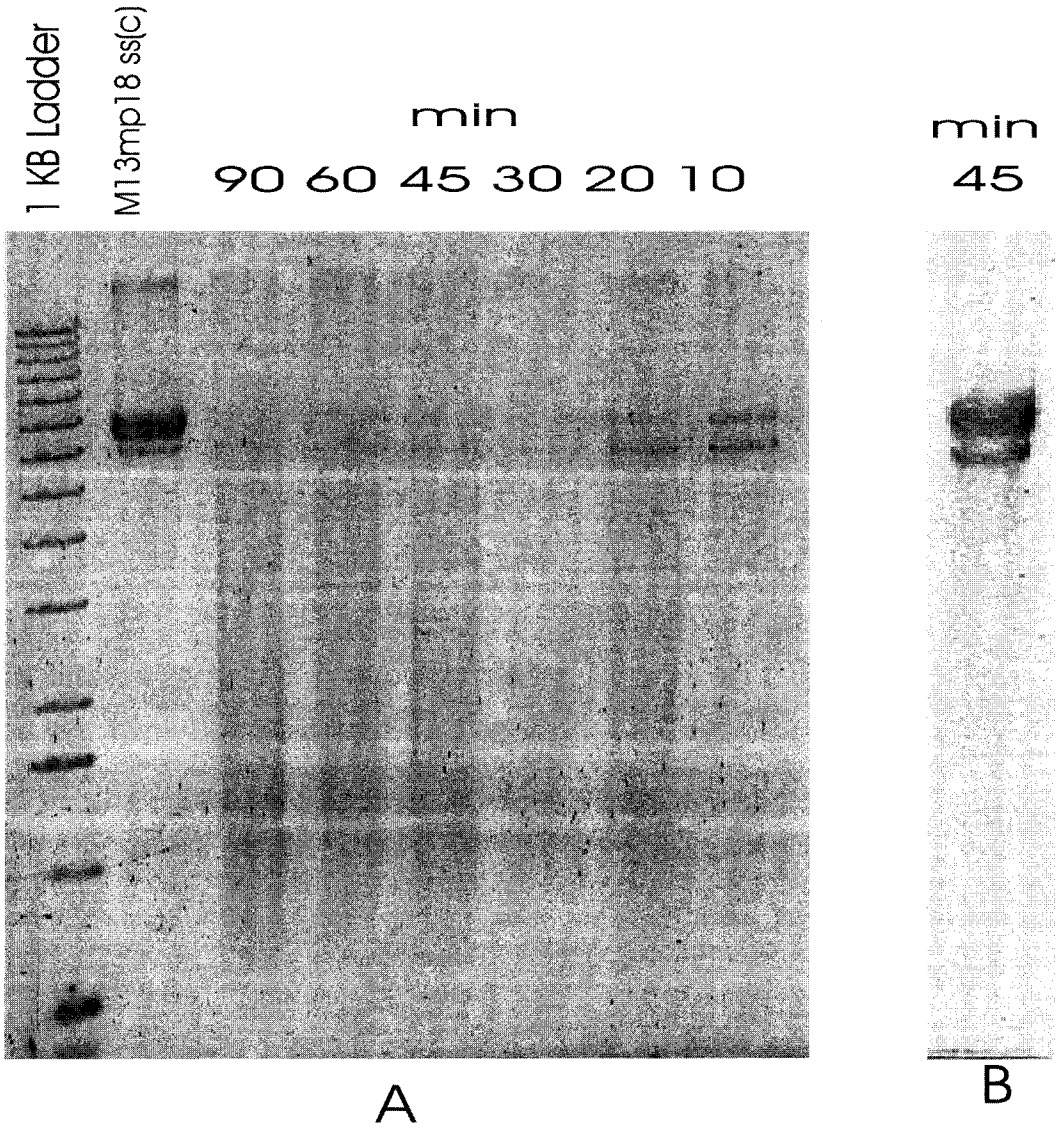

Figure 15 The comparison of the two reductase samples used for the cross-linking reaction.
The samples were NADH cytochrome c reductase purchased from Sigma, and NADPH cytochrome P-450 reductase purified in our lab. Panel A shows fluoroimage of a 1.0% agarose gel into which six reactions ,each containing 1 μg of ss(c) M13mp18 DNA and 1.0 unit of NADH cytochrome c reductase sample, were loaded. Each reaction was allowed to proceed for the time indicated. As a control, a reaction containing 1.0 μg of DNA without the NADH cytochrome c reductase sample was taking place for 90 min, and loaded all into the gel. As can be seen, nuclease activity was very strong in this enzyme sample, comparing to the very low nuclease activity in the reductase sample prepared in our lab (Panel B).

The cross-linking reactions were performed under the general conditions described in Materials and Methods. Each of the four cordycepin-5'-triphosphate - labeled mitomycin C-oligonucleotide conjugates was put into a separate microfuge tube containing ss(c)DNA in Tris buffer for hybridization. After NADPH was added, each reaction tube was flushed with argon. Following this, NADPH-cytochrome c (P-450) reductase was injected, and the cross-linking reaction was allowed to proceed under bubbling argon for 45 min at 37^0C. The four control reactions did not have the reductase. In order to visualize the cross-linking and estimate the efficiency of the cross-linking reaction, the products were run in a glyoxal loading buffer under denaturing conditions, as described in "Current protocols in molecular biology", pp.4.9.8-4.9.9, (Ausubel et al., 1998); the results for 21-mer are presented in Fig.16, next page, (the dot represenst known amount of radioactivity for calibration purposes). Before loading on the gel, after the reactions were terminated, the reaction tubes (and controls) were first put into hot water at 80-90^0C for 2-3 min to allow the dissociation of the non-cross-linked conjugates from the DNA, and then transferred on ice and loaded immediately (after mixing with a glyoxal loading buffer) into the gel that was allowed to run for several hours. The assumption was that the dissociated conjugates would run off the gel quickly but the conjugates cross-linked to the DNA would run together with the DNA. As can be seen, the control gave much weaker signal than the cross-linking reaction.

It was possible to calculate the efficiency of the cross-linking by comparing the intensities of the signals coming from the reaction samples run in the gel, and the dot representing known amount of radioactivity. The cross-linking reaction efficiency was

8.1%. Figure 17, page 75, shows in detail cross-linking reaction products for the 21-mer conjugate.

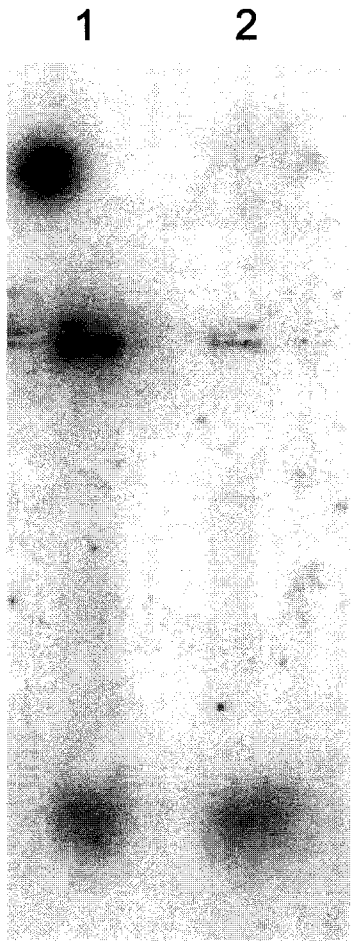

Figure 16 Phosphoimage of the cross-linking reaction product and control for the 21-mer conjugate.
The radioactive dot with known amount of radioactivity serve for the calibration purposes. A half of each reaction was mixed well by vortexing with sodium phosphate/DMSO/glyoxal solutions and loaded in glyoxal loading buffer on a 1.0%, 14 cm, agarose gel, using 10 mM sodium phosphate as a running gel buffer. The gel was run for 4 hrs with agitating the buffer every 20 min., lane # 1, cross-linking reaction product; lane # 2, control (no reductase).

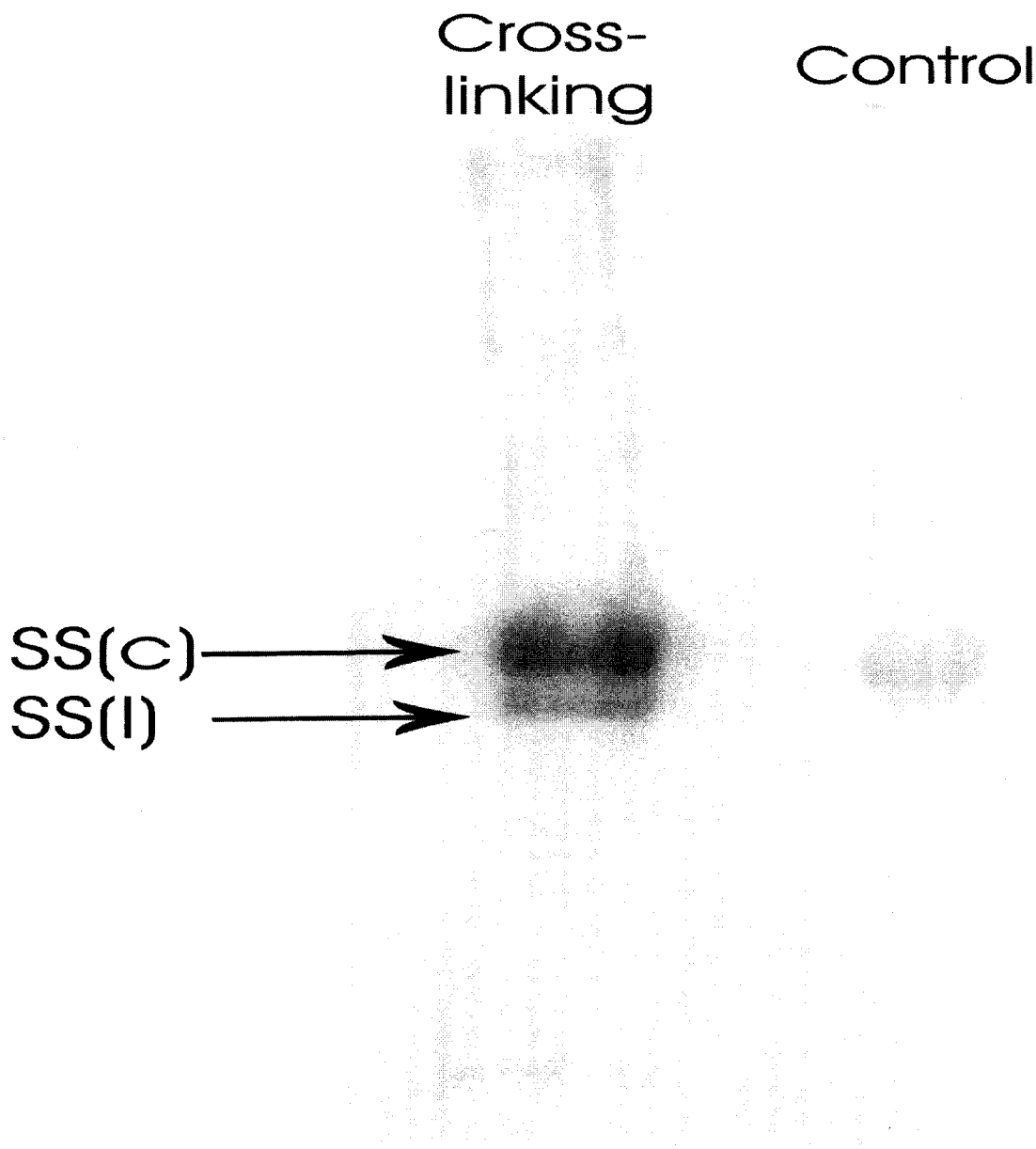

Figure 17 Phosphoimage of the cross-linking reaction products and control for 21-mer conjugate.
The products and the control were run in glyoxal loading buffer. Two bands for cross-linking reaction products can be identified; the larger, for potential cross-links in single-stranded, circular form of M13mp18 DNA, and the smaller band, for potential cross-links in single-stranded, linear form of DNA.

In vivo experiments in *E. coli*

A. Identification and analysis of potential mutation in M13mp18 DNA

Repair of the cross-link between the MC-oligonucleotide conjugate and the 5'-d(CG) in the target fragment of M13mp18 DNA can lead to a mutation in this fragment. *E. coli* has repair systems capable of repairing cross-linking in DNA (Min et al., 1996). In order to detect a mutation site the cross-linking reaction was performed as described before using 21-mer conjugate since this conjugate produced the highest efficiency of cross-linking. The target was G nucleotide on the border of EcoRI recognition site in the polylinker region of M13mp18. Primer extension of the 21-mer conjugate followed; a polymerase was Klenow fragment of *E.coli* which does not have the 5'→3' exonuclease activity that could degrade the conjugate. The products of the extension reaction were transformed into JM101 strain of *E. coli* that has an intact repair system which increases the effectiveness of mitomycin C as a mutagen. Transformed cells were plated on agar plates with X-gal (the β-galactosidase activated chromophore), and IPTG (isopropyl-1-thio-β-*D*-galactoside; the *lac* operon inducer) to detect potential mutations visually. The plates were incubated overnight at 37^0C. Among 255 blue plaques there was one colorless plaque indicating possible mutation in the targeted *lacZ* gene of M13mp18 DNA. Single-stranded DNA template for sequencing was prepared from plaque. DNA sequence in the polylinker region carrying the mutation was determined with the fluorescent dye-labeled terminators sequencing method using an ABI 310 Genetic Analyzer in Sequencing Facilities at Hunter College. Unfortunately, the sequence indicated the site of the mutation far away from the potential cross-linking site on the

border of *E.coRI* recognition site. Therefore, this mutation can not be attributed to the MC-oligonucleotide conjugate.

Since not all mutations might lead to colorless plaques (for example some single-point mutations may still give rise to the production of active β-galactosidase and, consequently, blue plaques) a wider screen was necessary to cover all plaques. Many of them could have a mixture of mutated and non-mutated M13 DNA. Screening bacteriophage plaques could be achieved by hybridization of radiolabeled oligonucleotide probe to target DNA sequence and plaque lifts. Differential washing with increasing temperature can reveal mutation. Theoretically, plaques that hybridize less strongly than others should give out less intense radioactive signal due to dissociation of the radioactive oligonucleotide from the mutagenized target sequence at lower temperature - even mismatch by a single base can speed up the dissociation. Consequently, according to this method, γ ^{32}P-labeled oligonucleotide complementary to the selected 5'-d(CG) site, on the border of EcoRI recognition site, where the potential cross-linking and subsequent mutagenesis could have taken place, Fig.18, and the flanking regions was hybridized to M13 DNA (present in plated plaques) that was first denatured, neutralized, and immobilized on replica plate filters.

Figure 18 M13mp18 DNA sequence with EcoRI recognition site and complementary 18-mer oligonucleotide probe. The probe was labeled with γ^{32}P and was used in plaque lifts to detect mutations. The approximate melting temperature for the probe was calculated at 50^{0}C. Large G indicates guanine targeted for the cross-link.

A plate that contained plaques of the original non-mutated M13mp18 DNA served as a control. Differential washings with increasing temperature were done to reveal mutations in the area of the 5'-d(CG) site on the border of EcoRI recognition fragment. Unfortunately, none of the several thousand screened plaques, resulting from new cross-linking experiment, indicated the presence of a mutated DNA sequence in the EcoRI cutting site.

B. Cross-linking *in vivo* catalyzed by the intracellular reductases of *E. coli.*

Direct transformation with the MC-oligonucleotide conjugate and M13mp18 DNA was performed as before, but this time without cross-linking step *in vitro*; the cross-linking was to depend on the intracellular activation of the MC-oligonucleotide conjugate by *E. coli* reductases. Plaque lifts with γ ^{32}P-labeled oligonucleotide complementary to the selected 5'-d(CG) site, on the border of *E.coRI* recognition site, followed as before. Differential washing again did not reveal any mutations in several thousand screened plaques.

Introduction of mutations in *Drosophila white* and *ard* genes

The experiments with *Drosophila* aim at introduction of a mutation into the *Drosophila ard* gene via repair of the cross-linking induced by mitomycin C-oligonucleotide conjugate, with oligonucleotide sequence complementary to the target sequence of this gene.

Before planning to employ MC-oligonucleotide construct against *Drosophila ard* gene, we targeted the construct against *Drosophila white* (w) gene. This gene encodes an ATPase transporter involved in transport of guanine and tryptophane required for eye pigmentation in *Drosophila.* A good target for the mitomycin C-oligonucleotide conjugate is a conserved Gly-Lys sequence which contains a putative nucleotide binding fold. Mutation of this motif is known to create a white eye color phenotype that can be easily identified and does not require any laborious, time-consuming procedures (Ewart et al., 1994) Preceding the glycine is an alanine - the nucleotide sequence is GCC GGA AAG for the three amino acids, generating the required 5'-d(CG) site for cross-linking. Figure 19 shows the target sequence with the complementary oligonucleotide sequence of the conjugate that was used for cross-linking. We have chosen the conjugate which has 18 nucleotides in the standard phosphodiester backbone and has aminolinker which is 12 carbons long.

Gly - Lys

5'- ATGGGCAGTCCGGTGCC**G**GAAAGA -3' DNA Coding Strand

3'- TACCCGTCAGGCCACGGC -5' 18-mer

Figure 19 *Drosophila white* gene target sequence with conserved motif and complementary 18-mer oligonucleotide.
Bold G indicates guanine targeted for the cross-link

The construct was microinjected into the posterior pole of *Drosophila* embryos as described in microinjections procedure in Materials and Methods. The timing of injections is critical for MC-oligonucleotide construct hybridization, cross-linking, and

potential mutagenesis, since during the first 1 hour after egg laying the nucleus of the *Drosophila* egg undergoes fast eight syncytial cleavages before cell formation begins, so there are no cell membranes impeding construct movement. During this period rapidly replicating DNA should be fully accessible for the interactions with the injected construct. Microinjections were performed on wild-type fly embryos. Previously we did experiments to check the tolerance of *Drosophila* embryos to mitomycin A, since in larger amounts this substance is toxic (as is mitomycin C) to living cells. After mastering my skills in microinjections, we calculated that about 20% of flies that originated from the mitomycin A-injected embryos have survived when those embryos were injected with the injection solution containing 2.0-2.7 ng/μl of MA. At slightly higher concentration (3.4 ng/μl) less than 6% of flies survived. Based on these numbers the injection solution was prepared in which the MC-oligonucleotide conjugate concentration was 34.8 ng/μl, that gives mitomycin C concentration 2.05 ng/μl, enough to guarantee 20% survival. The conjugate was injected into over 10,000 *Drosophila* embryos; 511 flies eclosed. Adults were checked under the microscope for mosaic-type of eye color. All males and virgin flies from G_0 generation were crossed (about 500 crosses total) with virgin and male $\mathbf{w^{1118}}$ strain flies, respectively, in which part of the *white* gene was deleted, causing a white color eyes. The rationale to choose for the injections the embryos of wild type, red eye flies, is as follows: *white* gene has two recessive alleles that are needed to confer red eye color in *Drosophila.* Consequently, mutation in one of the alleles is not enough to change red eye color into a white eye color. Both alleles have to be mutated to disrupt the transport of pigments and to cause white eye. For that reason G_0 flies were crossed with $\mathbf{w^{1118}}$ strain flies, in which both alleles with *white* gene were mutated. If in progeny G_1

fly one allele, mutated by MC-oligo action, "combines" with another mutated allele coming from $\mathbf{w^{1118}}$ line, then this G_1 fly will have white eye color. Consequently, G_1 generation was checked for white eye color. Unfortunately, after checking about 60-100 flies from each cross (that gives about 30,000-50,000 flies total from all 500 crosses), no white eye flies were found in G_1 generation, which indicated that mutation had not taken place or was too insignificant to cause any visible change in the phenotype. It is possible, that the phosphodiester backbone of the MC-oligonucleotide conjugates was destroyed by *Drosophila* nucleases; this could prevent targeted hybridization of the construct, and cross-linking. Therefore, new constructs with phosphorothioate (PS) backbone, very resistant to the nucleases destructive action, were attempted but, probably, due to different chemistry of phosphorothioates in solutions this attempt failed. As a result, we terminated our plans to introduce mutation into *Drosophila ard* gene using mitomycin C-oligonucleotide conjugate.

The results presented below reflect second part of our study in which the experiments were conducted aiming at the destruction or significant lowering of the *ard* mRNA using ribozymes.

Prediction of the *ard* mRNA secondary structures

Prediction of the *ard* mRNA secondary structures was done using a free energy minimization computer program available on the Internet. The program is based on the efficient algorithms for RNA secondary structure prediction using dymanic programming methods formulated by Prof. Michael Zuker, from Department of Mathematical Sciences

at Rensselaer Polytechnic Institute (Zuker, 2003). Fig. 20 shows optimal secondary structure of the *ard* mRNA calculated by the above program. Also, several "suboptimal" or near minimum energy secondary structures were predicted for the *ard* mRNA since, in general, the reliability of the computer modeling prediction is not very high for large RNA molecules. Therefore, the favorable regions targeted by ribozymes appear both on minimum and near minimum structures.

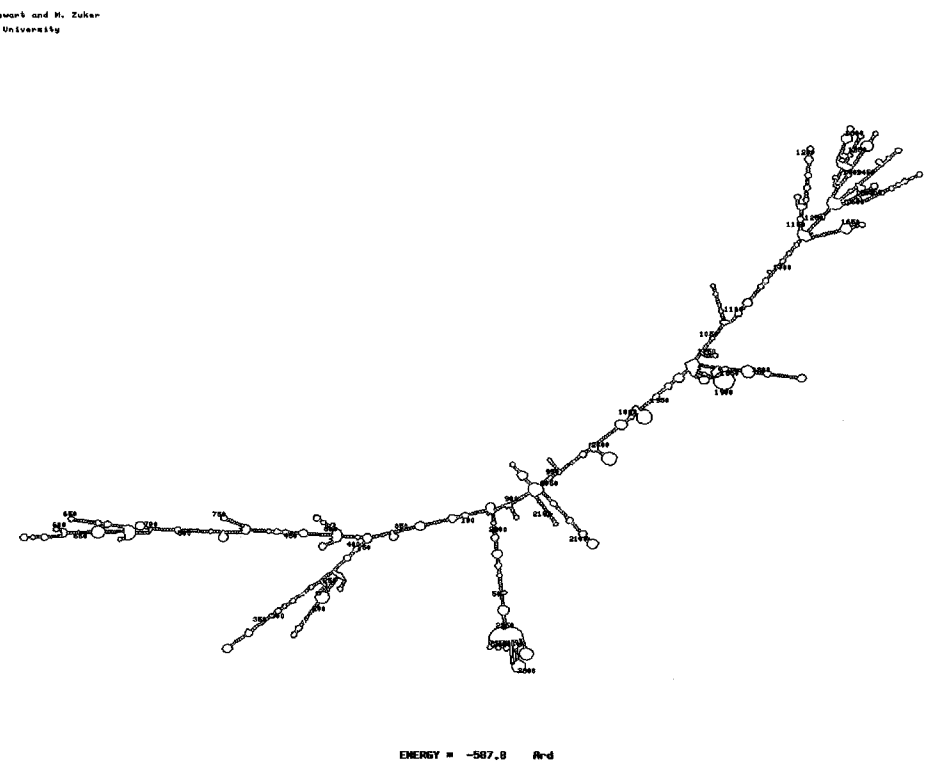

Figure 20 *ard* mRNA optimal secondary structures. Designed by "energy minimization" computer modeling program RNA Structure, Version 3.2, created by D. Stewart and M. Zuker.

Favorable target sequences on *ard* mRNA were chosen (employing Zhao and Lemke set of rules described before) to assure potentially efficient cutting by ribozymes. Figure 21 shows the magnified part of the *ard* mRNA optimal structure with the targeted sites.

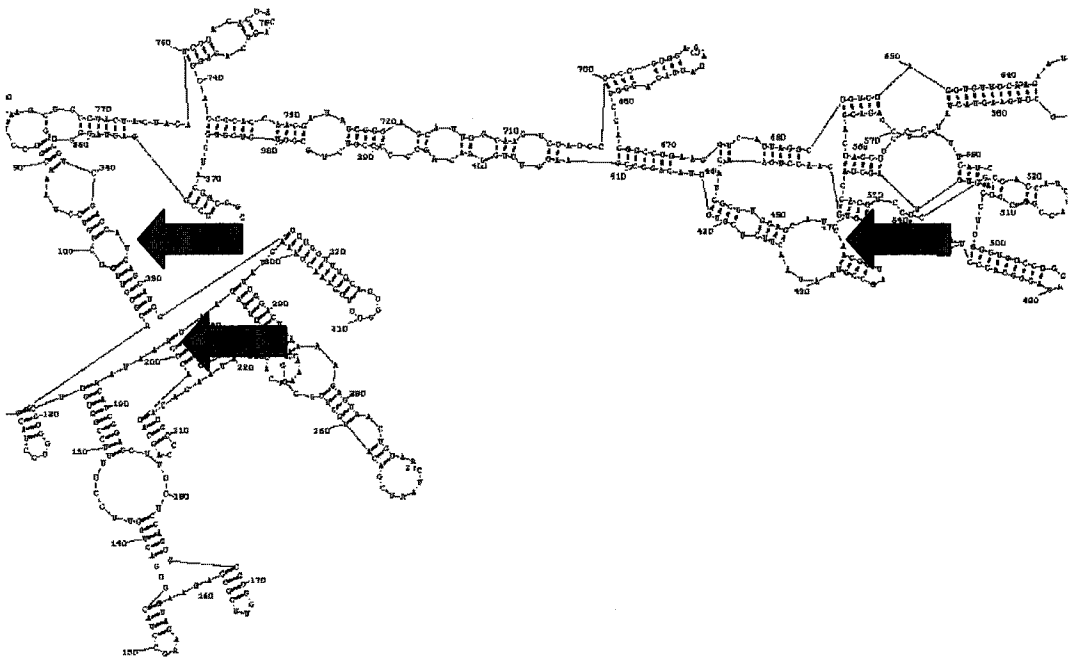

Figure 21 Enlarged region of the *ard* mRNA optimal secondary structures. The arrows point at the target sites.

Ribozyme design and the preparation of the ribozyme delivery construct

Four ribozyme constructs were designed after the optimal and suboptimal secondary structures were carefully analyzed and favorable regions were found. The Zhao and Lemke rules, described before, were taken into account. The DNA sequences of these 4 ribozymes and their target sites are shown in Table 2, next page.

cDNAs of RIBOZYMES	Target location on *ard* DNA
5'- AAT TCG GGG GCA CTG ATG AGT CCG TGA GGA AAC GCA ACT – 3' 5'- CTA GAG TTG CGT TTC GTC CTC ACG GAC TCA GTG CCC CCG – 3' Subcloned in sample named HAM	flanks: 438-444; 446-452 GTTGCGT TGCCCCC target: 443-445 GTC
5' – AAT TCG GGG CAA GAA CAA CAC CAG AGA AAC CGA CGT AAG TCG TGG TAC ATT ACC TGG TAT – 3' 5' – CTA GAT ACC AGG TAA TGT ACC ACG ACT TAC GTC GTG TGT TTC TCT GGT GTT GTT CTT GCC CCG – 3' Subcloned in sample named HP	Flanks: 439-442; 446-451 TTGC TGCCCC target: 443-445 GTC
5' – TTC TCA TTC TGA TGC CGT GAG GAC GAA ACA TTG AT - 3' 5' – AT CAA TGT TTC GTC CTC ACG GCA TCA GAA TGA GAA - 3' Subcloned in sample named J2	flanks 328-335; 338-344 ATCAATGT ATGAGAA target: 334-336 GTC
5' - GAT GCA CTC TGA TGC CGT GAG GAC GAA ACC AAC GA – 3' 5' - TC GTT GGT TTC GTC CTC ACG GAC TCA TCA GAG TGC ATC- - 3' Subcloned in sample named J1 and Y1	flanks 193-200; 202-209 TCGTTGGT AGTGCATC target: 198-200 GTC

Table 2 cDNAs of four subcloned ribozyme constructs.
On the right their target locations on the *ard* cDNA and flanks of the targets with numbered nucleotides.

One ribozyme was designed as having all the features of a hammerhead ribozyme, the others were hairpin ribozymes. Two ribozymes - one hammerhead and one hairpin - were directed against the same target site to investigate if there is a reactive difference between these two ribozyme constructs. Fig. 22, and Fig. 23, next page, show ribozyme delivery constructs and the *ard* RNA sequence specific ribozymes, with the target mRNA.

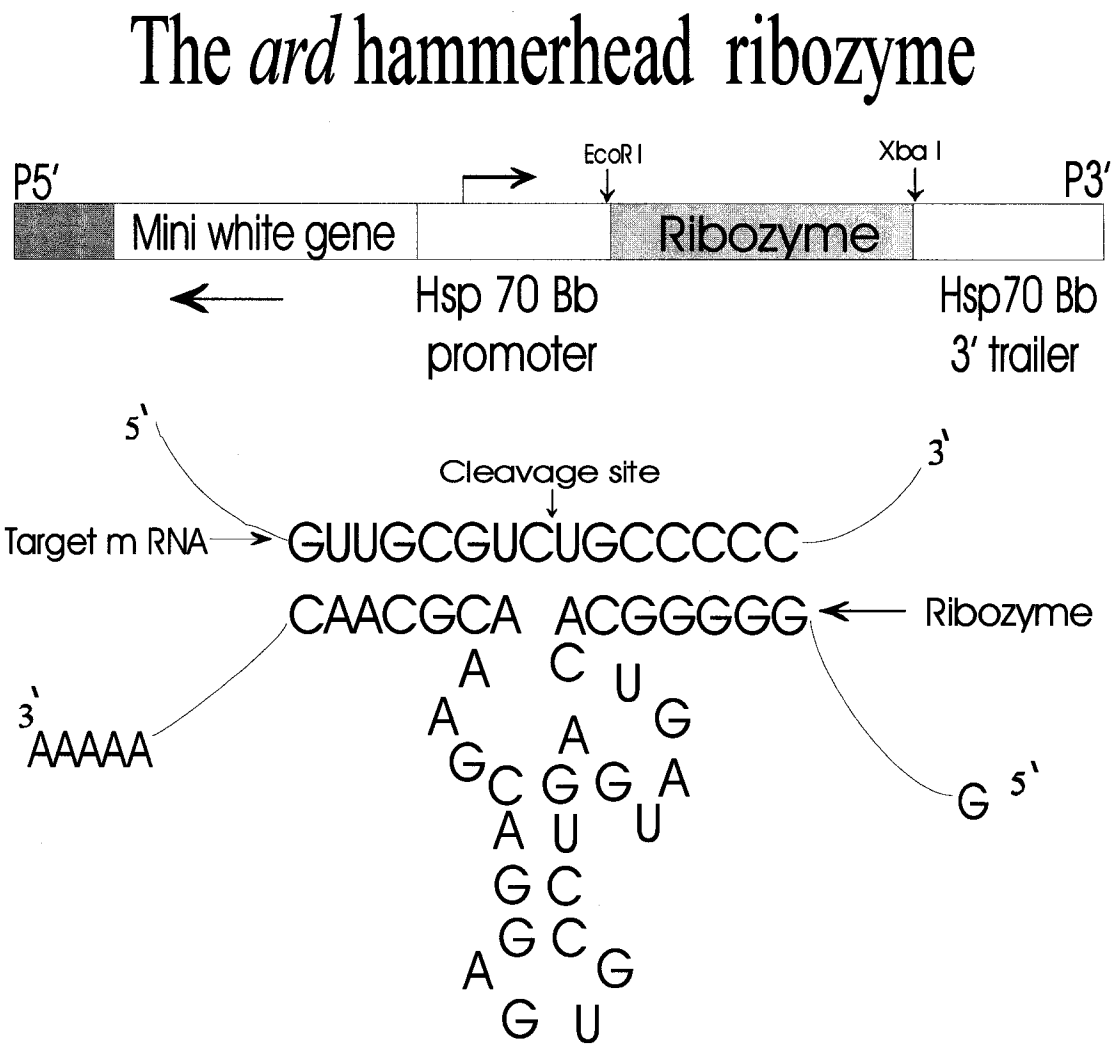

Figure 22 Schematic diagram of the hammerhead ribozyme delivery construct (top) and the target *ard* mRNA together with ribozyme (bottom).
pP{CaSpeR-hs} delivery plasmid contains a white mini gene as a marker and a heat-shock promoter.

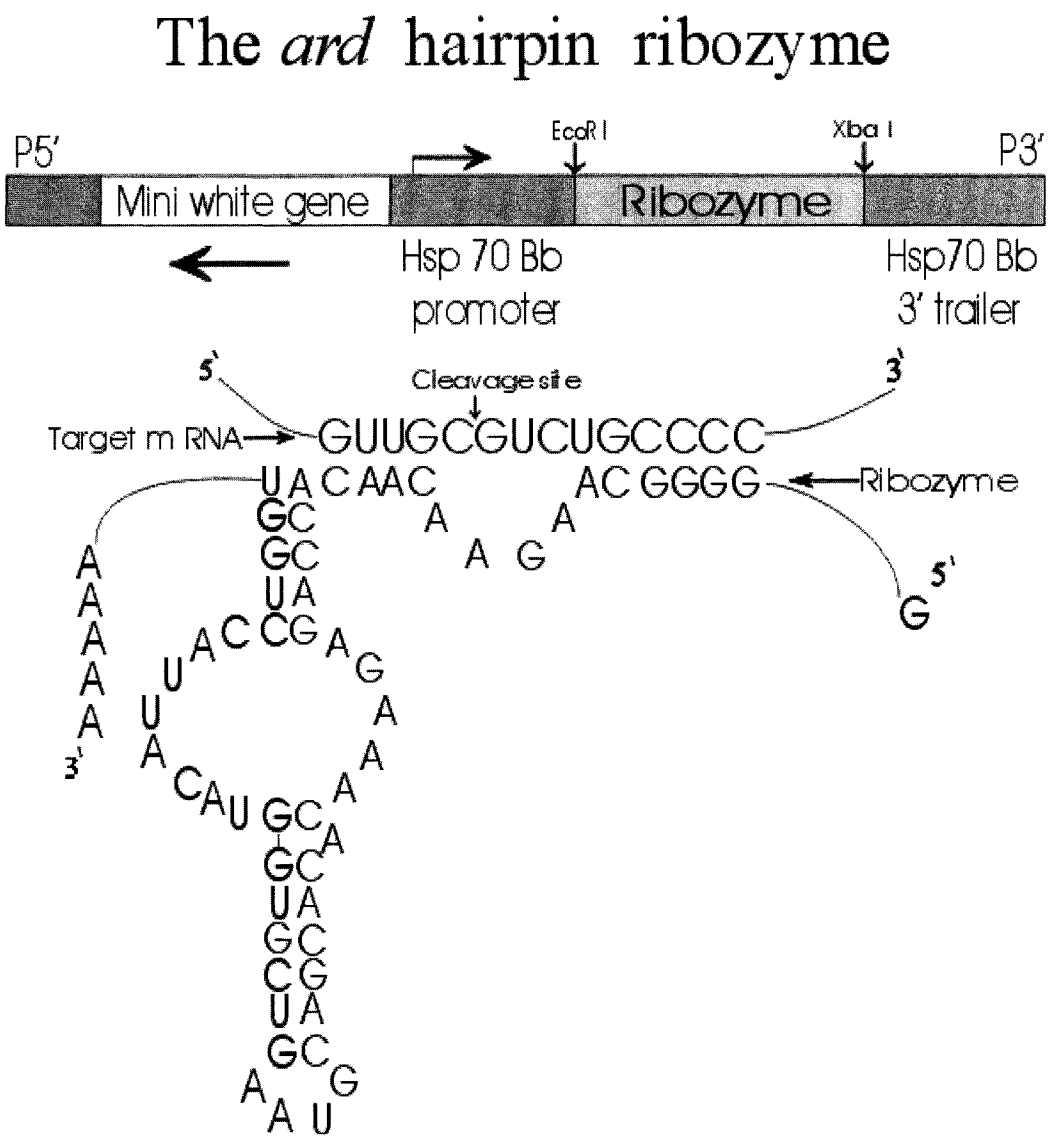

Figure 23 Schematic diagram of the hairpin ribozyme delivery construct (top) and the *ard* mRNA with the ribozyme(bottom).
pP{CaSpeR-hs} delivery plasmid contains a white mini gene as a marker and a heat-shock promoter.

The ribozyme DNA sequence was subcloned into the P-element transformation plasmid pP{CaSpeR-hs), between EcoRI and XbaI sites (Fig. 24). This vector allows heat-induced expression of inserted ribozyme construct because it contains a heat-shock promoter. Larger amounts of the delivery vector was prepared and purified from transformed *E.coli* XL-1 Blue bacteria.

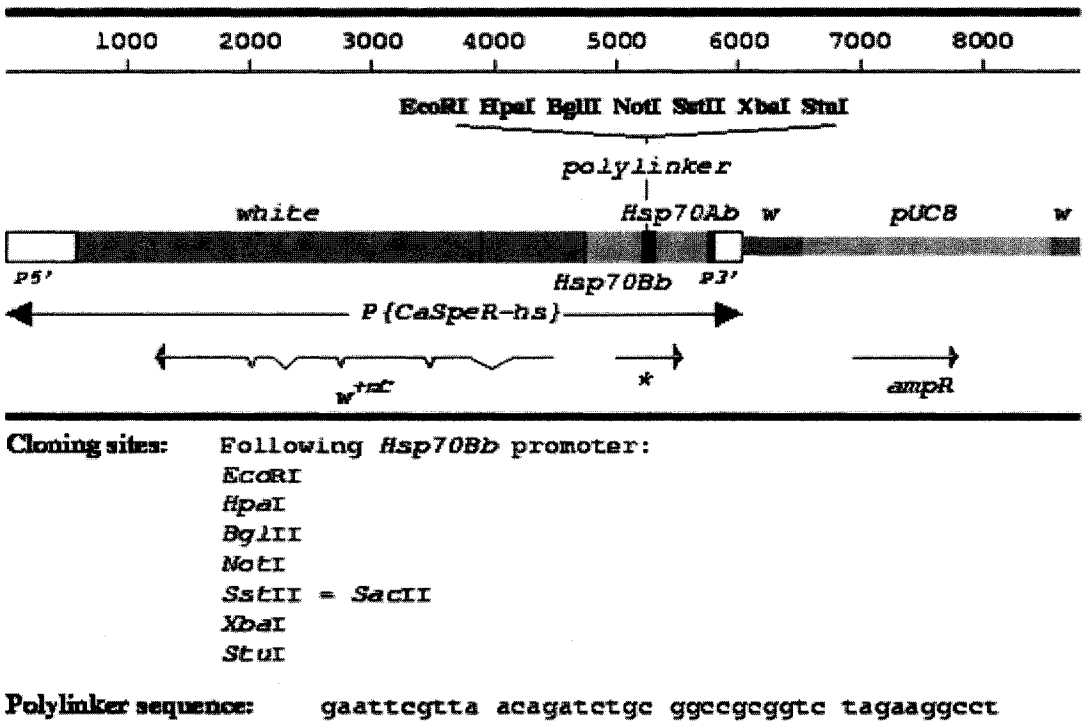

Figure 24 pP{CaSpeR-hs} vector.
Cloning vector that enables subcloning of smaller pieces of DNA into polylinker region. Carries mini white gene as a marker and heat-shock promoter.(GenBank U59056).Copied from website: ww.flybase.bio.indiana.edu

Generation of transgenic flies.

Transgenic flies were generated by P-element mediated transformation. Four pP{CaSpeR-hs} plasmids, each with the subcloned dissimilar ribozyme DNA sequence, were separately microinjected into *Drosophila* **yw** mutant embryos, together with the helper plasmid. Three transgenic flies were generated; one carrying hammerhead ribozyme construct, and two other flies, each carrying different hairpin ribozyme construct. Insertion linkage with *Drosophila* chromosome was made for each transgenic fly using the balancers and making the crosses according to the scheme described in details in Materials and Methods. The three lines of transgenic flies containing ribozyme constructs, and balancers, are maintained on a special recipe fly food in controlled conditions (RT ~25^0 C, ~60-70% humidity, 12/12 hrs day/night).

Lowering of ARD protein level by degradation of the *ard* mRNA

For ribozyme activation by heat-shock treatment of *Drosophila* embryos flies homozygous for the ribozyme insert were chosen, except for one transgenic line in which the ribozyme construct was inserted on the first, X, chromosome (the males are hemizygous for this construct). Previous heat-shock experiments, followed by Western blotting, indicated that one of the ribozymes could degrade *ard* mRNA leading to lower level of the ARD protein. Therefore, two independent heat-shock experiments were set up. *Drosophila* embryos with the same ribozyme construct in their genome were divided into two groups. One group was subjected to the heat-shock and another served as a control group.

Heat-shocks were applied on two different days to have two independent sets of data. After larvae collection and membrane protein preparation Western blotting followed.

The same anti-ARD antibody was used that was employed previously in our lab in immunoblotting with *Drosophila* head membrane preparation (Fig. 25). On that blot a band around 50 kDa (where –(Chamaon et al., 2000; Schuster et al., 1993) – the band for the ARD protein should be) is clearly visible.

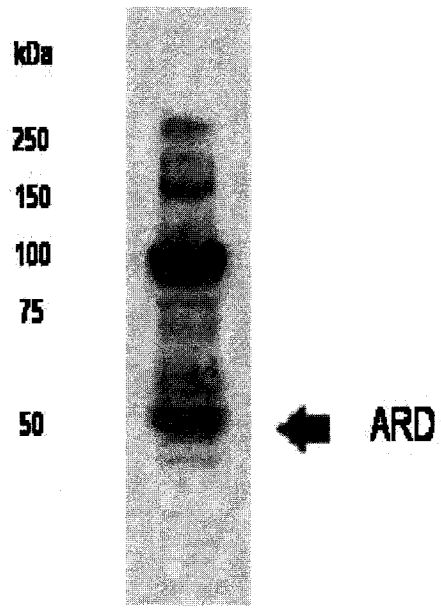

Figure 25. Picture of the SDS-polyacrylamide gel with solubilized membrane protein preparation from *Drosophila* head. Arrow points to presumed ARD band at 50 kDa
Polyclonal rabbit anti-ARD antibody was used (dilution 1:500).
100µg of the solubilized membrane prep. was loaded

We had problem with protease digestion of our larval membrane preparation. After Coomassie Blue staining, we found out that most likely proteases digested a substantial portion of proteins above 37kD (Fig. 26, gel 1, left, next pages). After substantially increasing the amounts of most protease inhibitors and adding new ones contained in the Sigma inhibitor cocktail, the problem with the protease digestion was overcome.

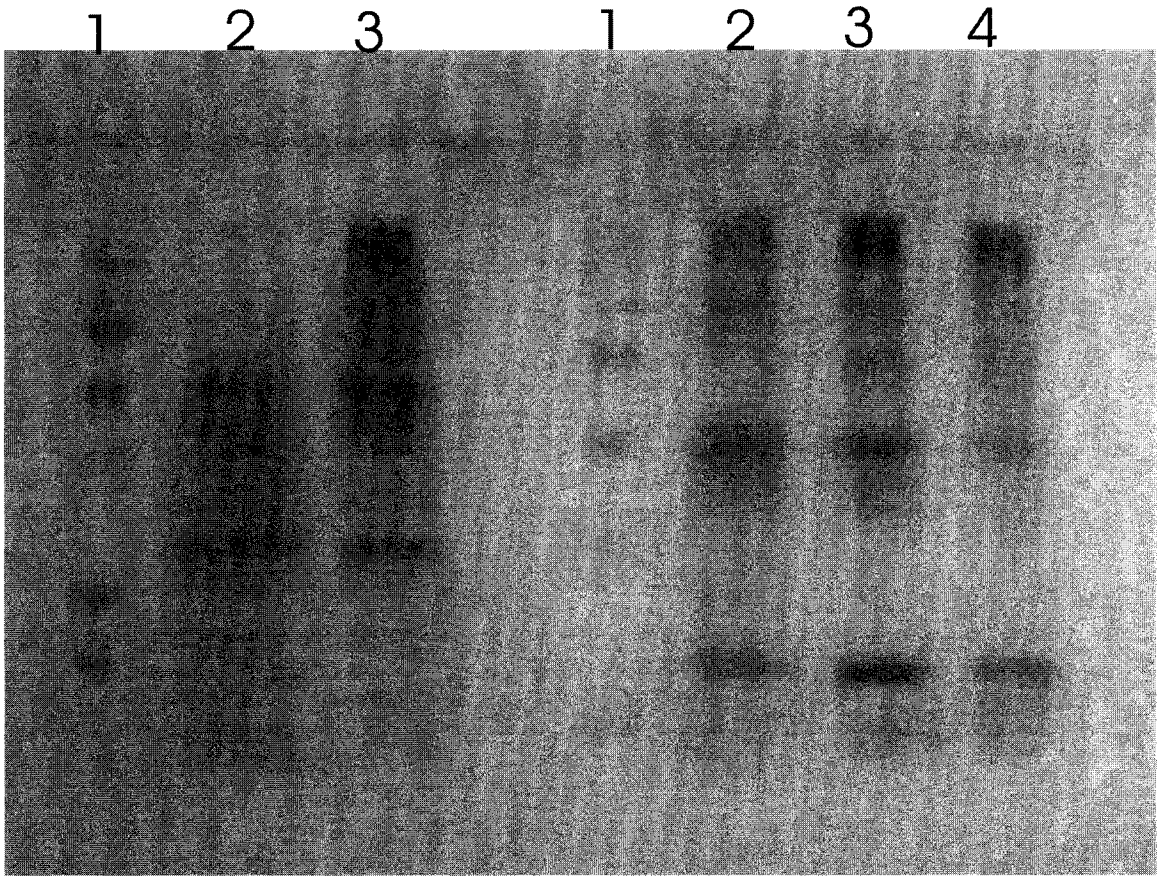

Figure 26 Protease digestion of the solubilized larval membrane preparation (gel 1,left) and the results of the increased amount of protease inhibitors (gel 2, right).
Gel 1: lane 1, MW marker
lane 2, larval membrane prep. digested by proteases
lane 3, a control, fly head membrane prep. free from proteases
Gel 2: lane 1, MW marker;
lane 2, larval membrane prep. with higher amounts of protease inhibitors
lane 3, a control, head membrane prep. free from proteases
lane 4, fly body membrane prep. with higher amounts of protease inhibitors

The results of the final Western blotting are presented in Fig.27, next page. Based on relative protein bands intensities calculations were done using software available for free on Internet, called SCION IMAGE. The results indicate that the level of the presumed ARD protein, band around 50kDa, was 39-40% lower in larvae hatched from the embryos that were subjected to heat- shock in comparison with the larvae hatched from the embryos not heat- shocked (control). There was not much change in protein levels in the other two visible bands, except in the lower band, around 29kDa, where the protein level (averaged from the two experiments) was about 14% lower in the larvae hatched from heat-shocked embryos.

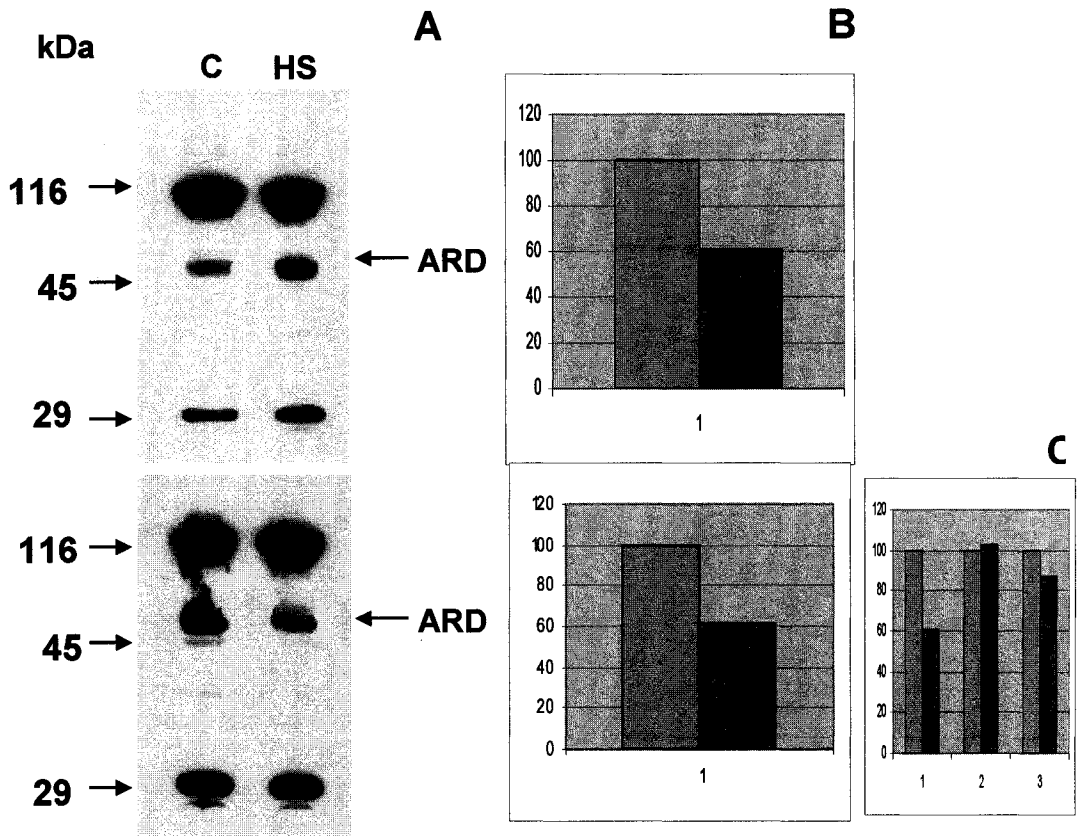

Figure 27 Western blotting results of heat-shock experiments..
A: Western blotting results from 2 independent experiments. HS- indicates the lane with the solubilized extract of larval membrane protein preparation made from HS embryos. C-indicates the CONTROL lane with the solubilized extract of larval membrane protein preparation made from non-HS embryos. The arrow indicates presumed ARD protein band. B: Two corresponding diagrams showing drop in ARD level when HS was applied (40-39%). C: shows average changes in protein level in three bands present on the blots: #1. ARD band; #2. 116 kDa band; #3. 29 kDa band. Darker bar indicates HS conditions.

IV. DISCUSSION

Mitomycin C, as stated before, is a potent mutagen known to cross-link DNA in the cell. The cross-link may be bypassed by the DNA polymerase during DNA replication and the replication may continue, which can result in mutations. Both the monofunctional and bifunctional DNA lesions can occur if MC activation is mediated by various reductases (Paz et al., 1999). The nature of these mutations was broadly investigated. For example, when shuttle vector pSP189 was exposed to activated MC, replicated in permissive mammalian cells and then amplified in indicator bacteria, mitomycin C caused a substantial increase in the mutation frequency; the mutations were predominantly base substitutions, mostly transversions, with G:C to T:A the major transversion. Also, single base deletions, mostly G:C, were common. Clusters of mutations were found in GC-rich areas (Maccubbin et al., 1997; Srikanth et al., 1994). Many scientists, cited before, had suggested and proved that this mutational spectrum was due to binding of MC to guanine residue of DNA, preferentially at 5'-d(CG) sequence. Therefore, our choice to select mitomycin C for our experiments for forming cross-links at these sequences was justified. Obviously, for site-selected targeting we had to conjugate MC to an aminolinker oligonucleotide complementary to a target DNA sequence. Such types of constructs were made and used effectively in many experiments before. For instance, mitomycin C-oligodeoxynucleotide conjugates were synthesized, mitomycin residue of the conjugate was bioreductively activated to cross-link to targeted guanine in complementary oligonucleotides, and cross-linked products were isolated and structurally characterized (Maruenda and Tomasz, 1996). In similar experiment cross-linking efficiencies of some conjugates were 25-50% (Maruenda and Tomasz, 1997)

Unfortunately, we failed to identify potential mutations in M13mp18 vector after transforming *E. coli* with the product of the cross-linking reaction after the cross-linking reaction the 21-mer conjugate was subjected to primer extension with Klenow fragment of *E.coli* which does not have the 5'→3' exonuclease activity that could degrade the conjugate. Plaque screening by plaque lifts with the radiolabeled probe and differential washings did not identify any mutations in this experiment nor *in vivo* experiments, in which cross-linking was to depend on the intracellular activation of the MC-oligonucleotide conjugate by *E. coli* reductases. The main reason could rest on wrong selection of bacterial system; according to some scientific papers. For example, Ramos (Ramos et al., 1998), showed that in *E. coli* mitomycin C was not mutagenic, or insignificantly mutagenic. Repair system of *E. coli* could be error-free when repairing cross-linking lesions caused by MC. But other groups, for instance (Fram et al., 1986), had showed mutagenic effects of mitomycin C in *E. coli.*

Unsuccessful attempts to introduce mutation in *Drosophila white* gene could be explained by many factors. The phosphodiester (PE) backbone of the oligonucleotide part of the MC- oligo construct is one of them, because as mentioned before, the PE backbone is prone to nuclease digestion. Therefore, large amount of the constructs was most likely hydrolyzed by *Drosophila* exonucleases. As a result, the concentration of the conjugates with the intact oligonucleotide complementary to the *white* gene could have been too low to effectively find the target; moreover, these constructs had, under those conditions, to compete then with the products of the MC-oligonucleotide conjugate disintegration. In order to overcome this problem we made many attempts to synthesize a MC-oligonucleotide construct with phosphorothioate (PS) backbone, much more resistant

to hydrolysis by nucleases; unfortunately we were unable to make MC-oligonucleotide construct with PS backbone. We were also unable to find commercially available aminolinker oligonucleotide with PS backbone in the form that would guarantee successful attachment of mitomycin A to this oligo. We found only one scientific paper (Huh et al., 1996), in which the authors were capable of synthesizing mitomycin-tethered oligonucleotide constructs with phosphorothioate backbone. They used these constructs to successfully (40%-65% inhibition for some constructs) inhibit cultured human aortic smooth muscle cell (HASMC) growth. The method to make these constructs was however quite different from the one we were using to make our conjugates. The authors used mitomycin C derivative, porfiromycin, as active part of the conjugate. Furthermore, they used MC as starting material; we were using MA.

Other reason for failure to introduce mutations in *Drosophila white* gene may have to do with the mechanism of the cross-linking reaction. MC has to be reductively activated to alkylate and cross-link DNA. The active form has a short life and decomposes rapidly, lowering in consequence the efficiency of covalent alkylation and cross-linking of DNA (Paz et al., 1999). Some processes, like hydrolysis, may quickly and permanently inactivate MC and convert it to MC derivatives, which may compete effectively with the site-specific guanine alkylation. In addition, MC-oligonucleotide constructs can bind non covalently with DNA at non cross-linkable sites, blocking the movement of other conjugates to the targeted sites (Paz et al., 1999).

Injected more concentrated MC-oligonucleotide constructs to fly's egg could increase more effective concentration of the conjugates in the embryo and improve chances for annealing at target site and cross-linking. As a control MA was injected; it inserts itself

randomly into DNA strands, increasing this way its toxicity. Random interaction of the conjugates with DNA should be much lower than in case of MA, since the complementary oligonucleotide of the conjugate would direct it to the specific target sequence, lowering overall toxicity in the fly's embryo. For that reason, higher concentration of the MC-oligonucleotide construct could be injected.

Finally, the aminolinker part of the construct may not be always adequately flexible to position mitomycin C moiety for the reaction with the guanine at the target site.

Generally, it is very difficult to cause mutations in *Drosophila* nicotinic acetylcholine receptor subunits inside of this fly. To my knowledge, and the author of the following reference, mutants defective in individual nAChR genes in *Drosophila* have not yet been described (Schafer, 2002).

There are many mutagenic agents that have been traditionally used to induce mutations in *Drosophila;* the most commonly used are ethyl methanesulfonate (EMS), N-ethyl-N-nitrosurea (ENU), triethylenemelamine (TEM), formaldehyde, and ionizing radiation (Roberts, 1998). The problem arises how to efficiently screen for the mutation which phenotype is unknown. That is, so far, the case with *Drosophila* nAChR genes.

This investigation aimed at the disruption of the gene expression in *Drosophila melanogaster.* The target was the *ard* gene coding for the ARD subunit of the neuronal nAChR. The interference with the gene expression was more successful on the transcriptional level when one of the hairpin ribozymes used against the *ard* mRNA caused about 40% decrease in the amount of the protein that most probably is the ARD subunit. In one of these experiments the decrease was 40%, in another 39%. The target

was a small loop on the *ard* mRNA secondary structure predicted by the "mfold" energy minimization program. It is difficult to say why only this ribozyme, out of three, seemed to work. Immunoprecipitation experiments should be done to confirm if the 50 kDa band on the Western blots is really ARD. Indirect proofs could be the results of the two independent experiments illustrated in Fig. 27, on page 85; if heat-shock activated ribozyme directed against *ard* mRNA destroyed large amount of it then the level of the ARD protein should decrease. The only band that was substantially smaller under heat-shock conditions was the band around 50kDa. The other two bands on the blots, around 116 kDa and 29 kDa, can not be ARD subunits since, according to scientific publications (Chamaon et al., 2000; Schuster et al., 1993), the *Drosophila* ARD protein migrates at about 50 kDa in SDS-PAGE. So the outcome of the experiments suggests that the ~ 50 kDa band is really ARD protein. Nevertheless, to clarify this the immunoprecipitation experiments could be helpful, because immunoprecipitation allows the partial purification of the proteins (antigens) from the solubilized membrane protein preparation mixture of many proteins. The design of this experiment should include membrane preparation from the larvae hatched from the embryos not subjected to the heat-shock (control) and the membrane preparation from the larvae hatched from the heat-shock embryos (experimental).

In order to investigate if our anti-ARD antibody was specific for the ARD subunit an excess of the purified peptide against which our antibody had been raised should be used in immunoprecipitation experiments. If this peptide was added then the precipitation of the ARD would be blocked, since the immunoprecipitated protein would compete with

the peptide, there would be no ~50 kDa band visible, or its intensity would be drastically reduced. Unfortunately, we are not in a possession of such peptide.

If the direct proof was required for the cleaving action of the ribozyme, then Northern blotting could be done. It is known, that in *Drosophila* embryos *ard* transcripts are rapidly spliced to form the mature 3.2 kb mRNA, and that splicing intermediates can not be detected (Hermans-Borgmeyer et al., 1989). Our hairpin ribozyme cuts the *ard* transcripts at about 400 bases from the transcription start site. Therefore, the mature *ard* mRNA purified from the heat-shock embryos should be about 400 bases smaller and might be identified on the blot.

Assuming that our disruption of the *ard* mRNA was successful we could try to improve the results by, for example, varying the timing of the heat-shock itself. Heat-shock was applied when the embryos were about 10- 22 hrs old; at that period of time the *ard* mRNA level increases rapidly and reaches its peak at the end of embryogenesis. On the average, the embryos were about 16 hrs old when the heat-shock started. It is possible that by delaying the heat-shock for 1-2 hrs the amount of destroyed *ard* mRNA would be larger, because the closer to the end of the embryogenesis the more *ard* mRNA is synthesized.

Also, designing and using larger number of ribozymes to larger number of targets could lead to finding more efficient ribozyme or optimal target.

Other researches were frequently more successful with their work with ribozymes in *Drosophila*. In one classic paper (Zhao and Pick, 1993) the authors were describing how they generated complete inhibition of *Drosophila fushi tarazu(ftz)* protein synthesis after induction of the *ftz* ribozyme in transgenic embryos.

Currently some different methods are being used in *Drosophila* to inhibit gene activity, most promising is RNA interference. In many instances, RNAi injected in *Drosophila* embryos caused loss-of-function phenotype (Dzitoyeva et al., 2003; Kennerdell and Carthew, 1998), or effective degradation of transcripts in *Drosophila* (Geng et al., 2004) Therefore, this method could be investigated as an alternative or auxilary to ribozymes in efficient disruption of gene expression in *Drosophila.*

In summary, this study, if followed by more research, may have achieved the goal of disruption of the ARD subunit of *Drosophila* neuronal nicotinic acetylcholine receptor. The hairpin ribozyme seemed to be an effective agent in damaging mRNA of the *ard* gene in *Drosophila melanogaster.*

V. BIBLIOGRAPHY

M13 cloning/dideoxy sequencing. Instruction manual, (Bethesda Research Laboratory) (1994).

Sequencing support service. Instruction manual, (Cleveland, United States Biochemical) (1994).

Andang, M., Hinkula, J., Hotchkiss, G., Larsson, S., Britton, S., Wong-Staal, F., Wahren, B., and Ahrlund-Richter, L. (1999). Dose-response resistance to HIV-1/MuLV pseudotype virus ex vivo in a hairpin ribozyme transgenic mouse model. Proc Natl Acad Sci U S A *96*, 12749-12753.

Arias, H. R. (2000). Localization of agonist and competitive antagonist binding sites on nicotinic acetylcholine receptors. Neurochem Int *36*, 595-645.

Ashburner, M. (1989). *Drosophila*: a laboratory handbook (Cold Spring Harbor, Cold Spring Harbor Laboratory Press).

Ausubel, F. M., Brent, R., Kingston, R. E., Moore, D. D., Seidman, J. G., Smith, J. A., and Struhl, K., eds. (1998). Current protocols in molecular biology (John Wiley & Sons, Inc.).

Basu, A. K., Hanrahan, C. J., Malia, S. A., Kumar, S., Bizanek, R., and Tomasz, M. (1993). Effect of site-specifically located mitomycin C-DNA monoadducts on in vitro DNA synthesis by DNA polymerases. Biochemistry *32*, 4708-4718.

Baumann, A., Jonas, P., and Gundelfinger, E. D. (1990). Sequence of D alpha 2, a novel alpha-like subunit of Drosophila nicotinic acetylcholine receptors. Nucleic Acids Res *18*, 3640.

Bertrand, D., Ballivet, M., Gomez, M., Bertrand, S., Phannavong, B., and Gundelfinger, E. D. (1994). Physiological properties of neuronal nicotinic receptors reconstituted from the vertebrate beta 2 subunit and Drosophila alpha subunits. Eur J Neurosci *6*, 869-875.

Birikh, K. R., Heaton, P. A., and Eckstein, F. (1997). The structure, function and application of the hammerhead ribozyme. Eur J Biochem *245*, 1-16.

Boorman, J. P., Groot-Kormelink, P. J., and Sivilotti, L. G. (2000). Stoichiometry of human recombinant neuronal nicotinic receptors containing the b3 subunit expressed in Xenopus oocytes. J Physiol *529 Pt 3*, 565-577.

Bossy, B., Ballivet, M., and Spierer, P. (1988). Conservation of neural nicotinic acetylcholine receptors from Drosophila to vertebrate central nervous systems. Embo J *7*, 611-618.

Boulter, J., Connolly, J., Deneris, E., Goldman, D., Heinemann, S., and Patrick, J. (1987). Functional expression of two neuronal nicotinic acetylcholine receptors from cDNA clones identifies a gene family. Proc Natl Acad Sci U S A *84*, 7763-7767.

Chamaon, K., Schulz, R., Smalla, K. H., Seidel, B., and Gundelfinger, E. D. (2000). Neuronal nicotinic acetylcholine receptors of Drosophila melanogaster: the alpha-subunit dalpha3 and the beta-type subunit ARD co-assemble within the same receptor complex. FEBS Lett *482*, 189-192.

Chawla, A. K., and Tomasz, M. (1988). Interaction of the antitumor antibiotic mitomycin C with Z-DNA. J Biomol Struct Dyn *6*, 459-470.

Chen, C. H., and Sigman, D. S. (1986). Nuclease activity of 1,10-phenanthroline-copper: sequence-specific targeting. Proc Natl Acad Sci U S A *83*, 7147-7151.

Corringer, P. J., Bertrand, S., Galzi, J. L., Devillers-Thiery, A., Changeux, J. P., and Bertrand, D. (1999). Mutational analysis of the charge selectivity filter of the alpha7 nicotinic acetylcholine receptor. Neuron *22*, 831-843.

Dzitoyeva, S., Dimitrijevic, N., and Manev, H. (2003). Identification of a novel Drosophila gene, beltless, using injectable embryonic and adult RNA interference (RNAi). BMC Genomics *4*, 33.

Ewart, G. D., Cannell, D., Cox, G. B., and Howells, A. J. (1994). Mutational analysis of the traffic ATPase (ABC) transporters involved in uptake of eye pigment precursors in Drosophila melanogaster. Implications for structure-function relationships. J Biol Chem *269*, 10370-10377.

Fram, R. J., Sullivan, J., and Marinus, M. G. (1986). Mutagenesis and repair of DNA damage caused by nitrogen mustard, N,N'-bis(2-chloroethyl)-N-nitrosourea (BCNU), streptozotocin, and mitomycin C in E. coli. Mutat Res *166*, 299-242.

Francois, J. C., Saison-Behmoaras, T., and Helene, C. (1988). Sequence-specific recognition of the major groove of DNA by oligodeoxynucleotides via triple helix formation. Footprinting studies. Nucleic Acids Res *16*, 11431-11440.

Geng, C., Pellegrino, A., Bowman, J., Zhu, L., and Pak, W. L. (2004). Complete RNAi rescue of neuronal degeneration in a constitutively active Drosophila TRP channel mutant. Biochim Biophys Acta *1674*, 91-97.

Georgiev, P. G., Korochkina, S. E., Georgieva, S. G., and Gerasimova, T. I. (1990). Mitomycin C induces genomic rearrangements involving transposable elements in Drosophila melanogaster. Mol Gen Genet *220*, 229-233.

Glover, D. M., ed. (1985). DNA cloning: a practical approach (Oxford, IRL Press Limited).

Gotti, C., and Clementi, F. (2004). Neuronal nicotinic receptors: from structure to pathology. Prog Neurobiol *74*, 363-396.

Grauso, M., Reenan, R. A., Culetto, E., and Sattelle, D. B. (2002). Novel putative nicotinic acetylcholine receptor subunit genes, Dalpha5, Dalpha6 and Dalpha7, in Drosophila melanogaster identify a new and highly conserved target of adenosine deaminase acting on RNA-mediated A-to-I pre-mRNA editing. Genetics *160*, 1519-1533.

Grutter, T., and Changeux, J. P. (2001). Nicotinic receptors in wonderland. Trends Biochem Sci *26*, 459-463.

Gundelfinger, E. D. (1992). How complex is the nicotinic receptor system of insects? Trends Neurosci *15*, 206-211.

Gundelfinger, E. D., and Hess, N. (1992). Nicotinic acetylcholine receptors of the central nervous system of Drosophila. Biochim Biophys Acta *1137*, 299-308.

Hall, Z. W., and Sanes, J. R. (1993). Synaptic structure and development: the neuromuscular junction. Cell *72 Suppl*, 99-121.

Hampel, A., DeYoung, M. B., Galasinski, S., and Siwkowski, A. (1997). Design of the hairpin ribozyme for targeting specific RNA sequences. Methods Mol Biol *74*, 171-177.

Haseloff, J., and Gerlach, W. L. (1992). Simple RNA enzymes with new and highly specific endoribonuclease activities. 1988. Biotechnology *24*, 264-269.

Helene, C. (1991). The anti-gene strategy: control of gene expression by triplex-forming-oligonucleotides. Anticancer Drug Des *6*, 569-584.

Helene, C., Montenay-Garestier, T., Saison, T., Takasugi, M., Toulme, J. J., Asseline, U., Lancelot, G., Maurizot, J. C., Toulme, F., and Thuong, N. T. (1985). Oligodeoxynucleotides covalently linked to intercalating agents: a new class of gene regulatory substances. Biochimie *67*, 777-783.

Helene, C., Thuong, N. T., and Harel-Bellan, A. (1992). Control of gene expression by triple helix-forming oligonucleotides. The antigene strategy. Ann N Y Acad Sci *660*, 27-36.

Hermans-Borgmeyer, I., Hoffmeister, S., Sawruk, E., Betz, H., Schmitt, B., and Gundelfinger, E. D. (1989). Neuronal acetylcholine receptors in Drosophila: mature and immature transcripts of the ard gene in the developing central nervous system. Neuron *2*, 1147-1156.

Hille, B. (2001). Ionic channels of excitable membranes (Sunderland, Sinauer Associates, Inc.).

Hucho, F., Tsetlin, V. I., and Machold, J. (1996). The emerging three-dimensional structure of a receptor. The nicotinic acetylcholine receptor. Eur J Biochem *239*, 539-557.

Huh, N., Rege, A. A., Yoo, B., Kogan, T. P., and Kohn, H. (1996). Design, synthesis, and evaluation of mitomycin-tethered phosphorothioate oligodeoxynucleotides. Bioconjug Chem *7*, 659-669.

Jackson, W. H., Jr., Moscoso, H., Nechtman, J. F., Galileo, D. S., Garver, F. A., and Lanclos, K. D. (1998). Inhibition of HIV-1 replication by an anti-tat hammerhead ribozyme. Biochem Biophys Res Commun *245*, 81-84.

Jonas, P., Baumann, A., Merz, B., and Gundelfinger, E. D. (1990). Structure and developmental expression of the D alpha 2 gene encoding a novel nicotinic acetylcholine receptor protein of Drosophila melanogaster. FEBS Lett *269*, 264-268.

Karess, R. E., and Rubin, G. M. (1984). Analysis of P transposable element functions in Drosophila. Cell *38*, 135-146.

Karlin, A., and Akabas, M. H. (1995). Toward a structural basis for the function of nicotinic acetylcholine receptors and their cousins. Neuron *15*, 1231-1244.

Kennerdell, J. R., and Carthew, R. W. (1998). Use of dsRNA-mediated genetic interference to demonstrate that frizzled and frizzled 2 act in the wingless pathway. Cell *95*, 1017-1026.

Lansdell, S. J., and Millar, N. S. (2002). Dbeta3, an atypical nicotinic acetylcholine receptor subunit from Drosophila : molecular cloning, heterologous expression and coassembly. J Neurochem *80*, 1009-1018.

Lansdell, S. J., Schmitt, B., Betz, H., Sattelle, D. B., and Millar, N. S. (1997). Temperature-sensitive expression of Drosophila neuronal nicotinic acetylcholine receptors. J Neurochem *68*, 1812-1819.

Le Doan, T., Perrouault, L., Praseuth, D., Habhoub, N., Decout, J. L., Thuong, N. T., Lhomme, J., and Helene, C. (1987). Sequence-specific recognition, photocrosslinking and cleavage of the DNA double helix by an oligo-[alpha]-thymidylate covalently linked to an azidoproflavine derivative. Nucleic Acids Res *15*, 7749-7760.

Lena, C., and Changeux, J. P. (1999). The role of beta 2-subunit-containing nicotinic acetylcholine receptors in the brain explored with a mutant mouse. Ann N Y Acad Sci *868*, 611-616.

Ma, D. D. (2004). Characterization of upstream sequences required for transcriptional control of the *als* gene encoding a subunit of a neuronal nicotinic acetylcholine receptor from *Drosophila.* Department of Biology, City University of New York, New York.

Maccubbin, A. E., Mudipalli, A., Nadadur, S. S., Ersing, N., and Gurtoo, H. L. (1997). Mutations induced in a shuttle vector plasmid exposed to monofunctionally activated mitomycin C. Environ Mol Mutagen *29*, 143-151.

Maher, L. J., 3rd, Wold, B., and Dervan, P. B. (1991). Oligonucleotide-directed DNA triple-helix formation: an approach to artificial repressors? Antisense Res Dev *1*, 277-281.

Marks, M. J., Whiteaker, P., Calcaterra, J., Stitzel, J. A., Bullock, A. E., Grady, S. R., Picciotto, M. R., Changeux, J. P., and Collins, A. C. (1999). Two pharmacologically distinct components of nicotinic receptor-mediated rubidium efflux in mouse brain require the beta2 subunit. J Pharmacol Exp Ther *289*, 1090-1103.

Marubio, L. M., del Mar Arroyo-Jimenez, M., Cordero-Erausquin, M., Lena, C., Le Novere, N., de Kerchove d'Exaerde, A., Huchet, M., Damaj, M. I., and Changeux, J. P. (1999). Reduced antinociception in mice lacking neuronal nicotinic receptor subunits. Nature *398*, 805-810.

Maruenda, H., and Tomasz, M. (1996). Antisense sequence-directed cross-linking of DNA oligonucleotides by mitomycin C. Bioconjug Chem *7*, 541-544.

Maruenda, H., and Tomasz, M. (1997). Antisense sequence-directed cross-linking of RNA oligonucleotides by mitomycin. Anticancer Drug Des *12*, 473-479.

Mathews, C. K., Kensal E. van Holde, Kevin G. Ahern (2000). Biochemistry, 3rd edn (San Francisco, Addison Wesley Longman).

McGehee, D. S., and Role, L. W. (1995). Physiological diversity of nicotinic acetylcholine receptors expressed by vertebrate neurons. Annu Rev Physiol *57*, 521-546.

Millar, N. S. (2003). Assembly and subunit diversity of nicotinic acetylcholine receptors. Biochem Soc Trans *31*, 869-874.

Miller, P. S., and Ts'o, P. O. (1987). A new approach to chemotherapy based on molecular biology and nucleic acid chemistry: Matagen (masking tape for gene expression). Anticancer Drug Des *2*, 117-128.

Min, Z., Gill, R. D., Cortez, C., Harvey, R. G., Loechler, E. L., and DiGiovanni, J. (1996). Targeted A --> T and G --> T mutations induced by site-specific deoxyadenosine and

deoxyguanosine adducts, respectively, from the (+)-anti-diol epoxide of dibenz[a,j]anthracene in M13mp7L2. Biochemistry *35*, 4128-4138.

Moser, H. E., and Dervan, P. B. (1987). Sequence-specific cleavage of double helical DNA by triple helix formation. Science *238*, 645-650.

Nai, Q., McIntosh, J. M., and Margiotta, J. F. (2003). Relating neuronal nicotinic acetylcholine receptor subtypes defined by subunit composition and channel function. Mol Pharmacol *63*, 311-324.

Nishiyama, M., Suzuki, K., Kumazaki, T., Yamamoto, W., Toge, T., Okamura, T., and Kurisu, K. (1997). Molecular targeting of mitomycin C chemotherapy. Int J Cancer *72*, 649-656.

Orr-Urtreger, A., Goldner, F. M., Saeki, M., Lorenzo, I., Goldberg, L., De Biasi, M., Dani, J. A., Patrick, J. W., and Beaudet, A. L. (1997). Mice deficient in the alpha7 neuronal nicotinic acetylcholine receptor lack alpha-bungarotoxin binding sites and hippocampal fast nicotinic currents. J Neurosci *17*, 9165-9171.

Ortiz-Acevedo, A., Melendez, M., Asseo, A. M., Biaggi, N., Rojas, L. V., and Lasalde-Dominicci, J. A. (2004). Tryptophan scanning mutagenesis of the gammaM4 transmembrane domain of the acetylcholine receptor from Torpedo californica. J Biol Chem *279*, 42250-42257.

Paz, M. M., Das, T. A., and Tomasz, M. (1999). Mitomycin C linked to DNA minor groove binding agents: synthesis, reductive activation, DNA binding and cross-linking properties and in vitro antitumor activity. Bioorg Med Chem *7*, 2713-2726.

Peterson, G. L. (1977). A simplification of the protein assay method of Lowry et al. which is more generally applicable. Anal Biochem *83*, 346-356.

Picciotto, M. R., Zoli, M., Lena, C., Bessis, A., Lallemand, Y., Le Novere, N., Vincent, P., Pich, E. M., Brulet, P., and Changeux, J. P. (1995). Abnormal avoidance learning in mice lacking functional high-affinity nicotine receptor in the brain. Nature *374*, 65-67.

Praseuth, D., Perrouault, L., Le Doan, T., Chassignol, M., Thuong, N., and Helene, C. (1988). Sequence-specific binding and photocrosslinking of alpha and beta oligodeoxynucleotides to the major groove of DNA via triple-helix formation. Proc Natl Acad Sci U S A *85*, 1349-1353.

Purves, W. K., Sadava, D., Orians, G. H., and Heller, C. H. (2001). Life: the science of biology, 6th edn, Sinauer Associates, Inc.(W.H. Freeman And Company).

Ramos, L. A., Lipman, R., Tomasz, M., and Basu, A. K. (1998). The major mitomycin C-DNA monoadduct is cytotoxic but not mutagenic in Escherichia coli. Chem Res Toxicol *11*, 64-69.

Rigas, B., Welcher, A. A., Ward, D. C., and Weissman, S. M. (1986). Rapid plasmid library screening using RecA-coated biotinylated probes. Proc Natl Acad Sci U S A *83*, 9591-9595.

Roberts, D. B., ed. (1998). *Drosophila:* a practical approach, 2nd edn (New York, Oxford University Press Inc.).

Rossi, J. J. (1997). Therapeutic applications of catalytic antisense RNAs (ribozymes). Ciba Found Symp *209*, 195-204; discussion 204-196.

Rubin, G. M. (1988). Drosophila melanogaster as an experimental organism. Science *240*, 1453-1459.

Rubin, G. M., and Spradling, A. C. (1983). Vectors for P element-mediated gene transfer in Drosophila. Nucleic Acids Res *11*, 6341-6351.

Sambrook, J., Fritsch, E. F., and Maniatis, T. (1989). Molecular cloning: a laboratory manual, 2nd edn (Cold Spring Harbor, Cold Spring Harbor Laboratory Press).

Sandor, Z., and Bredberg, A. (1994). Repair of triple helix directed psoralen adducts in human cells. Nucleic Acids Res *22*, 2051-2056.

Sargent, P. B. (1993). The diversity of neuronal nicotinic acetylcholine receptors. Annu Rev Neurosci *16*, 403-443.

Sawruk, E., Udri, C., Betz, H., and Schmitt, B. (1990). SBD, a novel structural subunit of the Drosophila nicotinic acetylcholine receptor, shares its genomic localization with two alpha-subunits. FEBS Lett *273*, 177-181.

Schafer, W. R. (2002). Genetic analysis of nicotinic signaling in worms and flies. J Neurobiol *53*, 535-541.

Schloss, P., Betz, H., Schroder, C., and Gundelfinger, E. D. (1991). Neuronal nicotinic acetylcholine receptors in Drosophila: antibodies against an alpha-like and a non-alpha-subunit recognize the same high-affinity alpha-bungarotoxin binding complex. J Neurochem *57*, 1556-1562.

Schloss, P., Hermans-Borgmeyer, I., Betz, H., and Gundelfinger, E. D. (1988). Neuronal acetylcholine receptors in Drosophila: the ARD protein is a component of a high-affinity alpha-bungarotoxin binding complex. Embo J *7*, 2889-2894.

Schmidt-Nielsen, B. K., Gepner, J. I., Teng, N. N., and Hall, L. M. (1977). Characterization of an alpha-bungarotoxin binding component from Drosophila melanogaster. J Neurochem *29*, 1013-1029.

Schulz, R., Bertrand, S., Chamaon, K., Smalla, K. H., Gundelfinger, E. D., and Bertrand, D. (2000). Neuronal nicotinic acetylcholine receptors from Drosophila: two different types of alpha subunits coassemble within the same receptor complex. J Neurochem *74*, 2537-2546.

Schuster, R., Phannavong, B., Schroder, C., and Gundelfinger, E. D. (1993). Immunohistochemical localization of a ligand-binding and a structural subunit of nicotinic acetylcholine receptors in the central nervous system of Drosophila melanogaster. J Comp Neurol *335*, 149-162.

Srikanth, N. S., Mudipalli, A., Maccubbin, A. E., and Gurtoo, H. L. (1994). Mutations in a shuttle vector exposed to activated mitomycin C. Mol Carcinog *10*, 23-29.

Strobel, H. W., and Dignam, J. D. (1978). Purification and properties of NADPH-cytochrome P-450 reductase. Methods Enzymol *52*, 89-96.

Sun, L. Q., Ely, J. A., Gerlach, W., and Symonds, G. (1997). Anti-HIV ribozymes. Mol Biotechnol *7*, 241-251.

Takasugi, M., Guendouz, A., Chassignol, M., Decout, J. L., Lhomme, J., Thuong, N. T., and Helene, C. (1991). Sequence-specific photo-induced cross-linking of the two strands of double-helical DNA by a psoralen covalently linked to a triple helix-forming oligonucleotide. Proc Natl Acad Sci U S A *88*, 5602-5606.

Unwin, N. (1995). Acetylcholine receptor channel imaged in the open state. Nature *373*, 37-43.

Vazquez-Tello, A., Castan, P., Moreno, R., Smith, J. M., Berenguer, J., and Cedergren, R. (2002). Efficient trans-cleavage by the Schistosoma mansoni SMalpha1 hammerhead ribozyme in the extreme thermophile Thermus thermophilus. Nucleic Acids Res *30*, 1606-1612.

Wadsworth, S. C., Rosenthal, L. S., Kammermeyer, K. L., Potter, M. B., and Nelson, D. J. (1988). Expression of a Drosophila melanogaster acetylcholine receptor-related gene in the central nervous system. Mol Cell Biol *8*, 778-785.

Ward, B., Skorobogaty, A., and Dabrowiak, J. C. (1986). DNA cleavage specificity of a group of cationic metalloporphyrins. Biochemistry *25*, 6875-6883.

Wilson, G. G., and Karlin, A. (1998). The location of the gate in the acetylcholine receptor channel. Neuron *20*, 1269-1281.

Yasukochi, Y., and Masters, B. S. (1976). Some properties of a detergent-solubilized NADPH-cytochrome c(cytochrome P-450) reductase purified by biospecific affinity chromatography. J Biol Chem *251*, 5337-5344.

Yu, Q., Pecchia, D. B., Kingsley, S. L., Heckman, J. E., and Burke, J. M. (1998). Cleavage of highly structured viral RNA molecules by combinatorial libraries of hairpin ribozymes. The most effective ribozymes are not predicted by substrate selection rules. J Biol Chem *273*, 23524-23533.

Zamecnik, P. C., Goodchild, J., Taguchi, Y., and Sarin, P. S. (1986). Inhibition of replication and expression of human T-cell lymphotropic virus type III in cultured cells by exogenous synthetic oligonucleotides complementary to viral RNA. Proc Natl Acad Sci U S A *83*, 4143-4146.

Zhao, J. J., and Lemke, G. (1998). Rules for ribozymes. Mol Cell Neurosci *11*, 92-97.

Zhao, J. J., and Pick, L. (1993). Generating loss-of-function phenotypes of the fushi tarazu gene with a targeted ribozyme in Drosophila. Nature *365*, 448-451.

Zuker, M. (2003). Mfold web server for nucleic acid folding and hybridization prediction. Nucleic Acids Res *31*, 3406-3415.